Modeling Nutrient Legacies and Time Lags in Agricultural Landscapes: A Midwestern Case Study

by

Idhaya Chandhiran Ilampooranan

A thesis
presented to the University of Waterloo
in fulfillment of the
thesis requirement for the degree of
Doctor of Philosophy
in
Civil and Environmental Engineering (Water)

Waterloo, Ontario, Canada, 2019

Examining Committee Membership

The following served on the Examining Committee for this thesis. The decision of the Examining Committee is by majority vote.

External Examiner	Indrajeet Chaubey Dean of the College of Agriculture- Health and Natural Resources University of Connecticut
Supervisor	Nandita Basu Associate Professor Department of Civil and Environmental Engineering University of Waterloo
Internal Member	Bryan Tolson Associate Professor Department of Civil and Environmental Engineering University of Waterloo
Internal-external Member	Merrin Macrae Associate Professor Department of Geography and Environmental Management University of Waterloo
Other Member(s)	Bruce MacVicar Associate Professor Department of Civil and Environmental Engineering University of Waterloo

Author's Declaration

This thesis consists of material all of which I authored or co-authored: see Statement of Contributions included in the thesis. This is a true copy of the thesis, including any required final revisions, as accepted by my examiners

I understand that my thesis may be made electronically available to the public

Statement of Contributions

All the four research chapters were written in the journal manuscript format. I am the first author of all these chapters, and the contribution of co-authors are summarized below

Chapter 2: Estimation of Legacy Nitrogen Storage in Agricultural Landscape using data synthesis approach

Nandita B Basu (NBB) and Idhayachandhiran Ilampooranan (II) designed the study. II and Kimberly J Van Meter (KJV) synthesized the data, and II lead the analysis. II wrote this chapter with help from NBB

Chapter 3: Pitfalls in Model Calibration - Getting the Right Answers for the Wrong Reasons

II and NBB designed the study. Jerald L. Schnoor provided the base SWAT model. II collected the data, re-built and calibrated the model and performed the analysis. II and NBB wrote the chapter

Chapter 4: A Race against Time: Modelling Time Lags in Watershed Response

II and NBB designed the study. II collected data, built the models (SWAT-LAG and TTD and coupling) and performed the analysis. KJV provided some nitrogen inputs data and offered valuable feedbacks. II performed the analysis. II and NBB wrote the chapter and KJV improved the manuscript

Chapter 5: Intensive Agriculture, Nitrogen Sequestration, and Water Quality: Intersections and Implications

NBB, KJV, and II designed the study. II collected data, built the model, and performed the analysis. II, NBB, and KJV wrote the chapter

Abstract

Land-use change and agricultural intensification have increased food production but at the cost of polluting surface and groundwater. Best management practices implemented to improve water quality have met with limited success. Such lack of success is increasingly attributed to legacy nutrient stores in the subsurface that may act as sources after reduction of external inputs. These legacy stores have built up over decades of fertilizer application and contribute to time lags between the implementation of best management practices and water quality improvement. However, current water quality models lack a framework to capture these legacy effects and corresponding lag times. The overall goal of this thesis is to use a combination of data synthesis and modeling to quantify legacy stores and time lags in intensively managed agricultural landscapes in the Midwestern US. The specific goals are to (1) quantify legacy nitrogen accumulation using a mass balance approach from 1949 - 2012 (2) develop a SWAT model for the basin and demonstrate the value of using crop yield information to increase model robustness (3) modify the SWAT (Soil Water Assessment Tool) model to capture the effect of nitrogen (N) legacies on water quality under multiple land-management scenarios, and (4) use a field-scale carbon-nitrogen cycling model (CENTURY) to quantify the role of climate and soil type on legacy accumulation and water quality. For objectives 1 and 2, the analysis was performed in the Iowa Cedar Basin (ICB), a 32,660 km^2 watershed in Eastern Iowa, while for objective 3, the focus has been on the South Fork Iowa River Watershed (SFIRW), a 502 km^2 sub-watershed of the ICB, and for objective 4 the focus was at the field scale.

For the first objective, a nitrogen mass balance analysis was performed across the ICB to understand whether legacy N was accumulating in this watershed and if so, the magnitude of accumulation. The magnitude of N inputs, outputs, and storage in the watershed was quantified over 64 years (1949 – 2012) using the Net Anthropogenic Nitrogen Inputs (NANI) framework. The primary inputs to the system were atmospheric N deposition (9.2 ± 0.35 kg/ha/yr), fertilizer N application (48 ± 2 kg/ha/yr) and biological N fixation (49 ± 3 kg/ha/yr) and while the primary outputs from the system was net food and feed that was estimated as 42 ± 4.5 kg/ha/yr. The Net Anthropogenic Nitrogen Input (NANI) to the system was estimated to be 64 ± 6 kg/ha/yr. Finally, an estimated denitrification rate constant of 12.7 kg/ha/yr was used to estimate the

subsurface legacy nitrogen storage as 33.3 kg/ha/yr. This is a significant component of the overall mass budget and represents 48% of the NANI and 31% of the fertilizer added to the watershed every year.

For the second objective, the effect of crop yield calibration in increasing the robustness of the hydrologic model was analyzed. Using a 32,660 km^2 agricultural watershed in Iowa as a case study, a stepwise model refinement was performed to show how the consideration of additional data sources can increase model consistency. As a first step, a hydrologic model was developed using the Soil and Water Assessment Tool (SWAT) that provided excellent monthly streamflow statistics at eight stations within the watershed. However, comparing spatially distributed crop yield measurements with modeled results revealed a strong underestimation in model estimates (PBIAS Corn = 26%, PBIAS soybean = 61%). To address this, the model was refined by first adding crop yield as an additional calibration target and then changing the potential evapotranspiration estimation method -- this significantly improved model predictions of crop yield (PBIAS Corn = 3%, PBIAS soybean = 4%), while only slightly improving streamflow statistics. As a final step, for better representation of tile flow, the flow partitioning method was modified. The final model was also able to (i) better capture variations in nitrate loads at the catchment outlet with no calibration and (ii) reduce parameter uncertainty, model prediction uncertainty, and equifinality. The findings highlight that using additional data sources to improve hydrological consistency of distributed models increases their robustness and predictive ability.

For the third objective, the SWAT model was modified to capture the effects of nitrogen (N) legacies on water quality under multiple land-management scenarios. My new SWAT-LAG model includes (1) a modified carbon-nitrogen cycling module to capture the dynamics of soil N accumulation, and (2) a groundwater travel time distribution module to capture a range of subsurface travel times. Using a 502 km^2 SFIR watershed as a case study, it was estimated that, between 1950 and 2016, 25% of the total watershed N surplus (N Deposition + Fertilizer + Manure + N Fixation – Crop N uptake) had accumulated within the root zone, 14% had accumulated in groundwater, while 27% was lost as riverine output, and 34% was denitrified. In future scenarios, a 100% reduction in fertilizer application led to a 79% reduction in stream N load, but the SWAT-LAG results suggest that it would take 84 years to achieve this reduction, in

contrast to the two years predicted in the original SWAT model. The framework proposed here constitutes a first step towards modifying a widely used modeling approach to assess the effects of legacy N on time required to achieve water quality goals.

The above research highlighted significant uncertainty in the prediction of biogeochemical legacies -- to address this uncertainty in the last objective the field scale CENTURY model was used to quantify SON accumulation and depletion trends using climate and soil type gradients characteristic of the Mississippi River Basin. The model was validated using field-scale data, from field sites in north-central Illinois that had SON data over 140 years (1875-2014). The study revealed that across the climate gradient typical of the Mississippi River Basin, SON accumulation was greater in warmer areas due to greater crop yield with an increase in temperature. The accumulation was also higher in drier areas due to less N lost by leaching. Finally, the analysis revealed an interesting hysteretic pattern, where the same levels of SON in the 1930s contributed to a lower mineralization flux compared to current.

Acknowledgments

I would like to thank Nandita Basu, my supervisor, for invaluable support and guidance, without which this thesis would not have been completed. I also thank her for introducing me to the world of Nitrogen, a big step which enabled me to learn nutrient dynamics and management and acquire water quality modeling skills.

I would like to thank my committee members Bryan Tolson, Bruce MacVicar and Merrin Macrae for their time, support, and feedbacks.

Thanks to Michael Steiff and Kimberly J Van Meter for their support. I cherish those initial days when we three were the only students in the group. Thanks to other members of Basu Lab and special thanks to Tejasvi Hora and Shadman Chowdhury - I could not forget the endless technical and personal conversations we had about modeling, hydrology, psychology, and ethics. Thanks to my roommates Rahul Deshpande and Abhishek Singhi -my stay at Waterloo wouldn't be pleasant without you both.

Special thanks to my Master's supervisor, Krishnaveni Muthiah, for her help and support. I would like to thank Dhanesh Yeganantham for his ideas and support during job search and thanks to Sriniranjan Sridharan, Thirunavukkarasu and Soundararajan for their continuous support. You three were always there for me.

Finally, I would like to thank my mother and sister for relieving me from family responsibilities and supporting me to pursue my dreams.

Dedication

To my family

Table of Contents

List of Figures

List of Tables

Chapter 1: Introduction

1.1 Background

Nitrogen (N) is one of the essential nutrients that support life on earth (Keeney and Hatfield, 2008). It is consumed by living organisms for the production of bio-molecules such as carbohydrates, proteins, lipids, and nucleic acids. Abundant nitrogen (78%) in the atmosphere is in the form of inert di-nitrogen gas (N_2), which is not readily available for assimilation by living organisms. Plants can only make use of inorganic forms of N such as ammonium (NH_4^+) and nitrate (NO_3^-) from soil solution for their growth. The inert N_2 gas is converted into readily available inorganic N (NH_4^+) through the process of fixation. Fixation occurs naturally through lightning, lava flow, and forest fires or through biological nitrogen fixation, where symbiotic bacteria (Rhizobia) in the root nodules of certain crops fix N that can be utilized by the plants. Other types of N inputs that sustain plant growth are fertilizer application (mineral and manure) and atmospheric N deposition (wet depositions: ammonium, nitrate; dry depositions: ammonia, nitrous oxide, etc.). The readily available N (mineral form) contributed by fertilizers and atmospheric deposition are utilized for plant growth, and the rest is stored in the soil root zone. Apart from these inputs, the soil receives inputs from the dead roots and crop residues after the harvest. These inputs to the soil are mainly in organic form and are immobile, and not readily available for crop growth, though, the organic N in soil is subjected to decomposition, where the fresh residues are broken down into simpler organic compounds. The simpler organic compounds are then converted into ammonium ions (NH_4^+) through the mineralization process while the reverse process by which ammonium ions are converted into organic form by micro-organisms is referred to as immobilization. Mineralization and immobilization are controlled by factors such as crop residues, soil moisture content, and pH (Haynes, 1986; Bingner *et al.,* 2018). A portion of the ammonium ions is converted into nitrite and then subsequently the nitrites (NO_2^-) are converted into nitrates (NO_3^-). This process of conversion of ammonium ions into nitrate is known as nitrification. The nitrates stored in the soil stores are subjected to leaching through which the nitrate particles move to the groundwater stores. Also, the nitrates in the soil stores are subjected to denitrification process by which nitrates are converted into NO_2, N_2O, NO, and N_2 (gaseous atmospheric losses), when the soil is saturated for a long period, and

the oxygen is depleted. In addition to these atmospheric losses, another loss from the soil system, to the atmosphere, occurs through the volatilization process. The ammonium ion resulting from mineralization and fertilizer application could be converted into ammonia gas. Factors favoring volatilization may include high soil temperature, high pH, windy conditions, coarse soil texture, etc. (Johnson *et al.,* 2005).

Human modification of the Nitrogen (N) cycle has resulted in a twofold increase in fixation of reactive N compared with pre-industrial levels (Galloway *et al.,* 1995). This increase has primarily occurred through emissions from burning fossil fuels, fertilizer production, and leguminous crop production (Galloway *et al.,* 2004; Vitousek *et al.,* 1997). Use of inorganic fertilizers for crop production increased dramatically after the discovery of the Haber-Bosch process for producing ammonia at an industrial scale, allowing for large increases in crop productivity (Smil, 2011). The food produced as a result of inorganic N fertilizer use now feeds more than 45% of the world's population (Smil, 2011). High levels of N fertilizer use have now significantly perturbed the global N cycle, and it has been argued that planetary boundaries for maintaining human and ecosystem health have been exceeded by the intensive use of N in modern agriculture (Rockström *et al.,* 2009).

Excess nitrogen in the atmosphere (Chameides *et al.,* 1994) due to fossil fuel combustion, burning of biomass, and fertilizer use deteriorates air quality leading to reactive airway disease, asthma and cardiovascular diseases (Pope *et al.,* 2002). Increased inputs of N to water bodies have resulted in water quality impairment that degrades human and ecosystem health. For example, in the U.S, 10-20% of groundwater sources exceed the nitrate limit of 10 ppm adopted by the World Health Organization (Townsend *et al.,* 2003). Excess nitrate in drinking water causes methemoglobinemia ("blue-baby" syndrome) in infants (Vitousek *et al.,* 1997). In Iowa, rising groundwater nitrate levels have been found to increase the risk of bladder and ovarian cancer (Weyer *et al.,* 2001).

Increased anthropogenic N inputs have increased the riverine N flux by 11-fold in the North Sea region, by six-fold in Europe and by threefold in the North American region (Howarth, 1998). Increased N inputs to the marine environment have altered the coastal nutrient cycling and accelerated eutrophication and hypoxia globally (Moss, 2011). Increased N flux to

coastal and inland waters has accelerated eutrophication, reduced biodiversity through species loss, and significantly reduced the long-term coastal fish catch (Vitousek *et al.,* 1997). The inputs are expected to increase even further in the future to meet the food demands of a growing global population through intensive agriculture (Vitousek *et al.,* 1997).

1.2 Time Lags in Catchment Response

Recognition of the detrimental effects of nitrate has led to the adoption of various best management practices (BMPs) for improving water quality. However, these practices have not led to expected improvements in water quality. For example, in the USA, the Gulf of Mexico experiences a massive dead zone formation which spreads across 20,000 km^2 (during 1999), with a 5-year running average size of 10,000 km^2 (for 1996-2000). In 2001, the Watershed Nutrient Task Force (WNTF) developed an Action Plan calling for reduction in size (5 year running average) of the dead zone to less than 5,000 km^2, by implementing a series of best management practices (e.g. wetland restoration, creation of riparian buffer zones, growing cover crops and improved nutrient management strategies). Even though millions of dollars have been spent on reducing the size of the dead zone, during 2015 the average size was still around 15, 000 km^2 and the target has been pushed to 2035 (Van Meter *et al.,* 2018). Attempts have been made to reduce inorganic fertilizer inputs in United Kingdom watersheds since 1980 though no substantial decrease has been observed in riverine N concentrations (Howden *et al.,* 2010). Nutrient input reductions in four Northern European ecosystems have also failed to restore past ecological conditions (Duarte *et al.,* 2008). Recently, in the Yongan river watershed of China, stream N concentrations have been observed to increase progressively, despite a reduction in inorganic fertilizer inputs since 1999 (Chen *et al.,* 2014). The same trend was observed in the watersheds of Finland and Poland in 1990s (Fenton *et al.,* 2011).

A time lag, defined as the time between implementation of agricultural BMPs and improvements in stream water quality, is often recognized as an important factor behind the "apparent failure" of these stream improvement measures (Fenton *et al.,* 2011; Meals *et al.,* 2010; Van Meter & Basu, 2015). For example, Fenton *et al.* (2011) have stated that most water bodies in the European Union will not attain good water quality status by the targeted year 2015

due to the influence of lag times, although improvements will be seen within a 6-12 year time frame. Meals *et al.* (2010) in a data synthesis study found that time lags can range from 5 to more than 50 years as a function of watershed size, soil type, climate, and management practices. Time lag can be conceptualized as made up of two components: (a) a hydrologic time lag that arises from dissolved nitrate in the vadose zone and groundwater reservoirs that take their time to show up in the stream due to slow groundwater pathways, and (b) a biogeochemical time lag arising due to accumulation of soil organic N in the root zones of agricultural soils. While the existence of hydrologic time lags is well accepted, the recognition of the possibility of biogeochemical time lags for N is relatively recent (Burt *et al.,* 2010; Chen *et al.,* 2014a; Van Meter & Basu, 2015) and to date no work has been on using process-based models to explore these lag times.

1.3 Nitrogen Mass Balance Studies: Is there a Legacy?

To quantify lag times, it is necessary to understand the fate of N applied to the landscape. Several mass balance studies have attempted to quantify the fate of applied N in the agricultural landscapes (Howarth *et al.,* 1996; Goolsby *et al.,* 1999; Baker *et al.,* 2001; Bouwman *et al.,* 2005; Hong *et al.,* 2011, 2013). The most widely used method for N mass balance at the watershed scale is the Net Anthropogenic Nitrogen Inputs (NANI) method formulated by Howarth *et al.* (1996), which is the summation of Atmospheric N Deposition, Fertilizer N Application, Biological Nitrogen Fixation, and Net food and Feed Import / Export. Boyer *et al*. (2002) and Howarth *et al.* (1996) have used this approach for global watersheds and found that only ~ 25% of net inputs were exported as riverine N flux. So, what could be the fate of the remaining nitrogen? While it is well established that the remaining N is either denitrified or stored in subsurface reservoirs, the exact mass of this stored N is not well known (Galloway & Cowling, 2002). Indeed, in most mass balance studies, it is assumed that the rates of soil N mineralization (Goolsby *et al.,* 1999; Han & Allan, 2008), immobilization (Goolsby *et al.,* 1999), ammonia volatilization (Bouwman *et al.,* 2005; Boyer *et al.,* 2002) and denitrification (Goolsby *et al.,* 1999) balance each other so that there is no net N accumulation. However, recent work suggests that this might not be the best assumption (Galloway *et al.,* 2008; Van Meter *et al.,* 2013; Worrall *et al.,* 2015). One study, for example, found that even after accounting for denitrification and the groundwater store, 17% of nitrogen inputs were unaccounted for at a

global scale (Schlesinger, 2009). Worrall *et al.* (2015) estimated that even after accounting for groundwater N accumulation beneath the river Thames drainage basin in the UK, the unaccounted for N was 55 kg/ha/yr, which they attributed to soil accumulation.

1.4 Evidence of Soil Nitrogen Legacy

While the above-mentioned mass balance studies have attributed the missing N to soil N accumulation, very few studies have quantified the potential of agricultural soils to retain N in the soil. David *et al.* (2009) which measured the changes in soil organic carbon (SOC) and total nitrogen (TN) at 19 locations in central Illinois, revealed significant increases in C and N concentrations in the soil profile. This study had resampled the soils by depth (0-100 cm) in 2002, at sites that were previously sampled during 1957. The results showed no significant change in C and N concentration in the first soil layer (0-20cm), however, from 20-100 cm, there was a significant increase in C and N concentrations, reflecting the translocation of nutrients to lower depths. Overall the study documented an increase in C and N concentrations in the soil profile. More recently, Van Meter *et al.* (2016) analyzed long term soil data from 1957 to 2010, at 2069 sites in Mississippi River Basin, and estimated the accumulation of N in croplands as 25 – 70 kg/ha/yr. Also, the study analyzed the soil data from 61 sites across Iowa that were sampled in 1959 and again in 2007 and observed a net 14% increase in soil total N (1478 ± 547 kg/ha) over the study depth of 0 to 100 cm, due to high inputs from agriculture (**Figure 1.1**). Similar to these field measurements, (Yan *et al.,* 2014) has documented the increase in total soil N content in croplands of China. Based on the total soil N content, measured in 1393 cropland sites across China. Yan *et al.* (2014) have estimated a 5.1% increase in total soil N content between 1979-1982 and 2007-2008. While N accumulation is evident in the above field measurements and data analysis studies, long term Broadbalk Continuous Wheat experiments in Rothamsted (UK) also indicates legacy N accumulation under two fertilizer application scenarios: (i) over a period of 115 years (1852-1967), an experimental plot that received 35 t/ha of farmyard manure showed two-fold increase in total soil N content (Jenkinson *et al.,* 1982) and (ii) another plot that received mineral N fertilizer application of 144 kg/ha/yr, over a period of 140 years (1852-1992) has increased total soil N content by 21% (Glendining *et al.,* 1996). In addition to the field measurements and experimental studies, few mass balance and modeling studies at national scales (Leip *et al.,* 2011- Europe; Science Advisory Board, 2011- U.S; Clair *et al.,* 2014-

Canada) have indicated that the agricultural soils have retained 15-20% of the total N inputs to the system. Furthermore, the global scale mass balance and modeling studies (Galloway *et al.,* 2004; Fowler *et al.,* 2013; Zaehle S., 2013) suggests that the terrestrial ecosystem may be sequestering N in the order of 20-100 Tg-N/yr. These findings highlight the accumulation of nitrogen in agricultural soils.

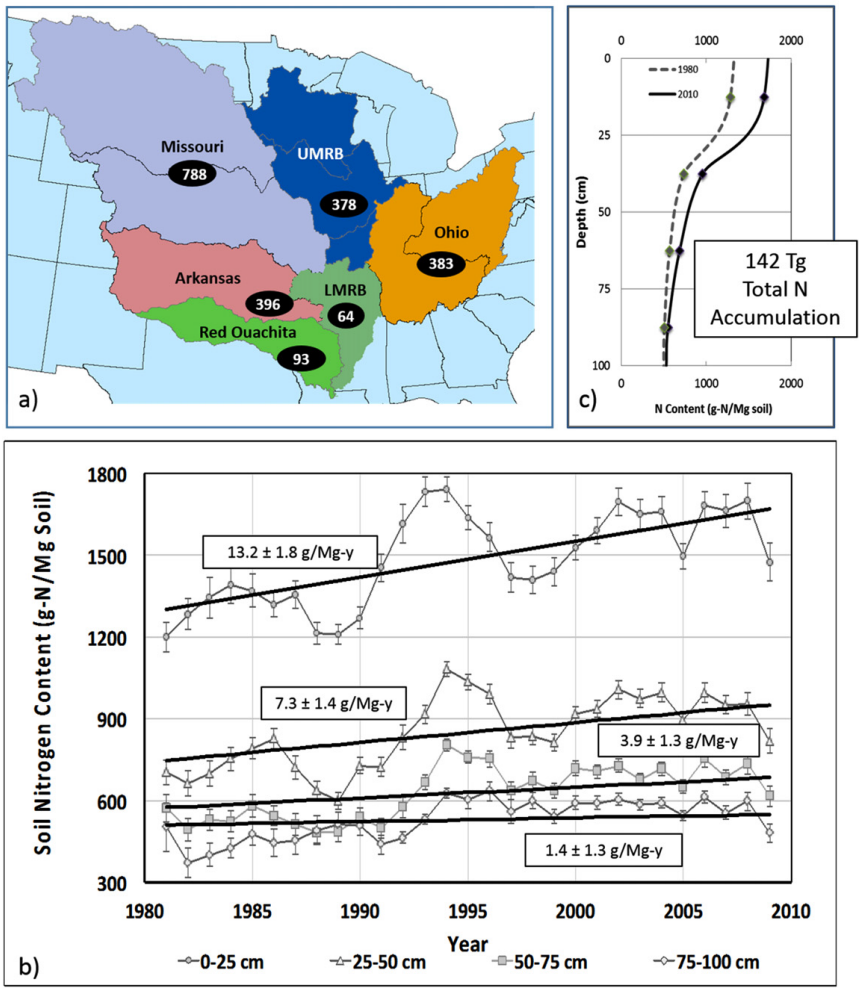

Figure 1.1. Accumulation of TN in agricultural soils across the MRB, 1980–2010, based on 2069 soil samples from the NCSS database. (a) The number of samples used for the TN analysis, by sub-basin. (b)TN accumulation rates for the four depth intervals (0–25 cm, 25–50 cm, 50–75 cm, 75–100 cm). Data points correspond to yearly means, and error bars to standard errors for the yearly means. Trend lines are obtained from multiple linear regression analysis of TN data. (c) Depth patterns of soil TN content in 1980 and 2010 reveal the greatest accumulation in the top 25 cm. Source: Van Meter *et al.,* (2016)

1.5 Modelling Nutrient Legacies and Time Lags

Despite the overall understanding that legacy nitrogen accumulation in soils and groundwater leads to lag times between implementation of best management practices and water quality improvement, most existing models can't predict these lag times. In the next section, the existing models, as well as some newer approaches that address legacy issues, are reviewed.

1.5.1 Brief Review of Existing Models: Capabilities and Gaps

In general, models that predict nutrient fluxes at stream outlet based on the inputs, land-use, and management practices are of three types: (i) empirical models (ii) conceptual and statistical models and (iii) process-based models, based on increasing complexity in process representations (Cherry *et al.,* 2008). Examples of empirical models are the (i) Export coefficient models and (ii) NANI based models. **Export coefficient models (ECM)** predict the nutrient loading in the stream network as function of export of nutrients from each of the sources (such as fertilizer application, atmospheric deposition etc.), in which the export coefficients (proportional nutrient loss from sources) are derived from literature review and field experiments (Johnes, 1996). Because of its simplicity and minimal data requirement, this approach has been used extensively by many studies (Mattikalli and Richards, 1996; Worrall and Burt, 1999; Ding *et al.,* 2010; Ma *et al.,* 2011) to estimate the stream nutrient export at watershed and regional scales (Alexander *et al.,* 2002).

Conceptual and statistical models include Spatially Referenced Regression on Watershed Attributes (**SPARROW**) and Geospatial Regression Equation for European Nutrient Losses (**GREEN**). SPARROW (Smith *et al.,* 1997) is a spatially explicit, statistical model that relates the total N and P riverine loads, with the nutrient sources (both point and nonpoint sources), stream-channel characteristics (channel depth and travel time) and watershed attributes (slope, soil permeability, percent wetlands etc.) (Preston *et al.,* 2011). SPARROW has been used at multiple scales, ranging from smaller watersheds to conterminous U.S. (Preston *et al.,* 2011) to understand (i) major sources of nutrients in the stream waters (ii) role of stream processes in nutrient delivery and (iii) impact of environmental factors on sediment export. The **GREEN** model is similar to SPARROW (Grizzetti *et al.,* 2008), and is a spatially explicit regression model but routes the N and P inputs from both diffuse and point sources to the outlet through the

internal sub-basins (Bouraoui and Grizzetti, 2014). Grizzetti *et al.* (2005, 2008) and Thieu *et al.* (2012) have used GREEN at the basin (Brittany) and continental scale (Europe) to predict the impact of various fertilizer and manure application scenarios on riverine nitrogen loads.

There is a wide variety of process-based models, with varying levels of complexity, including CENTURY, Environmental Policy Integrated Climate (EPIC) model, Hydrological Simulation Program – Fortran (HSPF), Annualized Agricultural Non-Point Source (AnnAGNPS), Soil Water Assessment Tool (SWAT) and MIKE-SHE. **CENTURY** is a plot scale, plant-soil-carbon interaction, biogeochemical model that predicts Nitrogen (as well as Carbon, Phosphorus, and Sulphur) dynamics in grassland, forest, and cropland systems at a monthly time-step (Parton *et al.,* 1988, 1993). CENTURY and its daily version, DAYCENT has been used extensively to analyze Soil Organic Carbon / Soil Organic Nitrogen dynamics (Parton *et al.,* 1988b, 1993; Del Grosso *et al.,* 2002) and estimate greenhouse gas emissions (Del Grosso *et al.,* 2002, 2005, 2008, 2009, 2011; Adler *et al.,* 2007; Davis *et al.,* 2012; Field *et al.,* 2016). **EPIC** is a field scale model that simulates hydrology, crop growth, nutrient cycling, and erosion processes, and runs at a daily time step. The model has the capability to estimate the SOC dynamics and impact of agricultural management practices changes on nutrients (Forster *et al.,* 2000; Izaurralde *et al.,* 2006, 2007; X. Wang *et al.,* 2006; Causarano *et al.,* 2008; Gaiser *et al.,* 2008; Balkovič *et al.,* 2011; Zessner *et al.,* 2017). **HSPF** (Bicknell *et al.,* 1996) is a semi-distributed, watershed scale model that includes hydrology, crop growth, and nutrient cycling processes in urban and agricultural landscapes. HSPF has multiple flow pathways such as surface runoff, lateral flow, and groundwater flow (Skahill, 2004). **AnnAGNPS** (Parsons *et al.,* 2004; Bingner *et al.,* 2018) is a distributed, watershed scale model that has hydrology, crop growth, and nutrient cycling processes modules. It simulates only surface runoff, lateral flow, and tile flow pathways and lacks groundwater component. Both HSPF and AnnAGNPS are being used widely for nutrient abatement strategy modeling (Suir., 2002; Shirinian-Orlando and Uchrin, 2007; Li *et al.,* 2012, 2017; Liu, 2015; Luo *et al.,* 2015) such as analyzing the impact of crop/land-use change, fertilizer application change, tillage practices change on nutrient loading. **SWAT** is a semi-distributed, watershed scale model that can simulate crop growth, hydrology, and nutrient cycling processes at a daily time step. It has multiple flow pathways (surface runoff, lateral flow, tile flow, and groundwater flow) and is used worldwide at various spatial scales (Arnold and

Fohrer, 2005; Gassman *et al.,* 2014). Due to its distributed and process-based nature, SWAT has been utilized for hydrological modeling, crop grow assessment, nutrient abatement strategies using agricultural Best Management Practices (BMPs), sediment transport estimation, land-use, and climate change and optimization and uncertainty analysis (Arnold and Fohrer, 2005; Krysanova and Arnold, 2008; Gassman *et al.,* 2014). **MIKE-SHE** is a physically based, distributed, fully integrated model that captures all components of the hydrological cycle. The model has multiple modules to simulate ET, channel flow, surface runoff, unsaturated zone flow, and saturated zone flow. It can be characterized with any desired spatial scale (grids) and offers multiple numerical solvers to simulate hydrologic and hydraulic processes based on the choice of lumped or fully distributed process representations (Frana, 2012; Butts and Graham, 2005; Hughes and Liu, 2008; Ma *et al.,* 2016).

Although empirical and statistical models like SPARROW and GREEN can estimate stream N loading at a watershed outlet, their ability to predict time lags instream responses induced by land-use changes are limited due to their inherent assumption of steady-state N in subsurface stores (Chen *et al.,* 2014b). Process-based field-scale models like CENTURY, EPIC and AnnAGNPS can predict field-scale SON accumulation and depletion but lack groundwater transport processes to capture hydrologic legacy. Watershed scale models like SWAT, HSPF, and MIKE-SHE have the groundwater transport processes; however, there has been no previous attempt to use them for time lag assessment. **Chapter 4** describes the modifications needed to achieve this goal.

1.5.2 New Modelling Frameworks to describe Legacy

In the recent past, a new modeling framework has been developed called the Exploration of Long Term Nutrient Legacies (ELEMeNT) model. This is a parsimonious, process-based model (Van Meter *et al.,* 2017) that couples SON accumulation and depletion dynamics in the soil profile with a travel time approach that includes the transformation and transport of nutrients in subsurface hydrologic pathways. Van Meter *et al.* (2017) applied this modeling framework at the Mississippi River Basin (MRB) and Susquehanna River Basin (SRB) to quantify the N legacies (both hydrological and biogeochemical) and time lags in stream nitrate response. Over 214 years (1800-2014), the modeling results highlight that soil legacies are dominant in MRB,

while groundwater legacies are dominant in SRB. Moreover, the study found that approximately 55% and 18% of the current annual N loads in the MRB and SRB are more than ten years old. Finally, the model predicted that if aggressive management strategies were implemented in MRB such that N application was achieved at 100% efficiency (all nitrogen applied was taken up by crops), it would take 35 years to achieve the 60% load reduction target suggested by the Gulf of Mexico Task Force.

Although the parsimonious process based ELEMeNT model developed by Van Meter *et al.* (2017) successfully captured the N legacies and time lags, it is difficult in the ELEMENT framework to estimate the impact of cropping pattern, soil texture and management changes (such as tillage) on SON dynamics and time lags. Thus, this thesis has focused on using widely accepted field-scale and watershed scale models, CENTURY and SWAT, to understand the accumulation and depletion of hydrologic and biogeochemical legacies as a function of climate, soil texture and land-use and land management.

1.5.3 Modelling Philosophy: Getting the right answers for the right reasons

One of the biggest limitations in describing water flow and solute transport through natural systems arises from a large number of unknown parameters that describe that physicochemical and biological processes, and the limited amount of measured data that the models are calibrated against. This leads to the problem of equifinality and non-uniqueness issues where multiple combinations of parameters can lead to similar streamflow and water quality responses at the catchment outlet (Basu *et al.,* 2010; Beven and Freer, 2001, Beven and Binley, 1992; Beven, 2006). Such models, if used to predict the future responses, will result in greater prediction uncertainties (Yen *et al.,* 2014).

An effective way of reducing equifinality and model prediction uncertainty is to include multiple data sources (Beven, 1993; Seibert and McDonnell, 2002) that govern the internal watershed processes in the model calibration. For example, spatially distributed soil moisture and crop yield data have been used in addition to streamflow measurements at the catchment outlet for model validation (Baumgart, 2005, Hu *et al.,* 2007). Kannan *et al.* (2007) and Nair *et al.* (2011) argued that the inclusion of crop growth components for calibration improves the

prediction efficiencies of the SWAT model. Furthermore, Cusack *et al.,* (1997), Yilmaz *et al.,* (2005), Spies *et al.,* (2014), Alazzy *et al.,* (2017), Hunink *et al.,* (2017), Ren *et al.,* (2018), Rajib *et al.,* (2016), & Qiao *et al.,* 2013, used spatially distributed rainfall, vegetation, soil moisture and Qiao *et al* 2013 & Seibert and McDonnell 2002 used field measured water table elevations in hydrological modeling to improve the model consistency.

The use of alternate data sources in improving the consistency of watershed models is a theme that runs through this thesis. Our overall hypothesis is that the inclusion of spatially distributed ancillary datasets like crop yield, and SON accumulation in soil and groundwater increases the consistency and predictive ability of hydrological and water quality models. In Chapter 3, we focused on modeling hydrology using SWAT, and show that including crop yield in model calibration increases model robustness, and improves the ability of the models to predict nitrate loads. In Chapter 4 and 5, we demonstrate the use of alternate sources of biogeochemical data, namely the build-up of soil organic nitrogen in the landscape to improve the robustness of water quality models.

1.6 Objectives

The overall objective of this research is to understand the N dynamics in agricultural landscapes and how stream nitrate responds to changes in land-use and management practices, with a specific focus on the role of legacy N stores in the landscapes in altering time lags between landscape changes and stream responses. This will be achieved through four closely related sub-objectives, as described below. This study focuses on Midwestern watersheds of the U.S.

Objective 1: Historical reconstruction of N data from 1949 to present, to quantify the fate of N Inputs, N output and legacy N storage in agriculture-dominated Midwestern US watershed, using a mass balance approach

Objective 2: Demonstrate the use of crop yield and flow partitioning data into model calibration to improve the hydrologic consistency and robustness of the SWAT model

Objective 3: Develop a framework to couple SWAT with the travel time distribution model to capture N accumulation in subsurface legacy stores (root zone and groundwater) and quantify time lags (combined biogeochemical and hydrologic time lags) for future land-use and management scenarios

Objective 4: Evaluate long term (> 100 years) SON accumulation and N leaching dynamics at the field scale, and understand how climate and soil texture control SON accumulation and depletion using the CENTURY model

1.7 Thesis Outline

The thesis has an introductory chapter (Chapter 1), four research chapters (Chapter 2 through 5) and a conclusion chapter (Chapter 6). **Chapter 2** focuses on the quantification of N dynamics, through a mass balance approach, in a 32,660 km^2 agricultural watershed in Iowa. The goal here was to quantify the magnitude of subsurface legacy nitrogen stores and develop input time-series that can be used in the SWAT model developed in Chapter 4. This is possibly the chapter that is further away from publication, but the results from here informed the watershed model. **Chapter 3**, which is to be submitted to *Hydrology and Earth System Sciences* (Ilampooranan, Schnoor, and Basu) demonstrates the value of using ancillary data (crop yield and flow partitioning) into model calibration to ensure proper representation of the internal watershed process and improve model robustness. **Chapter 4,** Ilampooranan *et al.* (2019), which was published in *Water Resources Research* (Ilampooranan, Van Meter and Basu) focuses on the development of a novel modeling framework (SWAT-LAG model) by coupling the SWAT model with a travel time distribution framework to capture biogeochemical and hydrologic legacies. The SWAT-LAG model is then applied to the South Fork Iowa River Watershed, a 502 km^2 watershed in the midwestern US, to ascertain lag times under various land-use and management scenarios. Finally, in **Chapter 5**, which is under preparation to be submitted to *Environmental Research Letters* (Ilampooranan, Van Meter and Basu), we delve deeper to understand the fate of soil organic nitrogen accumulation under changing the climate, land-use and management practices by using the field-scale carbon-nitrogen cycling model CENTURY.

Chapter 2: Estimation of Legacy Nitrogen Storage in Agricultural Landscapes using data synthesis approach

2.1 Abstract

Massive land-use changes and the industrial production of fertilizers have increased food production but at the cost of significantly altering the global nitrogen (N) cycle. Increased N concentrations in surface and groundwater bodies have severely affected human and ecosystem health. Best management practices implemented to improve water quality have generally met with limited success. Such lack of success can be attributed to the increased buildup of legacy N stores in the subsurface, that act as an additional source even when N inputs have been reduced. It is critical to understand the magnitude of such legacy stores, and their timescales of accumulation/depletion to predict water quality impacts following land-use shifts. Here, we propose a data synthesis framework to understand and quantify the magnitude of legacy stores and their timescales of accumulation/depletion in a 32,660 km^2 agricultural watershed in Eastern Iowa, the Iowa Cedar Basin. The magnitude of N inputs, outputs, and storage in this watershed over 64 years (1949–2012) was quantified using the Net Anthropogenic Nitrogen Inputs (NANI) framework. Inputs to the system, Atmospheric N Deposition, Fertilizer N Application and Biological N Fixation were estimated as 9.2 ± 0.35, 48 ± 2 and 49 ± 3 kg/ha/yr and outputs, Net Food and Feed, was estimated as 42 ± 4.5 kg/ha/yr, leading to Net Anthropogenic Nitrogen Input (NANI) as 64 ± 6 kg/ha/yr. Using the estimated values of riverine N export (18 kg/ha/yr) and denitrification (12.7 kg/ha/yr), we found that a significant portion of N (33.3 kg/ha/yr) was retained in the subsurface stores.

2.2 Introduction

Human activities over the last century have resulted in a twofold increase in nitrogen fixation in the terrestrial ecosystem through fossil fuel combustion, fertilizer production and cultivation of nitrogen-fixing crops (Galloway *et al.,* 1995, 2004; Vitousek *et al.,* 1997). Indeed, the inputs are expected to increase in the future to meet the growing demand for food (Vitousek *et al.,* 1997). Increased N inputs have significantly deteriorated water bodies and affect human and ecosystem health. To understand the fate of N in the agricultural system several studies (Bouwman, 2005; Howarth *et al.,* 1996; Goolsby *et al.,* 1999; Baker *et al.,* 2001; Han and Allan,

2008; Hong *et al.,* 2011, 2013; Hong, 2012) have quantified N by employing different mass balance frameworks. Within which the Net Anthropogenic Nitrogen inputs (NANI) framework introduced by Howarth *et al.* (1996) has been most commonly used to understand the fate of reactive N. NANI is estimated commonly as the summation of the four major components: (i) fertiliser application (ii) fixation by leguminous crops (iii) atmospheric deposition and (iv) net food and feed imported or exported. The NANI framework since then has been used most extensively using agricultural census and other databases. For example, Boyer *et al.,* (2002) used this framework in the 16 Northeastern U.S. watersheds and observed an average net N input of 30.8 kg /ha/yr. David *et al.* (2010) had found that the net N inputs to the Mississippi river basin have averaged 18.3 kg/ha/yr for the period 1997 to 2006.

Out of the total NANI, only a certain fraction shows up as a riverine output. Studies at large scale show this fraction to be around 25% for 14 major regions draining to the North Atlantic Ocean (Howarth *et al.,* 1996) and the same fraction was observed for 16 Northeastern U.S. watersheds (Boyer *et al.,* 2002). At the local scale, this fraction can be quite variable. Hong *et al.* (2013) analyzed the regional variation of NANI and riverine N flux by grouping 106 U.S. watersheds into five groups. The fraction of NANI exported by rivers varied from 25 to 35 due to regional variation in climate, discharge, and presence of tile drains. David and Gentry (2000) reported a high value, 51%, for Illinois rivers.

While it is well established that a fraction of NANI leaves the watershed as riverine N flux, the fate of the remaining NANI is mostly unknown (Galloway *et al.,* 2004). David and Gentry (2000), David *et al.* (2009) and Drinkwater *et al.* (1998) argues that there was no significant change in soil SON levels and assumes that the missing N in their studies was attributed to denitrification. However, Van Meter *et al.* (2016) has emphasized that a certain fraction of the inputs get stored in the soil as organic N. Van Meter *et al.* (2013) analyzed soil databases in Iowa and Illinois and found that soil organic N accumulates in the root zone of agricultural soils in fields under intensive agriculture. Similarly, Chen *et al.* (2014) highlighted the increase in soil organic nitrogen levels in Yongan River Watershed in Eastern China. Thus, in this study, the following questions were answered: (i) whether soil organic nitrogen accumulates in agricultural landscapes of Iowa and (ii) if it accumulates, what is the magnitude

of legacy N stores. The NANI based mass balance approach was used to understand the fate of missing N.

2.3 Site Description

The Iowa-Cedar Basin (ICB) which covers an area of 32,660 km^2, was selected as the study site. The ICB is drained by the Iowa and Cedar rivers, two major tributaries of the Mississippi River in the U.S. **(Figure 2.1)**. The ICB extends from southern Minnesota to the confluence with the Mississippi River at New Boston (downstream of Port Louisa). The region has a humid continental climate with cold winters and hot and humid summers. The average annual temperature is 10 ºC (ICRB Report, 2010), and the mean annual rainfall is approximately 864 mm (Seo *et al.,* 2013). Heavy rainfall occurs during spring and snowmelt events that often lead to flooding.

The Iowa landscapes, primarily tallgrass prairies, wetlands, and forests, were transformed into agricultural lands beginning in the 1850s (ICRB Report, 2010). Today the land is under intensive agriculture with predominantly corn and soybean crops, covering an area of ~73% of the Iowa Cedar Basin. The remaining area of the basin is in pasture and rangelands (11.7%), forests (3.4%), wetlands and water bodies (3.3%), and urban areas (8.7%). The intensive agriculture in Iowa has required excessive fertilizer application that has led to degraded water quality (Davis *et al.,* 2014). ICB has been ranked as one of the highest contributors of nutrients and sediments to the Upper Mississippi River Basin, causing Gulf Hypoxia (Davis *et al.,* 2014; ICRB Report., 2010). The nutrient concentration at the outlet of ICB has been slightly increasing between 1980 and 2008 (Sprague *et al.,* 2011). Furthermore, ICB exhibits annual flow normalized nitrate concentration levels of 4.8 mg/l, which is the one of the highest compared to other sites in the Mississippi River Basin (Murphy *et al.,* 2013). These factors make it important to study this watershed for developing nutrient reduction strategies.

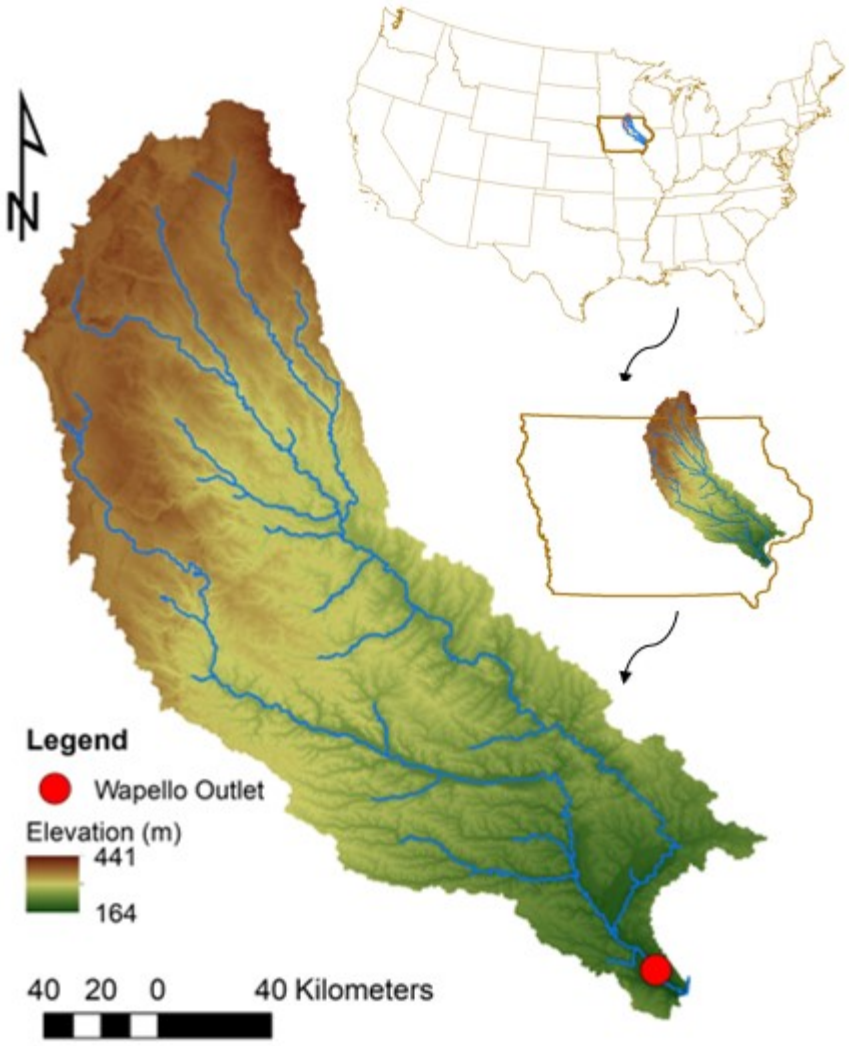

Figure 2.1. Location of Iowa Cedar Basin and Wapello Outlet for which discharge and nitrate concentration was measured

2.4 Methods

2.4.1 Historical reconstruction of nutrient budgets to estimate temporal trends in Net Anthropogenic N Inputs over the Iowa Cedar Basin (1949-2012)

The Net Anthropogenic Nitrogen Input (NANI) was estimated as the summation of atmospheric N deposition, fertilizer N application, agricultural N fixation, and net food and feed imports, following the approaches of Howarth *et al.* (1996) and Hong *et al.* (2013). Data required

for this study, such as fertilizer application, atmospheric deposition, human population, animal count, crop harvested area and crop yield for the period 1949 to 2012 (see **Table 2.1** for data sources), were collected at county scale (35 counties) and aggregated to watershed scale based on the area proportions i.e. based on the ratio of the watershed area over the county area. Ten crop types and nine animal groups were considered for Net Food and Feed component, and analysis was performed in MATLAB & ArcGIS at a yearly time step. Please refer the **Table 2.1** for details on data sources and spatiotemporal resolution of NANI components.

The NANI was estimated as the difference between total N inputs and total N outputs of the system. Total inputs include atmospheric N deposition (amount of N in rainfall), fertilizer N application (inorganic fertilizer applied for crops), agricultural N fixation (biological nitrogen fixation by leguminous crops) and human and animal consumption (amount of N present in human food and animal feed). Total N outputs include crop N production (nitrogen removed in crop harvest) and animal N production (amount of nitrogen in animal products, i.e., in the form of meat). Sewage and animal wastes (manure) are not considered as new inputs as they represent redistribution or recycling of nitrogen within the region (Howarth *et al.,* 1996). NANI was estimated as

$$NANI = DEP + FERT + FIX +/- NFF \quad \text{(Eq. 2.1)}$$

Where NANI is the Net anthropogenic nitrogen input (kg/ha/yr), *DEP* is the N in atmospheric deposition (kg/ha/yr), *FERT* is the N in inorganic fertilizer applied (kg/ha/yr), *FIX* is the N fixed by the crops (kg/ha/yr) and *NFF* is the N in net food and feed for humans and animals (kg/ha/yr). A schematic of this framework is presented in **Figure 2.2.**

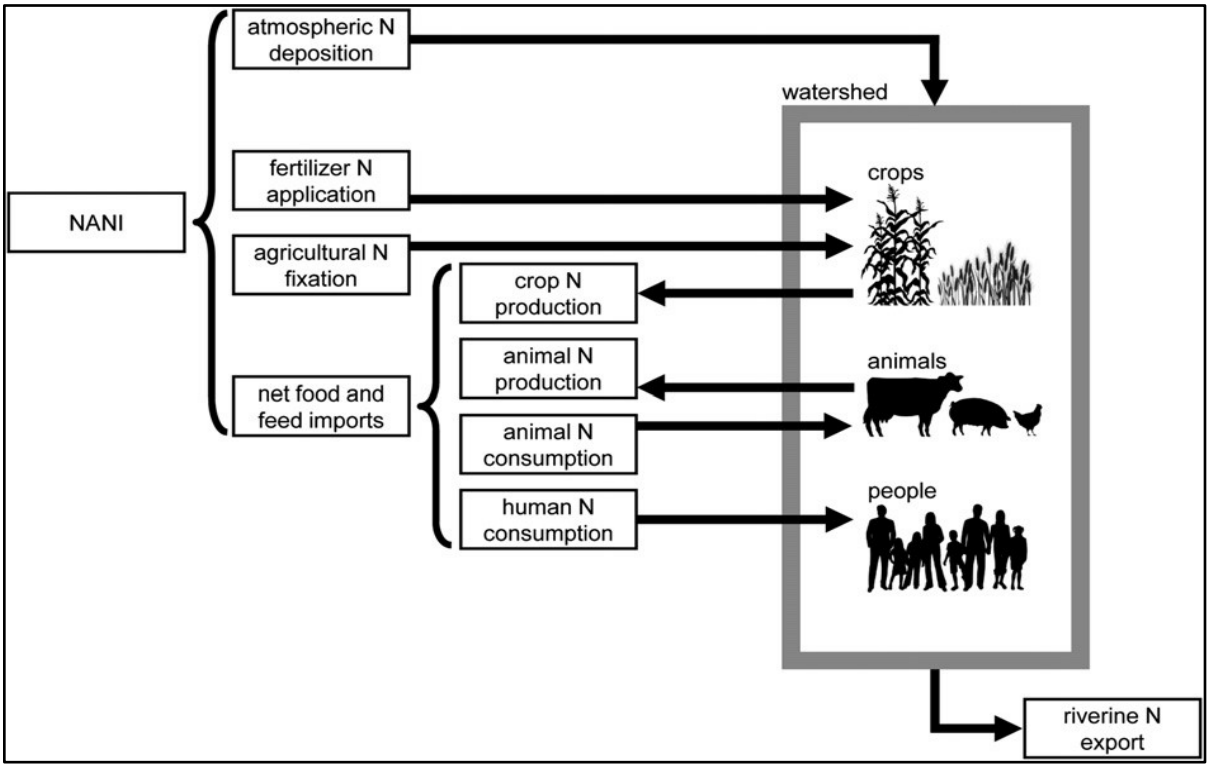

Figure 2.2. Schematic representation of NANI analysis (Howarth *et al.,* 1996)

Table 2.1. Summary table with the data type, source and spatiotemporal resolution of data for each component of NANI

NANI Components		Data Type	Data Sources	Temporal Resolution	Spatial Resolution
Atmospheric N Deposition		NOx (oxidized forms of N)	1949 to 1984, Dentener (2006) 1985 to 2012, NADP[1]	1949 to 2012 (annual data corresponding to census years were selected)	Station data
Fertilizer N Application		Annual N Fertilizer applied	Alexander and Smith (2000) USGS[2] (2012)	1949 to 2012 (every five years)	County-scale
Biological N Fixation		Crop production	Census of Agriculture, USDA[3]	1949- 2012 (every 5 years)	County-scale
		Crop harvested area	Census of Agriculture, USDA	1949 to 2012 (every five years)	County scale
Net food and Feed	***Crop N Production***	Crop production	Census of Agriculture, USDA	1949 to 2012 (every five years)	County scale
	Animal N Production	Animal inventory	Census of Agriculture, USDA	1949 to 2012 (every five years)	County scale
	Animal N Consumption	Animal inventory	Census of Agriculture, USDA	1949 to 2012 (every five years)	County scale
	Human N Consumption	Human population	U.S. Census Bureau	1949 to 2012 (annual data corresponding to census years were selected)	County scale

1-National Atmospheric Deposition Program,
2United States Geological survey and
3-United States Department of Agriculture

(i) Atmospheric N Deposition:

Only oxidized N (NO_X) is considered for analysis and reduced forms of nitrogen (NHx, i.e., ammonia and ammonium) were excluded based on the assumption that emissions from manure will get re-deposited in large watersheds (Howarth *et al.,* 1996). For the period 1985 to 2012, atmospheric N deposition data were obtained from NADP (2014) for four stations in and around Iowa and spatially interpolated in ArcGIS to obtain county scale deposition values. The NADP dataset is based on weekly precipitation samples that were collected and analyzed for nitrate, ammonium and other constituents at the NADP Central Analytical Laboratory, operated by Illinois State Water Survey in Champaign, Illinois. The point location of those sites was populated in ArcGIS for corresponding years and interpolated to get 250 m resolution grid cells that contain the atmospheric N deposition values. County scale annual deposition values were obtained by calculating the mean deposition rate of grid cells within the county boundary. Finally, county scale values were converted into watershed-scale values based on the area proportions. For the years before 1985, data was obtained from Dentener (2006) that provided global scale N deposition values.

(ii) Fertilizer application:

County-level fertilizer (kg/ha/yr) inputs were obtained from the United States Geological Survey (USGS) reports. In particular, data from 1949 to 1985 were obtained from Alexander and Smith (1990) and from 1985 to 2007, USGS (2012) data were used. The data obtained from Alexander and Smith (1990) and USGS (2012) were based on state-level fertilizer sales values that were disaggregated to county level values using (a) the county and states' fertilized acreage from 1949 to 1985 and (b) the county and states' expenditure on fertilizers from 1985 to 2012.

(iii) Biological Nitrogen Fixation:

The three major crops that perform biological nitrogen fixation in the Iowa Cedar Basin are soybeans, alfalfa hay, and non-alfalfa hay. Biological nitrogen fixation for soybeans and alfalfa hay was computed using yield based method (Hong *et al.,* 2013), as follows

$$FIX = FIX_{(\text{soybean \& alfalfa hay})} + FIX_{(\text{other hay})} \quad \text{(Eq. 2.2)}$$

$$FIX_{(soybean\ \&\ alfalfa\ hay)} = H * c * D\% * N\% * p\% * (1+b) \quad \text{(Eq. 2.3)}$$

Where $FIX_{(soybean\ \&\ alfalfa\ hay)}$ is the biological nitrogen fixation for soybean and alfalfa hay (kg/ha/yr), *H* is the harvested quantities (yield) reported in Census of Agriculture, United States Department of Agriculture (bushels), *C* is the conversion factor (from bushels to kg), *D* is the percent dry matter, *N* is the percent N in dry matter, *p* is the percent of harvested N that can be attributed to fixation, and *b* is the ratio of non-harvested N to harvested N. The *p* values adopted from Hong *et al.* (2013) for soybeans, and alfalfa hay is 74% and 82% respectively. The term b accounts for below-ground biomass nitrogen fixation, and the value adopted from Hong *et al.* (2013) was 50%. For non-alfalfa hay, area-based fixation was followed based on Hong *et al.* (2011):

$$FIX_{(other\ hay)} = A * n \quad \text{(Eq. 2.4)}$$

where $FIX_{(other\ hay)}$ is the biological nitrogen fixation for non-alfalfa hay (kg/ha/yr), A is the non-alfalfa hay harvested area (ha) and n is the fixation rate for non-alfalfa hay (117 kg/ha/yr, adopted from Hong *et al.* (2011)).

Harvested quantity (H) and harvested area (A) of crops were obtained from Census of Agriculture, United States Department of Agriculture from 1949 to 2012 (in a 5-year time interval) at the county scale. Biological nitrogen fixation rates were calculated using equations 2.2 to 2.4 and crop parameters D, and N in equations 2.3 and 2.4 were adopted from Hong *et al.* (2011) and Hong *et al.* (2013) (**Table 2.2**).

Table 2.2. Crop nitrogen parameters for NANI analysis, adapted from Hong *et al.* (2013)

			D	N	p_{human}	p_{animal}
Crops	**Yield Unit**	**Kilograms harvested per yield unit**	**Percent dry matter**	**Percent N in dry matter**	**Percent distributed to human**	**Percent distributed to animal**
Corn for Grain	Bushels	25.4	86.70%	1.64%	4%	96%
Corn for Silage or Green Chop	Green tons	907.2	28.40%	1.25%	0	100%
Sorghum for Grain or Seed	Bushels	25.4	89.40%	1.96%	0	100%
Soybeans for Beans	Bushels	27.2	90.60%	6.54%	2%	98%
Wheat for Grain	Bushels	26.1	88.50%	2.15%	61%	39%
Oats for Grain	Bushels	14.5	89.40%	2.05%	6%	94%
Barley for Grain	Bushels	21.8	88.90%	2.11%	3%	97%
Rye for Grain	Bushels	25.4	88.10%	2.17%	17%	83%
Alfalfa Hay	Dry tons	907.2	90.40%	2.79%	0	100%
Other Hay	Dry tons	907.2	86.70%	1.27%	0	100%

(iv) Net Food and Feed:

Net food and feed were calculated as the difference between human and animal nitrogen consumption and production as described below:

$$NFF = (C_A + C_H) - (P_{CA} + P_{CH}) - P_A \quad \text{(Eq. 2.5)}$$

Where NFF is the net food and feed (kg/ha/yr), C_A is animal N consumption (kg/ha/yr), C_H is human N consumption (kg/ha/yr), P_{CA} is crop N production distributed to animals (kg/ha/yr), P_{CH} is crop N production distributed to humans (kg/ha/yr), and P_A is animal N production (kg/ha/yr). It is assumed that the crops produced (P_{CA} & P_{CH}) in the watershed are consumed by the humans (C_H) and animals (C_A) in the watershed and the crop N production exceeding human and animal consumptions will be exported out of the watershed. Estimation of these subcomponents of NFF are described below

Animal and Human N consumption (C_A & C_H): The equations for calculating animal and human N consumption (Hong *et al.,* 2011) are as follows:

$$C_A = A_A * I_A \quad \text{(Eq. 2.6)}$$

$$C_H = A_H * I_H \quad \text{(Eq. 2.7)}$$

Where C_A is the animal N consumption (kg/ha/yr), A_A is the animal inventory. Animal inventory data for the six animal groups (beef cows, milk cows, hogs & pigs, sheep & lambs, chicken, and turkeys) were obtained from Census of Agriculture, United States Department of Agriculture. I_A (kg/animal/yr) is the parameter for animal N intake (Hong et al., 2011) (refer **Table 2.3**). Human consumption (C_H, in kg/ha/yr) was calculated by multiplying population (A_H, obtained from the United States Census Bureau) by the estimated human N intake rate I_H, 5 kg/person/yr (Boyer *et al.,* 2002; Hong *et al.,* 2011).

Table 2.3. Animal nitrogen requirement parameters used in Animal N consumption calculation, adopted from Hong *et al.* (2011)

	I_A	**E_A**
Animal groups	**Animal N intake (kg/animal/yr)**	**N in animal excretion (kg/animal/yr)**
Beef Cows	66.75	58.51
Milk Cows	156	121
Hogs and Pigs	8.51	5.84
Sheep and Lambs	5.97	5
Chickens	0.84	0.55
Total Turkeys	0.62	0.39

Crop N production distributed to animals and humans (P_{CA} & P_{CH}): Amount of N present in harvested crops is calculated as

$$P_{CA} = H * c * D\% * N\% * p_{animal}\% * 0.9 \quad \text{(Eq. 2.8)}$$

$$P_{CH} = H * c * D\% * N\% * p_{human}\% * 0.9 \quad \text{(Eq. 2.9)}$$

Where P_{CA} & P_{CH} are the crop N production distributed to animals and humans respectively (kg/ha/yr), H is the harvested quantities (yield) reported in Census of Agriculture, United States Department of Agriculture (bushels or tons), C is the conversion factor (from bushels or tons to

kg), D is the percent dry matter, N is the percent N in dry matter, p_{animal} and p_{human} are percent crop N distributed to animals and humans respectively **(Table 2.2).** A loss of 10% of crop N production during storage and processing, due to spoilage, consumption by insects and vermin were considered based on Hong *et al.* (2011). Ten crop groups (corn for grain, corn for silage, sorghum, soybean, wheat, oats, barley, rye, alfalfa hay, and other hay) were considered for analysis, and the crop yield data were obtained from the Census of Agriculture, United States Department of Agriculture at county scale from 1949 to 2012.

Animal N Production (P_A): Animal N production is calculated as the difference between animal N consumption (C_A) and animal N excretion (E_A), as follows:

$$P_A = (C_A - (A_A * E_A)) * 0.9 \quad \text{(Eq. 2.10)}$$

Where P_A is the animal N production in the form of meat and dairy products (kg/ha/yr), C_A is the animal N consumption (kg/ha/yr), A_A is the animal inventory. C_A and A_A were obtained from equation 2.6 and 2.7. E_A (kg/animal/yr) is the parameter corresponding to the N in animal excretion for each animal group **(Table 2.3).** A 10% loss of N is assumed for the animal production term due to losses incurred in the processing of animal products.

2.4.2 Uncertainty analysis

The parameters governing the NANI estimation though obtained from published literature were subject to variation. For example, different parameters for computing soybean fixation rates were adopted by Bouwman *et al.* (2005), David *et al.* (2009), and Hong *et al.* (2013) that led to a range of NANI values. In addition to the input parameters, the input data might also have uncertainty. To account for these variations in input parameters and input data, an uncertainty analysis was performed using Monte-Carlo simulation following Chen *et al.* (2014). Based on Chen et al (2014) and (Zhang, 2016), a normal distribution with coefficient of variation of 0.3 was assumed for each of the input parameters (mentioned in **Table 2.2 and Table 2.3**) and also for the input data (crop yield, animal count etc.,), resulting in 10,000 randomly generated NANI, Atmospheric N deposition, Biological N Fixation, Fertilizer N Application and Net Food and Feed for each year. The interquartile range (75^{th} percentile minus

25th percentile) obtained from 10, 000 Monte-Carlo runs was used to highlight the input and parameter uncertainty and the median values (50th percentile) were used for further analysis

2.4.3 Estimation of riverine N flux using WRTDS

Monthly nitrate concentration data for the Wapello outlet of ICB was obtained from USGS (2016) from 1977 to 2012 and Weighted Regression on Time Discharge and Season (WRTDS) model was used to obtain the daily nitrate concentration data from which annual nitrate flux data was estimated. The WRTDS model estimates daily nitrate concentration using the following equation

$$\ln(c) = \beta_o + \beta_1 t + \beta_2 \ln(Q) + \beta_3 \sin(2\pi t) + \beta_4 \cos(2\pi t) + \epsilon \qquad \text{(Eq. 2.11)}$$

where, c is concentration (mg l^{-1}), β_o to β_4 are fitted regression coefficients, Q is daily discharge (m^3 s^{-1}), t is time and ϵ is an error term. The WRTDS estimated daily nitrate concentration values were closer to observed values, with a flux bias statistic of 1.3%

2.5 Results and Discussion

2.5.1 Temporal trends of N fluxes and NANI

Nitrogen fertilizer application rate has increased from 1950 till 1982, at a rate of 10 ± 0.4 kg/ha/yr **(Figure 2.3)**. Such an increasing pattern in fertilizer application can be attributed to (i) the rapid increase in fertilizer production that took place after World War II and (ii) growing demand for food grains, during 1950s and 1980, leading to usage of high yielding, fertilizer intensive crop varieties (Ruddy *et al.,*2006; Cao *et al.,* 2018). After the peak usage in 1980, the fertilizer trends were stable till the early 2000s, following the corn acreage trend (USDA-Agricultural Census, 2012). From the early 2000s, there was a shift in corn acreage in Iowa, driven by the growing demand for corn-based biofuel (Green *et al.,* 2014). Due to the increase in corn prices, most productive lands in Iowa were put under continuous corn rotation in contrast to the conventional corn-soybean rotation (Secchi *et al.,* 2011). Increases in corn acreages at the expense of soybean acreages, since the early 2000s, lead to an increase in usage of commercial fertilizers by 57% when compared to 1950-1982 magnitudes.

Biological nitrogen fixation trend has also been increasing consistently since the 1950s due to the adoption of high yielding soybean varieties and increase in soybean acreages. Soybean acreages and yield have increased continuously since the 1950s till 2002, which in turn increased the biological nitrogen fixation magnitudes at a rate of 6 ± 0.5 kg/ha/yr. Since 2002, a significant reduction in soybean acreages occurred due to increasing land under corn for biofuels. This has reduced the biological nitrogen fixation magnitudes by 20%.

Finally, atmospheric nitrogen fixation values have remained relatively stable from 1950 to 2012, with an average magnitude of 9.2 ± 0.35 kg/ha/yr. The main N outputs from the system include crop and livestock production. In the NANI framework, the net food and feed (NFFI) indicate the food and feed produced that is in excess of the internal demand. The NFFI is zero till 1959 and then increases from 1959 till 2007 at a mean rate of -9 ± 5 kg/ha/yr.

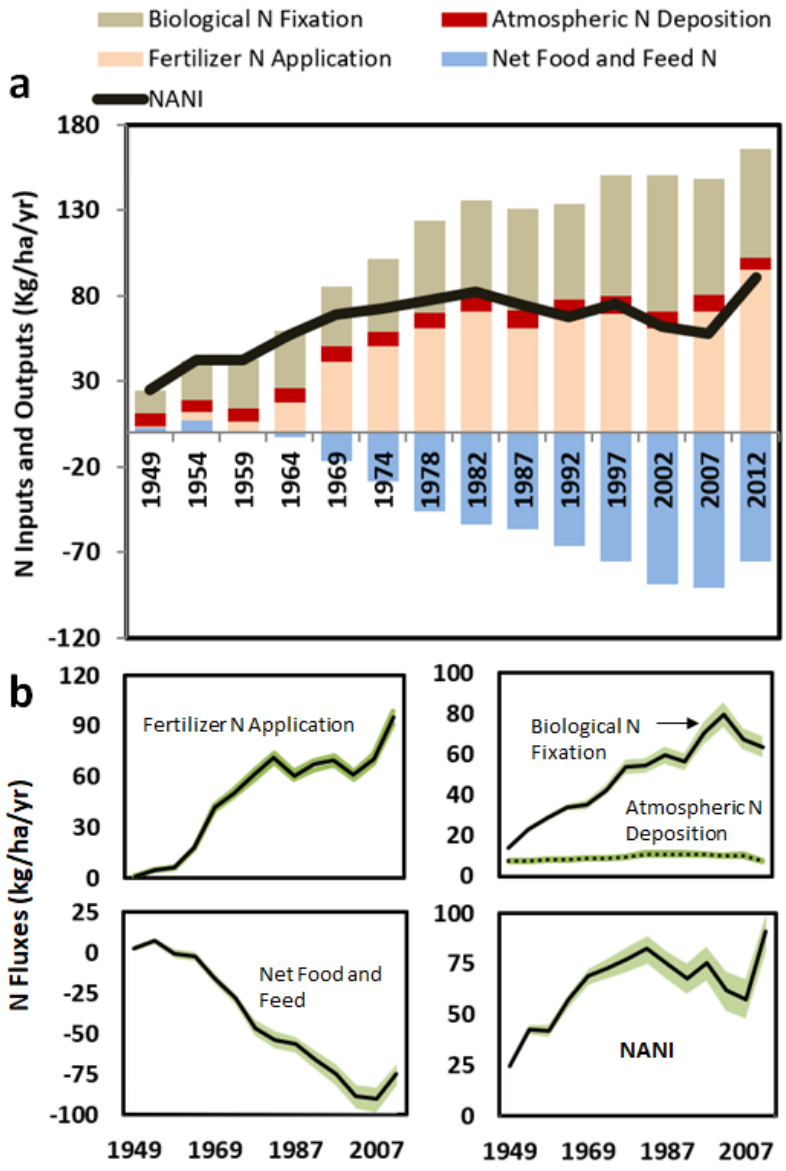

Figure 2.3. Temporal trend of Biological Nitrogen Fixation, Atmospheric Nitrogen Deposition, Fertilizer Nitrogen Application, Net Food, and Feed and Net Anthropogenic Nitrogen Input (NANI), for Iowa Cedar Basin from 1949 to 2012 (a). Values shown in the plots are the median values of 10,000 Monte-Carlo simulations. The interquartile range (green shaded area) and median (solid and dotted black lines) of individual NANI components were obtained from 10,000 Monte-Carlo simulations (b).

The Net Anthropogenic Nitrogen Inputs (NANI) increased from 1950 to 1982 due to an increase in fertilizer application, N fixation, and atmospheric deposition. However, from 1982 to 2007, though the biological N fixation has increased slightly (at a rate of 2.7 ± 0.3 kg/ha/yr), N fertilizer application has remained approximately constant while there was a substantial increase in net food and feed, at a rate of 7.3 ± 0.3 kg/ha/yr (**Figure 2.3**). This can be attributed to the use of higher-yielding crop varieties that are more efficient at harnessing fertilizer and soil N. Finally, there is an increase in NANI from 2007 – 2012 – this can be attributed to an increasing fertilizer application rates to meet biofuel demand driven corn production, coupled with 2012 being a drought year that led to decreased crop production (Rippey, 2015). Despite these annual trends, there was an overall significant decrease in NANI from 1977-2012.

2.5.2 River N Concentrations and Quantification of legacy N stores

The analysis of riverine N flux at the Wapello station (outlet of ICB) shows that there is a decreasing trend from 1977 to 2012 **(Figure 2.5).** This can be attributed to the decreasing trend in the NANI. The average annual NANI over the 50 years was estimated as 64 ± 6 kg/ha/yr, while the annual average riverine N flux was estimated as 18 kg/ha/yr.

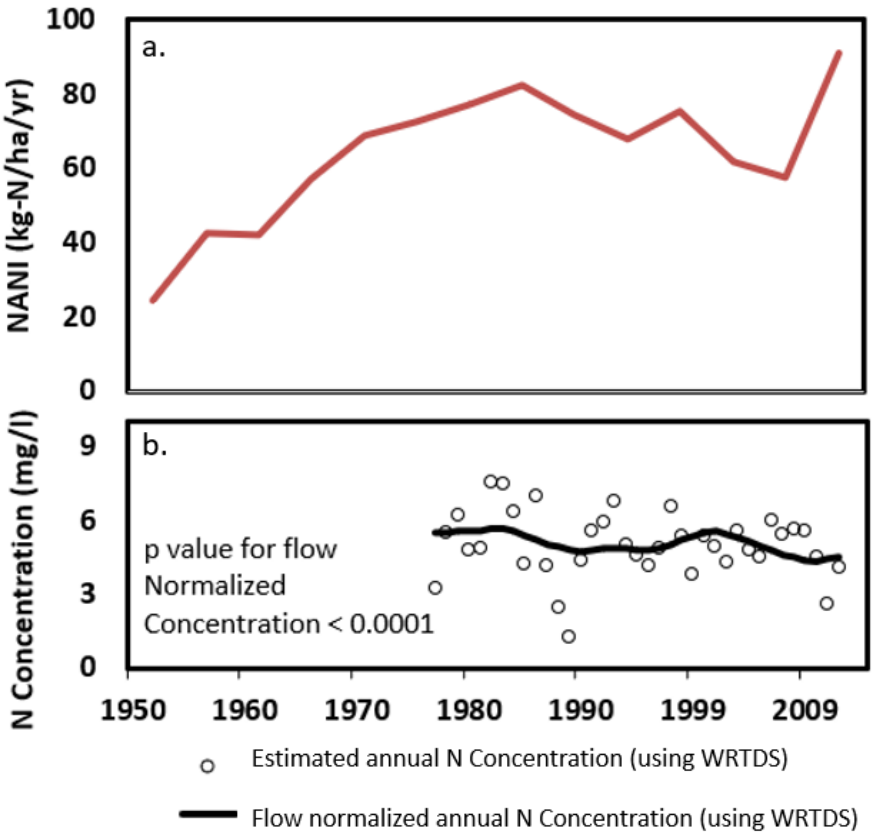

Figure 2.5. Net Anthropogenic Nitrogen Input (NANI) and mean annual riverine N flux from 1950 to 2012. (a) NANI decreasing significantly ($p<0.001$) from 1977-2012 (b) Circles: Observed nitrate concentration, Solid black line: Modelled riverine N flux using WRTDS method from 1977 to 2012

It is well known that the remaining nitrogen is either lost to denitrification or accumulates as legacy N stores in the landscapes. Denitrification fluxes at the landscape scale are difficult to quantify due to their great temporal and spatial variability and limitations in the measurement techniques to quantify the nitrous oxide and di-nitrogen gas fluxes due to the abundance of di-nitrogen gas in the environment (Groffman *et al.,* 2006). Following the uncertainty prevailing in the estimation of denitrification fluxes, David *et al.* (2009) performed a multi-modeling study to simulate the denitrification potential in a Central-Illinois watershed, which is similar to ICB in-terms of land-use, management practices, and weather. We used the David *et al.* (2009) value of 12.7 kg/ha/yr in this study and estimated legacy nitrogen as 33.3 kg/ha/yr (**Figure 2.6 and 2.7**). The estimated subsurface legacy N store (organic N in the root zone + dissolved nitrate in the

groundwater and soil water) value of 33.3 kg/ha/yr is close to the total soil organic nitrogen accumulation magnitude outlined in Van Meter *et al.* (2016) for Iowa soils (31 kg/ha/yr).

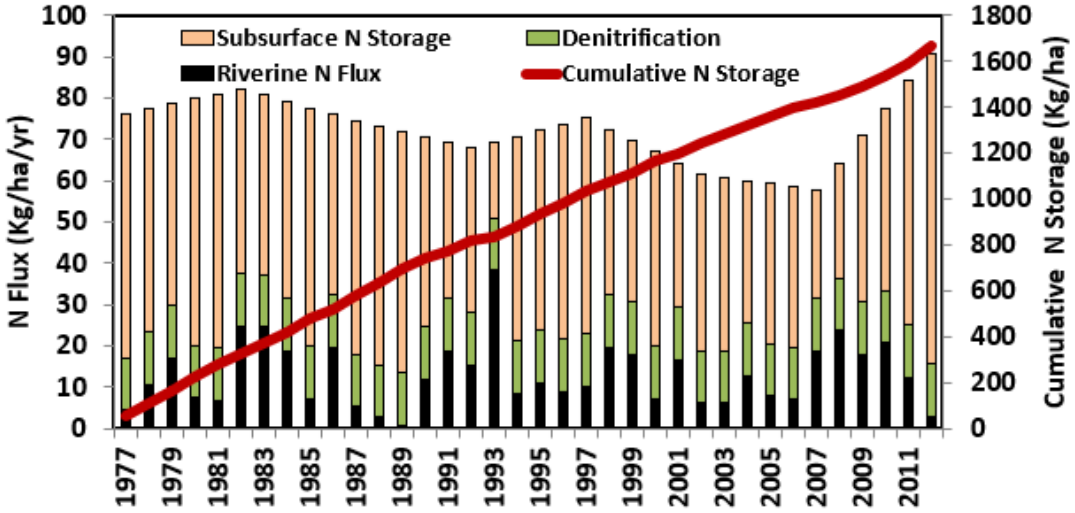

Figure 2.6. Temporal trend of N stores and fluxes from 1977 to 2012. Annual Riverine N flux obtained from WRTDS model using monthly nitrate data from USGS (2016). Denitrification rate of 12.7 kg/ha/yr was adopted from David *et al.* (2009). Note that NANI was initially estimated for 1 in 5 years (census years) (shown in Figure 2.3) and then interpolated to get the annual values

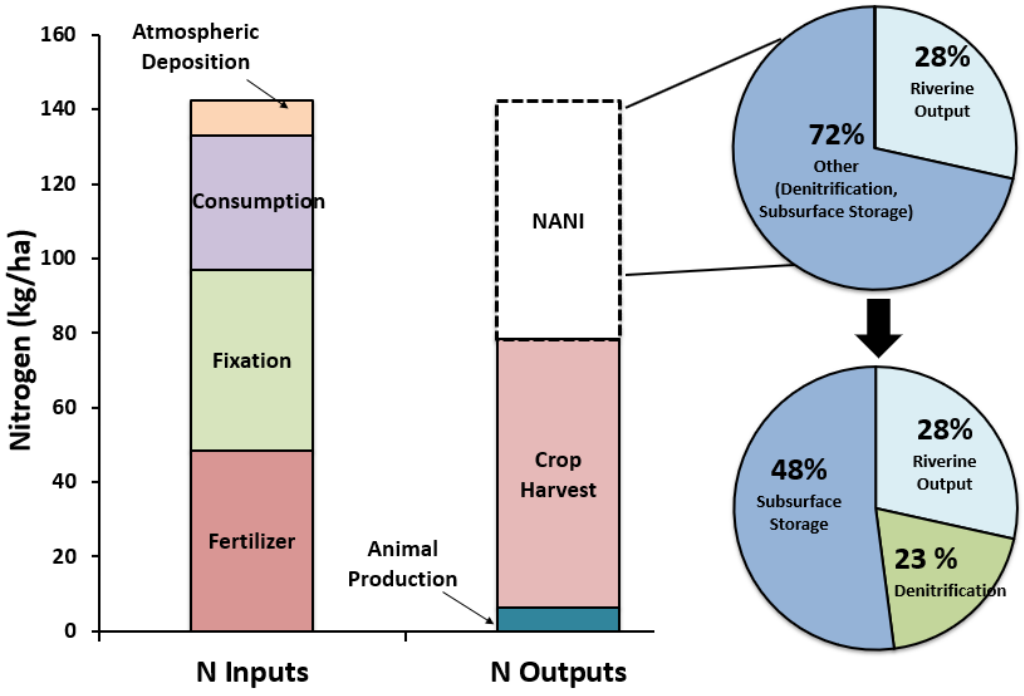

Figure 2.7. Mass balance showing N inputs, N outputs, NANI, riverine N output, denitrification, and subsurface N accumulation

2.6 Conclusion

Historical reconstruction of N inputs, outputs, and stores was performed from 1950 to 2012 for the Iowa Cedar Basin, agricultural watershed (i) to confirm the presence of legacy nitrogen stores and (ii) to quantify the magnitude of subsurface legacy nitrogen stores through mass balance approach. Using the most common Net Anthropogenic Nitrogen Inputs (NANI) method developed by Howarth *et al.* (1996), the N inputs such as atmospheric N deposition, fertilizer N application, and biological N fixation were estimated as 9.2 ± 0.35, 48 ± 2 and 49 ± 3 kg/ha/yr respectively. Net Food and Feed and NANI were estimated as 42 ± 4.5 kg/ha/yr. Then, the Riverine N Output was accounted for 28% of NANI (18 kg/ha/yr), and denitrification was estimated as 23% of NANI (12.4 kg/ha/yr). The rest, 48% of NANI (33.3 kg/ha/yr) was attributed to subsurface nitrogen storage. The quantification of legacy N storage implies that not all the missing N in the agricultural system is lost through denitrification and a significant

portion of the N inputs stays in the subsurface stores. Such accumulation of nitrogen in the soil root zone, predominantly in organic form, constitutes long-term mineralization and nitrate leaching – referred to as biogeochemical legacy (Van Meter et al., 2016). While the biogeochemical legacy of P in agricultural soils is well accepted, the biogeochemical legacy of N is relatively new, since it was neglected before due to non-sorbing and highly leaching nature of nitrate-nitrogen (Hamilton, 2012). Indeed, the evidence is now emerging recently (Sebilo *et al.,* 2013: Isotope tracer experiment; Van Meter et al., 2016: Parsimonious modeling and site measurements of SON accumulation), indicating the presence of biogeochemical nitrogen legacy in agricultural soils. In this chapter, rough estimates of nitrogen accumulation in subsurface stores were provided and there is a substantial need to employ modeling approaches (i) to quantify legacy nitrogen accumulation in soil and groundwater stores (ii) to understand the fate of legacy nitrogen under land-use and management changes and (iii) to quantify time lags between implementation of best management practices and corresponding improvement in riverine N exports

Chapter 3: Pitfalls in Model Calibration - Getting the Right Answers for the Wrong Reasons

3.1 Abstract

Hydrologic models are most commonly calibrated only for streamflow at one or multiple stations within the watershed. Using the distributed hydrologic models with large numbers of parameters, it is possible to get good streamflow statistics with the completely incorrect representation of the internal watershed processes. Consequently, these models fail when they are used to predict nutrient fluxes or effect of climate change. Using a 32,660 km^2 agricultural watershed in Iowa as a case study, a stepwise model refinement approach was used to show how the consideration of additional data sources can increase model consistency. We first developed a hydrologic model using the Soil and Water Assessment Tool that provided excellent monthly streamflow statistics (KGE, RSR and PBIAS values of 0.79, 0.59 and 6.5% during calibration and 0.75, 0.63 and 7.5% during the validation period, respectively) at eight stations within the watershed (Baseline Scenario, BS). However, comparing spatially distributed crop yield measurements with modeled results revealed a strong underestimation in model estimates (PBIAS Corn = 26%, PBIAS soybean = 61%). To address this, the model was refined by first adding crop yield as an additional calibration target (Scenario S1) and then changing the potential evapotranspiration estimation method (Scenario S2) -- this significantly improved model predictions of crop yield (PBIAS Corn = 3%, PBIAS soybean = 4%), while only slightly improving streamflow statistics. As a final step, for better representation of tile flow, the flow partitioning method (Scenario S3) was modified. While the model was developed for monthly streamflow, only version S3 was able to reproduce acceptable daily streamflow statistics. Furthermore, the S3 scenario was also able to (i) better capture variations in nitrate loads at the catchment outlet with no calibration and (ii) reduce parameter uncertainty, model prediction uncertainty, and equifinality. These findings highlight that using additional data sources to improve hydrological consistency of distributed models increases their robustness and predictive ability.

3.2 Introduction

Conventional distributed hydrologic models are most commonly evaluated using only streamflow information at one or multiple gaging stations within the watershed (Cao *et al.,* 2006; Rouhani *et al.,* 2007; Santhi *et al.,* 2008; Wang *et al.,* 2012, 2016; Boscarello *et al.,* 2013; Wi *et al.,* 2015; Xue Xianwu *et al.,* 2016). These models are often limited by a lack of adequate spatially distributed data (Grayson *et al.,* 2002) and rely on complex calibration-validation techniques for the estimation of a large number of model parameters (Madsen, 2003). This leads to what is commonly referred to as the equifinality issue, where multiple model combinations can lead to the same integrated response at the watershed outlet (Beven and Binley, 1992; Beven and Freer, 2001; Beven, 2006).

Recent studies have highlighted the ability of ancillary datasets, either spatially distributed information on vegetation and rainfall (Cusack *et al.,* 1997; Yilmaz *et al.,* 2005; Spies *et al.,* 2014; Alazzy *et al.,* 2017; Hunink *et al.,* 2017; Ren *et al.,* 2018) or soft data on flow partitioning (Seibert and McDonnell, 2002; Yilmaz *et al.,* 2008; Arnold *et al.,* 2015), to increase the consistency of hydrologic models. For example, models driven by remotely sensed meteorological data (e.g., NEXRAD rainfall data, and land surface temperature) had been shown to capture spatial patterns of runoff with greater accuracy than conventional hydrologic models (Andersen *et al.,* 2002; Stisen *et al.,* 2008; Zhang *et al.,* 2009; Cunha *et al.,* 2012). Remotely sensed vegetation data had been used as either model inputs to drive evapotranspiration (Glenn *et al.,* 2007, 2011) or for model calibration and validation (Immerzeel and Droogers, 2008; Liang and Qin, 2008). Rajib *et al.,* (2016) used remotely sensed soil moisture data to improve hydrologic predictions, while Qiao *et al.,* (2013) used GRACE-derived water storage and field measured water table information to reduce parameter uncertainty. Seibert and McDonnell, (2002) and Pfannerstill *et al.,* (2017) showed how soft data on flow partitioning could be used effectively in improving consistency in hydrologic modeling. Shafii *et al.,* (2017) observed adding additional flow partitioning constraints in model calibration, which helped improve the parameter identifiability and reduced model uncertainty. Incorrect flow partitioning can also affect solute transport since different pathways have unique biogeochemical signatures (Kannan *et al.,* 2007a; Yen *et al.,* 2014; Bieger *et al.,* 2015; Mockler *et al.,* 2016; Shafii *et al.,* 2017).

However, these examples of using ancillary data are few, and the vast majority of hydrologic model studies rely solely on streamflow data. A SCOPUS literature review was performed by the authors by considering modeling studies between 1995 - 2015 that used the Soil Water Assessment Tool (SWAT). The literature review revealed that only 31 (1.5%) of the 2084 SWAT papers used crop yield as a calibration target, in addition to streamflow. This is somewhat surprising, given that crop yield information, unlike remotely sensed data or ancillary field data, are relatively easy to obtain at the watershed scale since agricultural agencies in all countries routinely collect and curate this data. Furthermore, SWAT, unlike some hydrologic models, models crop growth and thus can provide information on crop yield that can be directly used in model calibration and validation.

The overall objective of this study is to demonstrate the value of ancillary data (crop yield and flow partitioning information) in increasing the consistency and robustness of hydrologic models by the proper representation of internal watershed processes, leading to the right answers for the right reasons (Kirchner, 2006). A secondary objective is to show how increasing model consistency with respect to water flow leads to a reduction in equifinality and increased predictive ability for solutes like nitrate.

3.3 Methods

3.3.1 Study Site

The 32,660 km^2 Iowa Cedar Basin (ICB) (**Figure 3.1**) is drained by the Iowa and Cedar Rivers, and the watershed extends from southern Minnesota to the confluence with the Mississippi River. The mean annual rainfall in ICB is approximately 864 mm (Seo *et al.,* 2013), and the average annual temperature is around 10 ^oC (ICRB Report, 2010). The ICB is an agricultural watershed with corn and soybean being the dominant crops. While the corn and soybean cultivation occupies approximately 42% and 26% of the watershed area respectively, 6% of the watershed is occupied by other crop varieties. Rest of the watershed area comprises pasture and rangelands (15%), urban areas (8%) and wetlands and water bodies (3%) (USDA, 2012). The predominant soils of ICB are loam and silty-loam soils, which cover approximately 96% percent of the watershed (Le, 2015).

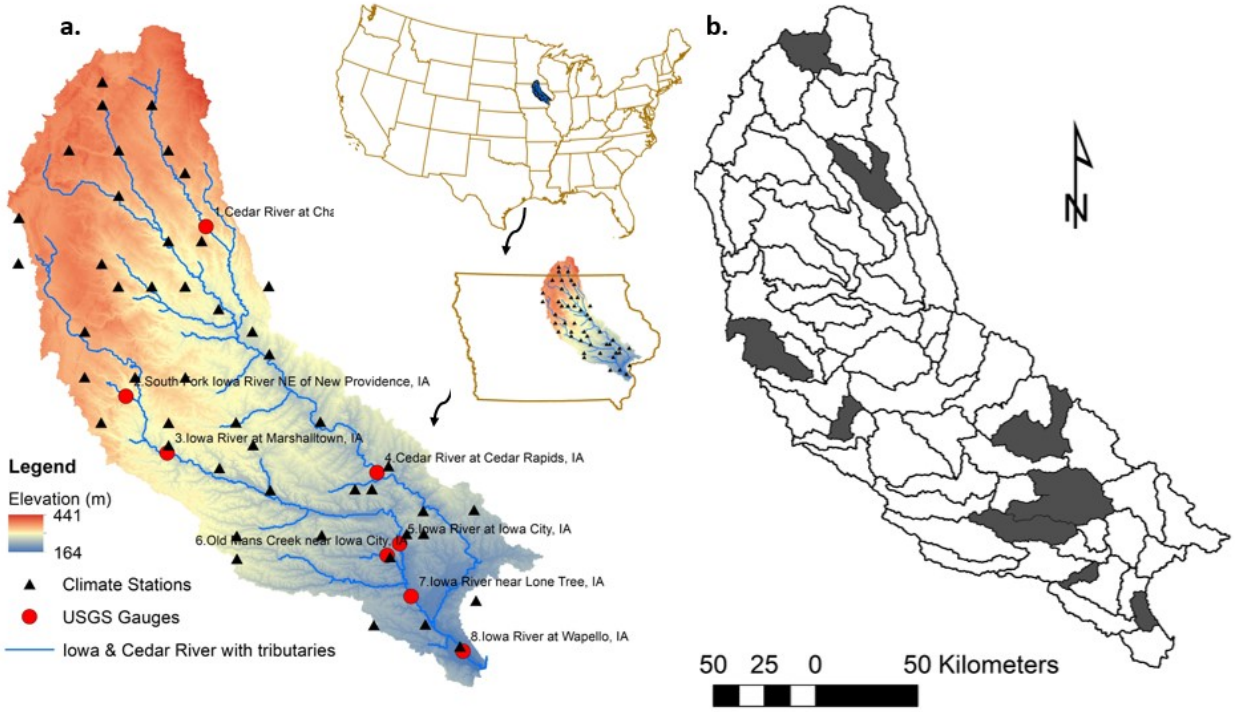

Figure 3.1. (a) Map showing the location of the Iowa Cedar Basin (ICB), with eight stream gauge locations (in red) that were used for model calibration (b) ICB with the location of sub-basins where crop yield calibration was performed

3.3.2 SWAT Model Description

Soil Water Assessment Tool (SWAT) is a watershed scale, process-based, continuous simulation model that runs at daily time steps to predict streamflow and nutrient loads. The watershed is divided into sub-basins that are further subdivided into Hydrologic Response Unit (HRU), characterized by the unique soil, land-use, and slope. Major modules of SWAT are climate, hydrology, plant growth, erosion, nutrients, pesticides, and management practices. Surface runoff is computed using either the SCS-curve number method that computes runoff under varying land-use and soil type, or the Green-Ampt infiltration method that requires sub-daily precipitation data. Infiltrated water is stored in soils and used for evapotranspiration or reaches the stream network as lateral flow. A portion of the infiltrated water also reaches the groundwater. Crop yield is calculated as the product of above ground biomass and crop-specific harvest index, where harvest index is the fraction of above-ground dry biomass removed during

harvest. The remaining fraction of crop, after the harvest, is converted into the residue. For more details on the modeling water and nutrient fluxes in SWAT, see Neitsch *et al.* (2011).

3.3.3 SWAT Model Setup, Input Data, and Parameters

The SWAT model developed by Le (2015) for ICB was used for this study. Digital Elevation Model (DEM) data (30 m resolution) was downloaded from United States Geological Survey (USGS) National Elevation Dataset (USGS, 2013), while soil data was obtained from the United States Department of Agriculture (USDA) STATSGO2 (Soil Survey Staff., n.d.) dataset. Land-use and land cover data were derived from the Iowa Department of Natural Resources (DNR) (Iowa DNR, 2012), the Multi-Resolution Land Characteristics Consortium's (MRLC), National Land Cover Dataset (NLCD) (Fry *et al.,* 2012), and the USDA's Crop Data Layer (CDL) (USDA-CDL., 2012). These three datasets had different spatial and temporal extents, and thus, all three were needed to capture the land-use trends appropriately. Using the DEM, the watershed was first divided into 67 sub-basins using a 1% flow accumulation area threshold (327 km^2), and the sub-basins were further discretized into hydrological response units (HRUs) using a threshold of 5% for land-use, soil, and slope. For more details on input data and model setup, please refer Le (2015)

Daily precipitation and temperature data for 48 weather stations (**Figure 3.1**) were obtained from the US National Weather Service (US-NWS, n.d.), United States Environmental Protection Agency (US-EPA, 2013) and Iowa Environmental Mesonet, n.d. while SWAT's automatic weather generator was used for relative humidity, wind speed and solar radiation data. Discharge data for the eight stream gauge stations were obtained from USGS (2016), from 1993 to 2012. The major crop varieties of ICB are corn and soybean. County scale annual corn and soybean yield data downloaded from the USDA-Agricultural survey (2012) was used for crop yield calibration. Annual crop yield data obtained for 35 counties of ICB in wet weight (bu/acre) was converted to dry weight (t/ha) based on guidelines outlined in Gassman (2008) to compare with SWAT simulated crop yield. Crop yield at the county scale was converted to the sub-basin scale using area weighting. Given the ICB is dominated with poorly drained and moderately drained soils (Sloan, 2013), and due to lack of information of the exact location of the tile drains, we assumed that tile drains were present on all agricultural HRUs. We explored alternate methods of estimating tile drain density based on databases provided by Iowa DNR (2017) that were based

on either (i) an incomplete digitized record of tile drains, or (ii) estimate of soils requiring based on slopes and soil type, as described by Kalcic *et al.* (2015). However, ground truthing in several sub-watersheds revealed that on-the-ground tile density was much greater than estimated by these maps. Indeed, with increasing high flow events, tile density has been increasing in Iowa, and thus, we used the conservative estimate that all agricultural areas were drained.

Auto-fertilization routine was used to estimate fertilizer application rates. The maximum amount of elemental nitrogen and P_2O_5 applied to corn and soybean per year was restricted to 218.5 kg/ha/yr and 45 kg/ha/yr based on the recommendations of Mallarino *et al.* (2013) and Sawyer (2015). Mineral fertilizer was applied through the surface broadcast method, and No-till tillage practice was considered for the model simulation. Fertilizer application and tillage methods - there is significant uncertainty in these input variables; however, the main goal of the nitrate model developed in this chapter is to evaluate how alternate streamflow calibration techniques impact nitrate loads.

3.3.4 Model Calibration and Validation

Discharge-specific calibration parameters were selected based on Le (2015), while crop growth parameters were selected based on Nair *et al.* (2011) (**Table A1**). The Sequential Uncertainty Fitting Algorithm version 2 (SUFI2) (Abbaspour *et al.,* 2007), which is capable of performing multi-objective calibration and uncertainty analysis, was used for model calibration and validation (Yang *et al.,* 2008, Faramarzi *et al.,* 2009). The model was calibrated from 1993 to 2002 and validated from 2003 to 2012 with a three-year warm-up period from 1990 to 1992. Stepwise model refinement was used to demonstrate the value of adding crop yield and flow partitioning. Since the development of each scenario was guided by the model results obtained from the previous scenario, details of the scenario development are described in **Section 3.1-3.3**.

The Kling-Gupta Efficiency (KGE) was used as the objective function in a multi-objective calibration, and the SUFI2 algorithm (Abbaspour, 2012) was used for model calibration and validation. While the streamflow was calibrated at a monthly time step (**Equation 3.4 and 3.5**), crop yields were calibrated at an annual time step (**Equation 3.5**). For the baseline scenario, simultaneous calibration was done at eight streamflow stations (**Figure 3.1**), with each station given equal weight, and the SUFI2 algorithm was used to maximize the

KGE*overall* (**Equation 3.4**). For the crop yield scenarios, the objective function (**Equation 3.5**) used is the average of 8 streamflow station KGEs, nine sub-basin level corn yield KGEs (at annual time step), and nine sub-basin level soybean yield KGEs (for a total of 26 KGEs; Figure 3.1). The SUFI2 algorithm tries to achieve a KGE value of 1 through multiple iterations.

All scenarios were subjected to three iterations, with 250 runs per iteration (750 runs in total). The SUFI2 algorithm produced a best parameter set at the end of each iteration and also provided the new calibration parameter ranges for the next iteration, which is narrower than the previous iteration's calibration parameter ranges. Results from the third iteration are then used for comparing between alternate model realizations. Although calibration and validation were done using only KGE, we also evaluated the performance of the models with respect to the performance metrics RMSE-observations Standard Deviation Ratio (RSR) and Percent Bias (PBIAS). The evaluation metrics were estimated using the best parameter set of the third iteration of each scenario.

$$\mathrm{KGE} = 1 - \sqrt{(r-1)^2 + (\alpha-1)^2 + (\beta-1)^2} \qquad \textbf{(Eq. 3.1)}$$

where r is the linear coefficient between simulated and measured data

$\alpha = \frac{\sigma_s}{\sigma_m}$; σ_s and σ_m are the standard deviation of simulated and measured data

$\beta = \frac{\mu_s}{\mu_m}$; μ_s and μ_m are mean of simulated and measured data

$$\mathrm{RSR} = \frac{\sqrt{\Sigma(Q_m - Q_s)^2}}{\sqrt{\Sigma(Q_m - \overline{Q_m})^2}} \qquad \textbf{(Eq. 3.2)}$$

where Q_m and Q_s are measured and simulated data & $\overline{Q_m}$ is the mean of measured data

$$\mathrm{PBIAS} = 100 * \frac{\Sigma(Q_m - Q_s)}{\Sigma Q_m} \qquad \textbf{(Eq. 3.3)}$$

where Q_m and Q_s are measured and simulated data. A positive PBIAS value indicates an underestimation, and a negative PBIAS value indicates an overestimation

$\mathrm{KGE}overall = \frac{1}{x}\sum_{i=1}^{x} KGE_{streamflow}$, for baseline scenario **(Eq. 3.4)**

where x = 8 (streamflow stations; Figure 3.1a)

$$\mathrm{KGE}overall = \frac{1}{n}\left[\frac{1}{x}\sum_{i=1}^{x} KGE_{streamflow} + \frac{1}{y}\sum_{j=1}^{y} KGE_{corn\ yield} + \frac{1}{z}\sum_{k=1}^{z} KGE_{soybean\ yield}\right]$$, for crop yield scenarios **(Eq. 3.5)**

where n = 3, x = 8 (streamflow stations; Figure 3.1a), y = 9 (sub-basin scale corn yield; Figure 3.1b), and z = 9 (sub-basin scale soybean yield; Figure 3.1b)

3.3.5 Uncertainty Analysis

Both parameter uncertainty and prediction uncertainty were evaluated using the methodologies developed by Abbaspour (2012). Parameter uncertainty was estimated based on behavioral solution sets that comprise of multiple parameter combinations that can produce equally satisfactory responses at the watershed outlet (Beven, 1993; Rajib and Merwade, 2016). Following Her and Chaubey (2015), a behavioral threshold was defined as parameter sets that produced the top 2.5% KGE values in the third iteration, and these are hereafter referred to as behavioral solutions. Then the normalized parameter uncertainty score Pn was defined as

$$\mathrm{Pn} = \left[\frac{Pb - Ll}{Ul - Ll}\right] * 100 \quad \text{(Eq. 3.6)}$$

Where, Pb is the behavioral parameter value, and U_l and L_l are the upper and lower limit of the parameter, respectively (Rajib and Merwade, 2016; Rajib *et al.,* 2016). The IQR of the Pn values for each of the key parameters was compared between model scenarios to evaluate the effect of modifications on parameter uncertainty. The prediction uncertainty was quantified using two metrics, the *p*-factor (defined as fraction of the observed data bracketed by the 95% prediction uncertainty (PPU)) and the *r*-factor (defined as average thickness of 95 PPU band divided by standard deviation of the observed data) (Yang *et al.,* 2008; Abbaspour., 2012). The p-factor and r-factor can vary between 0 and 1 and 0 and infinity, respectively, and higher p-factor value and

lower r-factor value imply a lower prediction uncertainty (Ekstrand *et al.,* 2010; Bouda *et al.,* 2012). Theoretically, a p-factor of 1 and r-factor of 0 is a simulation that corresponds exactly to observed data.

3.4 Results and Discussion

3.4.1 Streamflow Calibration and Validation (Baseline Scenario)

As mentioned previously, the model was calibrated from 1993 to 2002 and validated from 2003 to 2012. Simultaneous calibration and validation were done using monthly streamflow data at all eight stations within the watershed. The model performed well during the calibration and the validation periods, both at the outlet of the watershed in the Wapello station, and at all seven internal stations. The metrics KGE, RSR, and PBIAS, varied between 0.74 to 0.87, 0.42 to 0.68 and -13.7 to 8.6, respectively during the calibration period, and between 0.43 to 0.85, 0.49 to 0.92 and -25.9 to 8.7, respectively during the validation period (**Table 3.1**). This scenario is hereafter referred to as the Baseline Scenario (BS).

3.4.2 Crop Yield Performance Evaluation (Baseline Scenario)

The calibrated model was then used to estimate crop yield across the entire watershed. The model underpredicted both corn and soybean yields **(Figure 3.2b and 3.2c)**, with underestimation being greater for soybean compared to corn (26% underestimation of the mean yield for corn and 61% for soybean). Crop yields are generally low when there is water or temperature stress in the system. On exploring model outputs, it was identified that the corn HRUs were under water stress on an average for 27 days out of the 150-day growing season between 1993 and 2012, while, soybean HRUs were under water stress on an average for 33 days out of the 150-day growing season **(Figure 3.2d)**. Furthermore, the water storage within the soil profile was below the field capacity and wilting point, leading the system to water stress for the entire growing season **(Figure 3.2d)**. This explained the poor crop yield observed in the results and highlighted the need for adding crop yield as a calibration target.

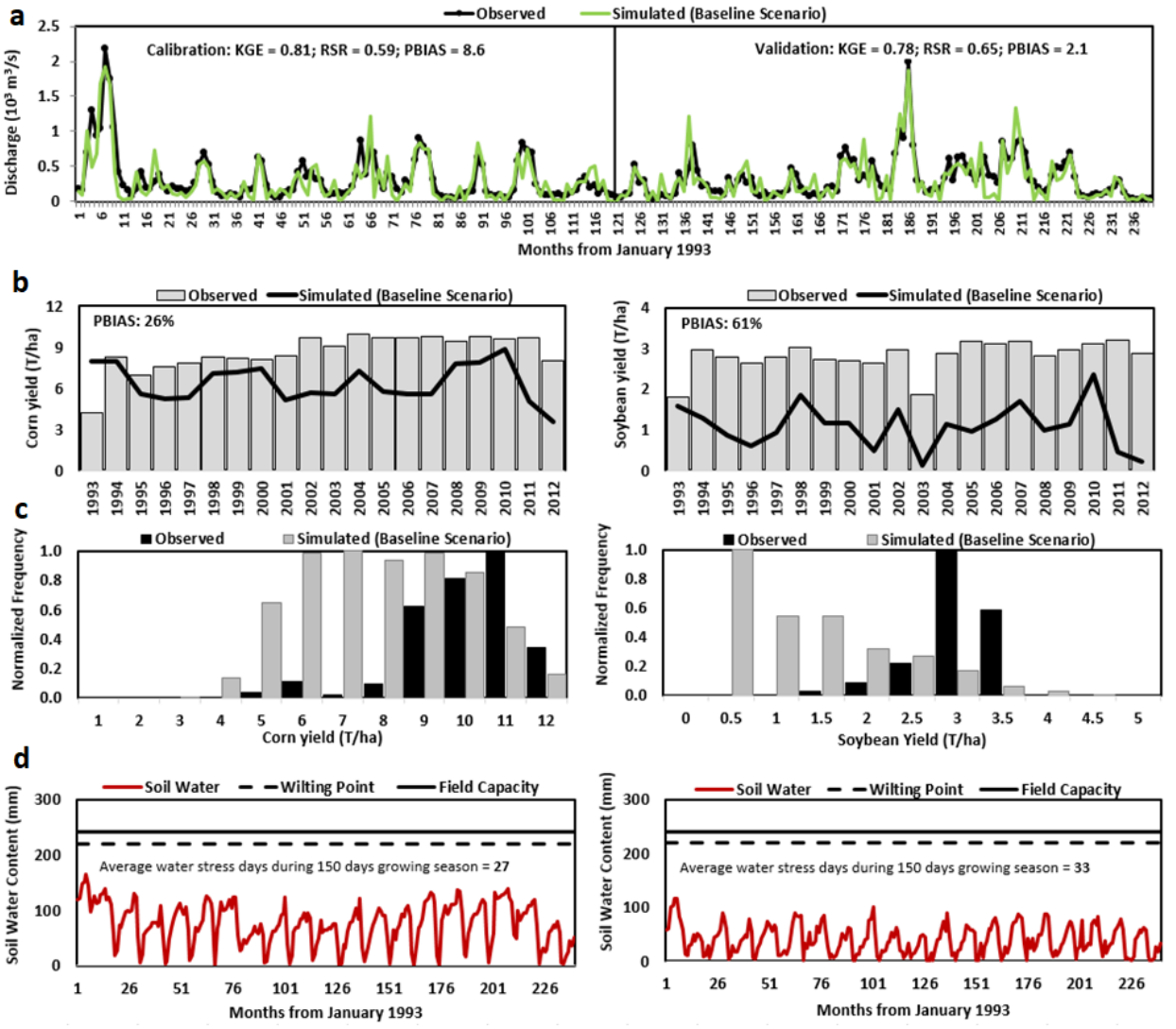

Figure 3.2. (a) Monthly discharge at the Wapello Station for the Baseline Scenario, (b) Annual Corn yield (left) and Soybean yield (right) at the Watershed Scale, (c) Histogram of Corn yield (left) and Soybean yield (right) and (d) Soil water content, Field capacity and Wilting point in the soil profile for Corn HRUs (left) and Soybean HRUs (right). Note: Corn and soybean HRUs were aggregated at the watershed scale to plot the figures

3.4.3 Stepwise Model Refinement: Crop Yield Calibration (Scenario S1)

In the next step of model refinement (**scenario S1**), the annual corn and soybean yields at nine internal sub-basins were added as calibration targets in addition to discharge. Crop-specific parameters like maximum potential leaf area index (BLAI), heat units (HEAT_UNITS), plant radiation use efficiency (BIO_E) and harvest index (HVSTI) were used for model calibration, in addition to streamflow specific parameters (Table A1). This led to a slight improvement in crop yield, but corn and soybean yield was still underpredicted by 27% and 52%, respectively (**Figure 3.3a and 3.3b**). Streamflow metrics were predicted with a similar level of accuracy as the baseline scenario **(Table 3.1)**. The crop water stress values and soil water content were also similar between the two scenarios **(Figure 3.3d)**, and much higher than what is typically expected in a humid climate like Iowa. We hypothesize that this can be created by overestimation of potential evapotranspiration (PET) which would potentially lead to "drying up" of the soil, contributing to water stress and reduced crop uptake of water. This led us to consider alternate model formulations for the estimation of evapotranspiration, as described below.

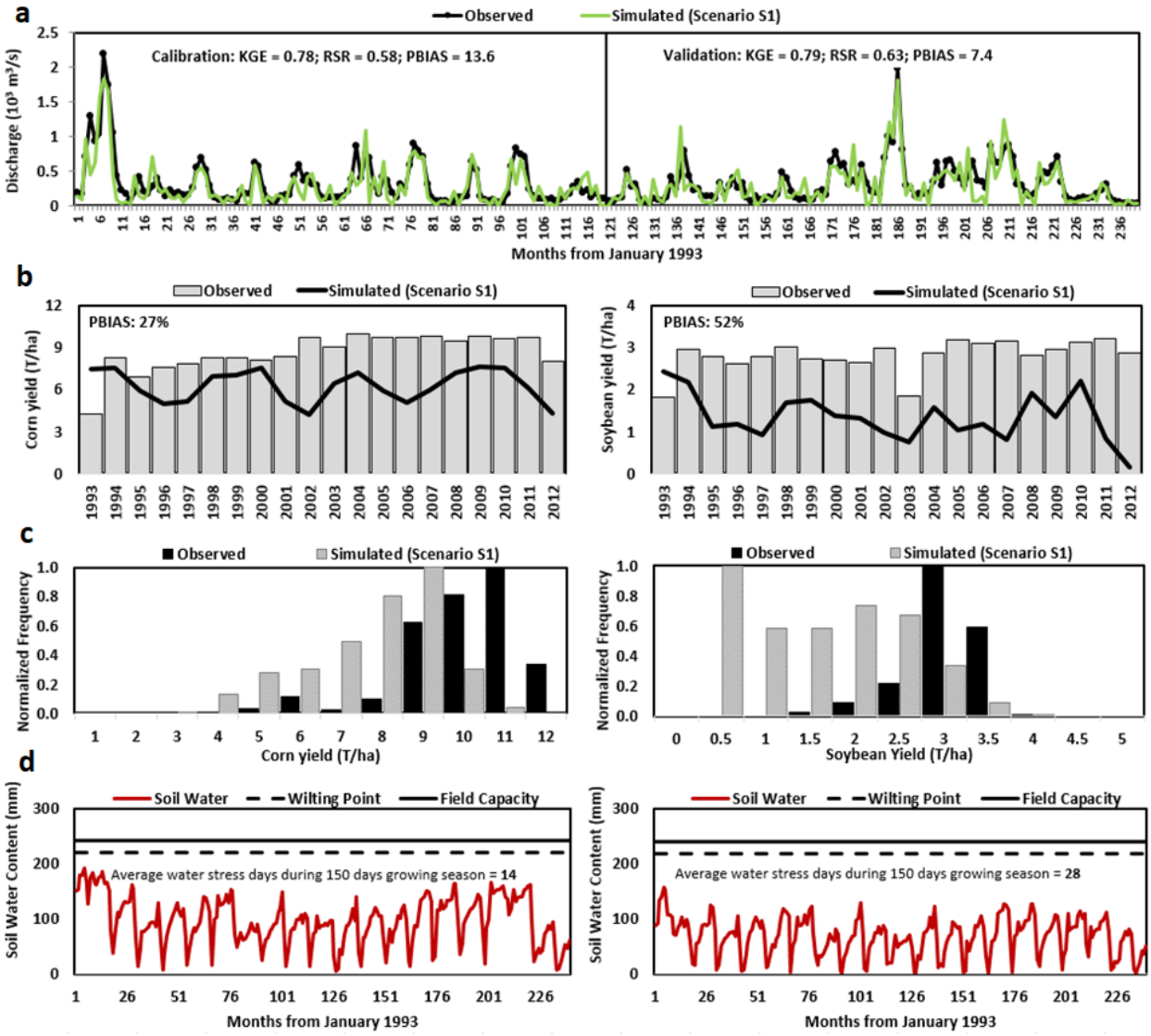

Figure 3.3. (a) Monthly discharge at the Wapello Station for the S1 Scenario, (b) Annual Corn yield (left) and Soybean yield (right) at the Watershed Scale, (c) Histogram of Corn yield (left) and Soybean yield (right) and (d) Soil water content, Field capacity and Wilting point in the soil profile for Corn HRUs (left) and Soybean HRUs (right). Note: Corn and soybean HRUs were aggregated at the watershed scale to plot the figures

3.4.4 Stepwise Model Refinement: Model Structural Changes - Improvement of Evapotranspiration (Scenario S2)

Due to its wide usage, the PM-PET method was used in the Baseline and the S1 scenario (Schneider *et al.,* 2007; Milly and Dunne, 2016). However, the average annual PET estimated by the model (1516 mm) seemed to be exceedingly high compared to estimated data in Iowa during the same years (Green *et al.,* 2006: 1190 mm; Daryl Herzmann, Iowa Environmental Mesonet, 2019: 1175 mm). To address this issue, the temperature-based Hargreaves (HG)-PET method was considered in the next step of model refinement (**Scenario S2**), with everything else being the same as scenario S1. This led to a significant improvement in crop yield (**Figure 3.4b and 3.4c**) with corn and soybean yield being underpredicted by only 2% and 9%, respectively. Potential evapotranspiration predicted by the HG method was lower than the PM method (963 mm compared to 1516 mm), and the average water stress days for both corn and soybean HRUs were reduced to zero days during the150-day growing season between 1993 and 2012 (**Figure 3.4d**).

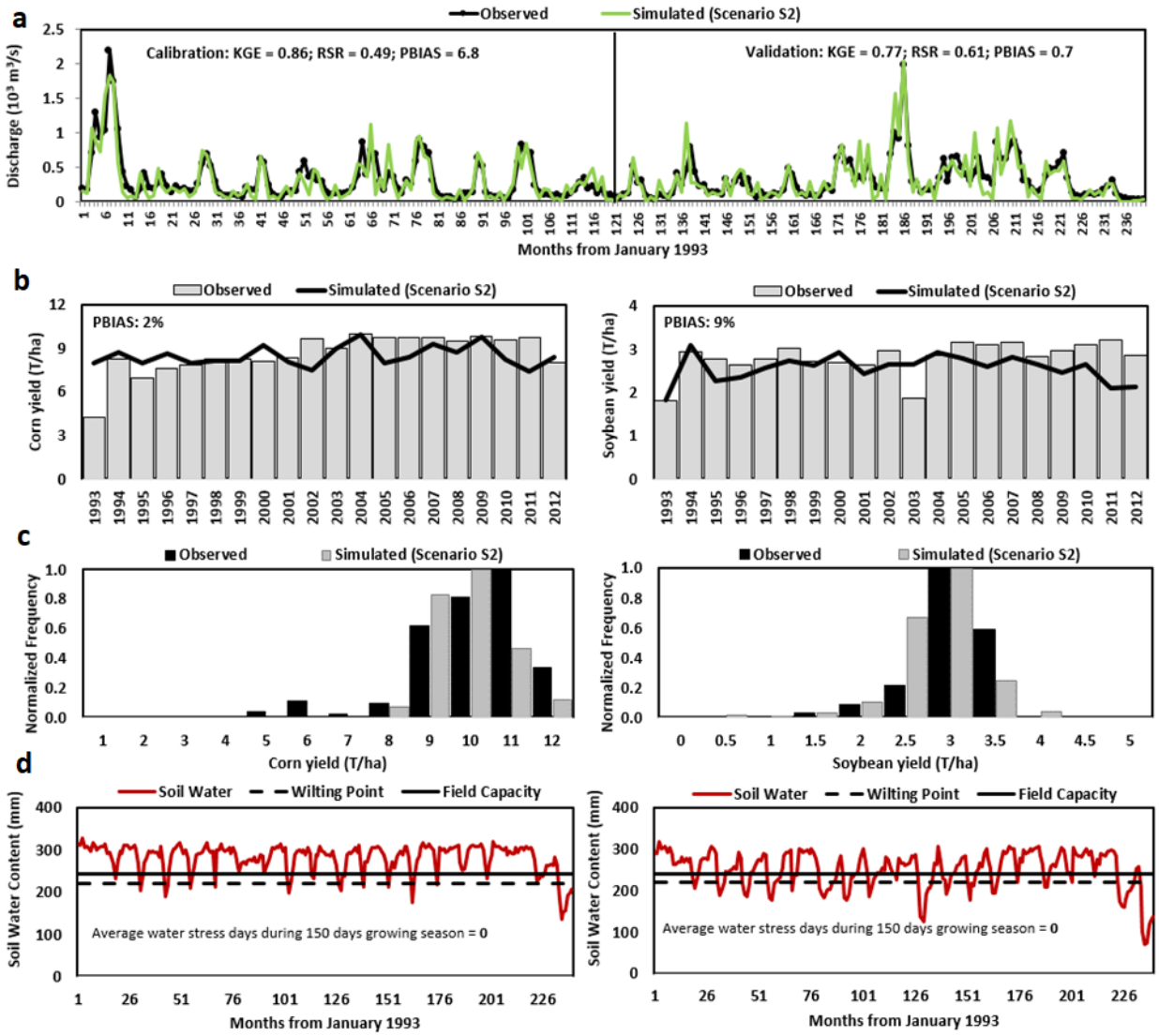

Figure 3.4. (a) Monthly discharge at the Wapello Station for the S2 Scenario, (b) Annual Corn yield (left) and Soybean yield (right) at the Watershed Scale, (c) Histogram of Corn yield (left) and Soybean yield (right) and (d) Soil water content, Field capacity and Wilting point in the soil profile for Corn HRUs (left) and Soybean HRUs (right). Note: Corn and soybean HRUs were aggregated at the watershed scale to plot the figures

3.4.5 Stepwise Model Refinement: Model Structural Changes - Improvement of Flow Partitioning (Scenario S4)

We then evaluated the effect of model refinement on the partitioning of water along the lateral flow pathways, namely, surface runoff, lateral flow, tile flow, and groundwater flow. Although scenario S2 yielded acceptable model statistics for both crop yield and streamflow, it led to the tile flow pathway contributing to only 17% of the total flow, while surface runoff, lateral flow, and groundwater flow corresponded to 74%, 7% and 2% of the total flow, respectively **(Table 3.2)**. This highlights serious underestimation of tile flow for a watershed that is 68% tile-drained. A review study conducted by (Howe and Moore, 2016) highlighted that the percent flow through tiles could range from 37-86% in North-American Watersheds, while a study in a neighboring watershed reported a tile flow percent of 67% (Green *et al.,* 2006). Thus, the next stage of model refinement involved interrogating the variables responsible for flow partitioning.

It has been argued that the traditional curve number method in SWAT that uses soil moisture based curve number prediction (ICN = 0 in SWAT manuals) generates too much surface runoff in shallow soils (Kannan et al., 2007; Neitsch et al., 2011; Amatya and Jha, 2011). There exists an alternate evapotranspiration based curve number method in SWAT (ICN=1) that links the retention parameter (S) in CN with soil moisture depletion, which in turn is governed by PET, rainfall, and runoff. In this method, it is possible to have control over the allocation of surface and subsurface flow (through infiltration) without affecting the ET (Amatya and Jha, 2011). Using the ET based CN prediction method, the CNCOEFF parameter was manually adjusted to achieve a tile flow of 67%, similar to Green *et al.* (2006) and Howe and Moore (2016). Also, this scenario (S3), was able to provide good streamflow **(Figure 3.5a)** and crop yield estimates a (**Figure 3.5b and 3.5c**). Better site-specific flow partitioning estimates can be used, if available, to refine the model further for reasonable flow partitioning, while still maintaining streamflow **(Table 3.1)** and crop yield statistics **(Table 3.3)**.

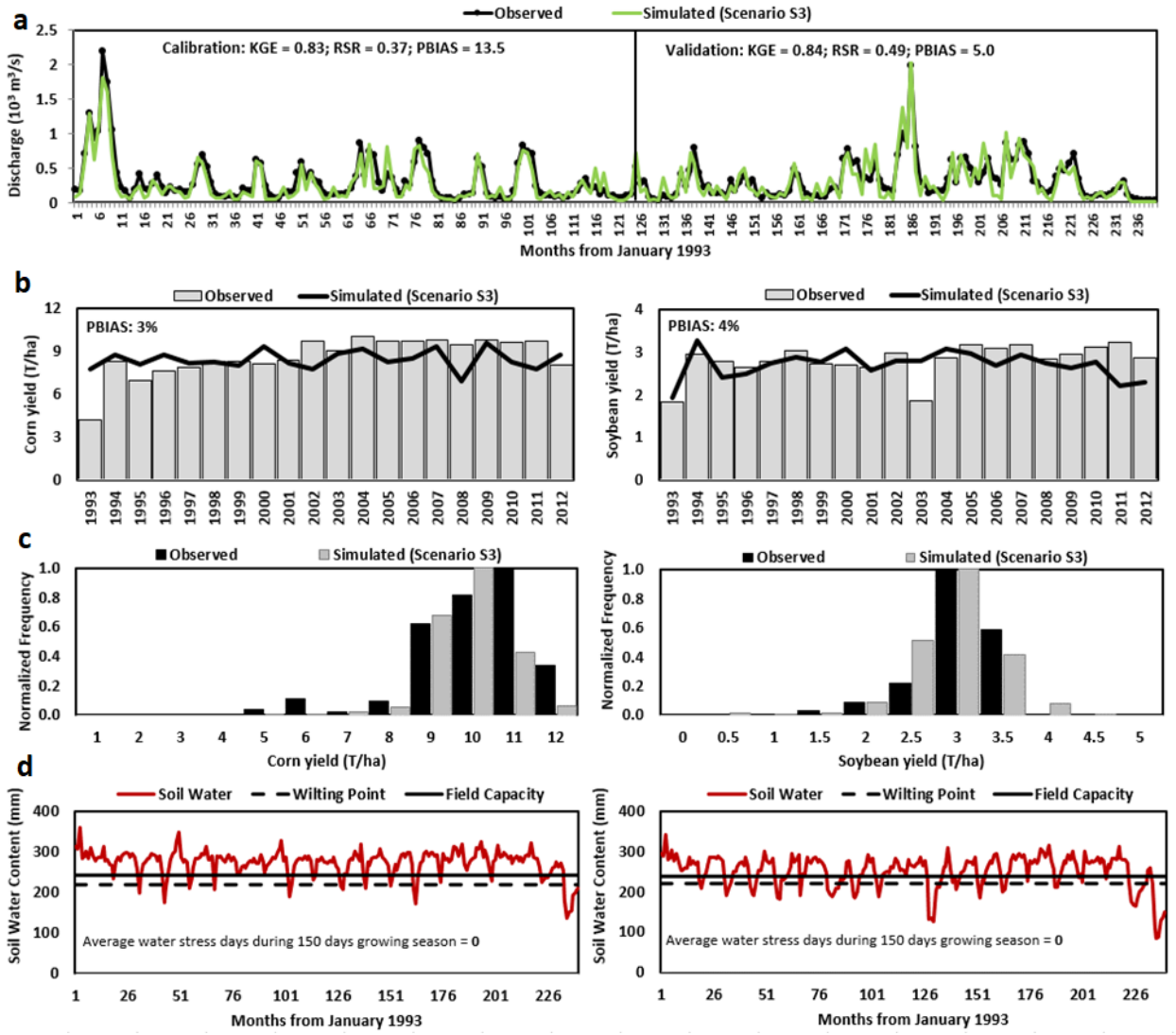

Figure 3.5. (a) Monthly discharge at the Wapello Station for the S3 Scenario, (b) Annual Corn yield (left) and Soybean yield (right) at the Watershed Scale, (c) Histogram of Corn yield (left) and Soybean yield (right) and (d) Soil water content, Field capacity and Wilting point in the soil profile for Corn HRUs (left) and Soybean HRUs (right). Note: Corn and soybean HRUs were aggregated at the watershed scale to plot the figures

3.4.6 Model Comparisons in Space and Time

Across the four scenarios analyzed in this paper (BS, S1, S2, S3), the addition of crop yield and flow partitioning parameters led to some improvement in streamflow prediction **(Table 3.2)**. The biggest improvement, however, occurred in crop yield estimates where watershed-scale PBIAS of corn decreased from decreased from 26 and 27% for the BS and S1 scenarios to 2 and 3% in the S2 and S3 scenarios and PBIAS of soybean decreased from 61 and 52% for the BS and S1 scenarios to 9 and 4% in the S2 and S3 scenarios **(Figures 3.2 to 3.5 and Table 3.3)**. Also, the crop yield estimates for nine selected sub-basins were significantly better for the S2 and S3 scenarios compared to the baseline and S1 scenarios (**Table 3.3**) due to the change in the representation of potential evapotranspiration in the model.

Table 3.1. Streamflow statistics (KGE, RSR, and PBIAS) for all eight stations and all four scenarios, during the calibration (validation) periods. The model was calibrated from 1993 to 2002 and validated from 2003 - 2012

Monthly streamflow statistics	**KGE**			
Stations	**BS**	**S1**	**S2**	**S3**
Charles City	0.74 (0.43)	0.76 (0.51)	0.87 (0.55)	0.92 (0.70)
New Providence	0.74 (0.83)	0.80 (0.83)	0.85 (0.86)	0.87 (0.89)
Marshalltown	0.85 (0.84)	0.81 (0.85)	0.91 (0.87)	0.92 (0.90)
Cedar Rapids	0.77 (0.78)	0.75 (0.82)	0.83 (0.81)	0.83 (0.91)
Iowa City	0.79 (0.75)	0.77 (0.71)	0.84 (0.81)	0.87 (0.83)
Lone Tree	0.87 (0.85)	0.81 (0.84)	0.87 (0.86)	0.82 (0.91)
Old Man's Creek	0.82 (0.81)	0.79 (0.77)	0.88 (0.86)	0.86 (0.87)
Wapello	0.81 (0.78)	0.78 (0.79)	0.86 (0.77)	0.83 (0.84)
Overall	**0.79 (0.75)**	**0.78 (0.76)**	**0.86 (0.79)**	**0.86 (0.85)**

Monthly streamflow statistics	**RSR**			
Stations	**BS**	**S1**	**S2**	**S3**
Charles City	0.68 (0.92)	0.66 (0.85)	0.50 (0.72)	0.34 (0.52)
New Providence	0.68 (0.59)	0.63 (0.58)	0.53 (0.48)	0.47 (0.42)
Marshalltown	0.54 (0.54)	0.54 (0.53)	0.44 (0.46)	0.36 (0.42)
Cedar Rapids	0.68 (0.63)	0.67 (0.60)	0.55 (0.54)	0.37 (0.40)
Iowa City	0.63 (0.64)	0.62 (0.64)	0.57 (0.61)	0.47 (0.55)
Lone Tree	0.42 (0.49)	0.43 (0.48)	0.39 (0.42)	0.36 (0.41)
Old Man's Creek	0.56 (0.56)	0.55 (0.56)	0.49 (0.53)	0.40 (0.48)
Wapello	0.59 (0.65)	0.58 (0.63)	0.49 (0.61)	0.37 (0.49)
Overall	**0.59 (0.63)**	**0.58 (0.61)**	**0.49 (0.55)**	**0.39 (0.46)**

Monthly streamflow statistics	**PBIAS**			
Stations	**BS**	**S1**	**S2**	**S3**
Charles City	-13.7 (-25.9)	-10.5 (-20.4)	0.0 (-17.0)	3.9 (-11.7)
New Providence	-11.3 (-0.1)	-3.1 (5.7)	-1.2 (8.0)	-5.6 (5.3)
Marshalltown	0.7 (-6.8)	7.5 (-0.6)	-1.0 (-5.9)	1.4 (-5.3)
Cedar Rapids	3.5 (-5.1)	8.3 (0.3)	7.2 (-1.7)	10.8 (1.6)
Iowa City	3.8 (8.7)	9.5 (14.2)	-2.2 (3.1)	6.0 (7.0)
Lone Tree	3.6 (3.7)	9.6 (6.2)	-11.1 (-8.2)	7.5 (0.2)
Old Man's Creek	5.4 (7.7)	11.1 (12.8)	-3.5 (0.2)	7.5 (5.4)
Wapello	8.6 (2.1)	13.6 (7.4)	6.8 (0.7)	13.5 (5.0)
Overall	**6.3 (7.5)[a]**	**9.1 (8.4)[a]**	**4.1 (5.6)[a]**	**7.0 (5.2)[a]**

[a] Average of absolute PBIAS values of individual stations

Table 3.2. Water balance components for all four scenarios (BS through S3)

Processes	BS (mm)	S1 (mm)	S2 (mm)	S3 (mm)
	ONLY FLOW (PM-PET+ICN0)	FLOW+CROP YIELD (PM-PET+ICN0)	FLOW+CROP YIELD (HG-PET+ICN0)	FLOW+CROP YIELD (HG-PET+ICN1)
Precipitation	892	892	892	892
Snowmelt	93	93	93	93
Surface runoff	294	278	225	35
Lateral flow	6	6	21	38
Tile flow	0	0	53	190
Base flow	1	1	7	21
Water yield	302	286	306	283
PET	1516	1516	963	963
ET	596	613	594	583
Change in Storage	87	86	85	118
Water stress days	27	15	1	1

Table 3.3. PBIAS of Corn (a) and Soybean yield (b) for nine internal basins for all four scenarios, during the calibration (validation) periods. The model was calibrated from 1993 to 2002 and validated from 2003 - 2012

Crop yield statistics	**Corn**			
Subbasins	**BS**	**S1**	**S2**	**S3**
Sub basin 1	30.7 (44.1)	31.0 (43.0)	-12.7 (6.0)	-9.9 (11.3)
Charles City	2.6 (20.8)	0.2 (12.6)	-19.7 (-2.3)	-19.5 (-0.4)
New Providence	31.2 (48.1)	33.4 (42.1)	-4.2 (11.8)	-5.6 (17.6)
Marshalltown	18.6 (40.0)	23.8 (37.7)	0.2 (15.3)	-1.0 (14.1)
Cedar Rapids	23.9 (31.0)	25.6 (29.7)	-0.9 (9.6)	-2.9 (7.5)
Iowa City	3.4 (28.1)	11.4 (27.8)	-4.9 (3.2)	-7.6 (1.7)
Lone Tree	16.7 (30.3)	15.6 (35.4)	-6.0 (9.9)	-6.5 (9.0)
Old Man's Creek	20.8 (20.5)	23.3 (31.2)	-2.0 (10.1)	-2.8 (10.4)
Wapello	21.5 (28.0)	20.9 (29.6)	-8.6 (8.3)	-10.8 (7.9)
Overall*	**18.8 (32.3)**	**20.6 (32.1)**	**6.5 (8.5)**	**7.4 (8.8)**
Crop yield statistics	**Soybean**			
Subbasins	**BS**	**S1**	**S2**	**S3**
Sub basin 1	62.3 (76.9)	57.3 (67.3)	-3.4 (1.5)	-8.8 (-3.7)
Charles City	60.2 (73.9)	38.7 (45.9)	2.3 (9.5)	-3.1 (4.3)
New Providence	57.4 (74.5)	64.3 (72.1)	2.6 (11.7)	-2.8 (7.1)
Marshalltown	70.2 (71.7)	50.2 (70.9)	10.1 (17.0)	5.4 (12.6)
Cedar Rapids	64.8 (70.0)	54.5 (60.1)	5.5 (7.0)	0.8 (2.2)
Iowa City	54.2 (61.3)	35.6 (59.4)	1.6 (4.0)	-4.3 (-1.4)
Lone Tree	57.6 (64.1)	50.4 (61.2)	9.7 (14.4)	5.3 (10.2)
Old Man's Creek	67.1 (61.7)	60.6 (54.2)	14.9 (14.9)	10.9 (10.7)
Wapello	65.2 (64.2)	57.2 (63.0)	3.8 (13.2)	-1.6 (8.6)
Overall*	**62.1 (68.7)**	**52.1 (61.6)**	**5.9 (10.3)**	**4.7 (6.7)**

Note. (i) * Average of absolute PBIAS values of individual stations (ii) KGE values were not reported since they were poor, due to the difficulty in matching the crop yield at the annual time-step

Since the model was calibrated for crop yield at only nine sub-basins, the ability of the model to describe spatial variations in crop yield for all 67 sub-watersheds within the Iowa Cedar Basin was evaluated further (**Figure 3.6**). For corn, only 12% of the sub-basins fell within the acceptable PBIAS window (-10 to 10%) for BS, while 95% and 97% of the sub-basins had acceptable PBIAS values for S2 and S3 scenarios, respectively. For soybean, the results were more dramatic, where no sub-basins with acceptable PBIAS existed in the BS scenario, while 51% and 78% of the sub-basins had acceptable PBIAS values for the S2 and S3 scenarios, respectively. It is possible that further model refinement of SWAT's crop representation is needed for better performance for soybean.

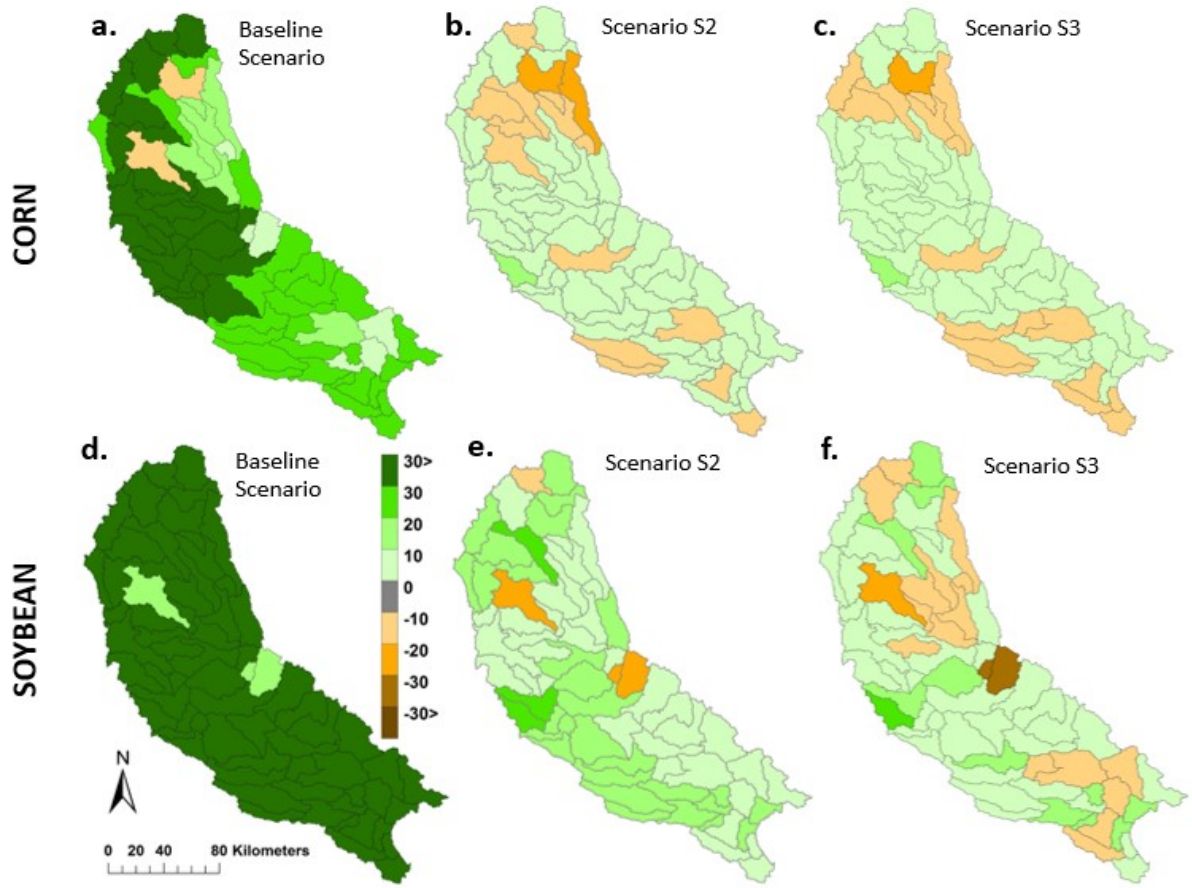

Figure 3.6. PBIAS estimates for corn (top row) and soybean (bottom row) at the sub-basin scale for BS (a and d), S2 (b and e) and S3 (c and f) scenarios. Note that, the S1 scenario was not included this point forward for comparison since results from S1 were very similar to the BS scenario

3.4.7 Model Performance Evaluation: Parameter Uncertainty

The impact of model refinement (BS vs. S2 vs. S3) on parameter uncertainty was evaluated by plotting the normalized uncertainty scores of the twelve parameters across all behavioral solutions (56 for BS, 19 for S2 and 19 for S3). A reduction in the interquartile range of the normalized uncertainty score indicates a reduction in uncertainty for the particular model scenario. Overall, there is a reduction in uncertainty for most of the parameters between the baseline and the S2 and S3 scenarios (CH_N2, SOL_Z, SOL_AWC, SOL_K, ESCO, EPCO, ALPHA_BF, and GW_REVAP), indicating that model refinement successfully constrained the parameter space. The reduction in uncertainty in the S3 scenario was generally more than the S2

scenario. Three of the parameters (SURLAG, GW_DELAY, and DEP_IMP) showed little difference in uncertainty between BS and S2 and S3 scenarios, while the most dramatic increase in uncertainty between the BS, S2 and S3 scenarios was apparent for CN2. The IQR of CN2 increased from 2 for the BS to 9 for the S2 and 14 for the S3 scenarios (**Figure 3.7**).

To understand this increase in uncertainty, the magnitude of the CN2 parameter was explored between the BS and the S2 and S3 scenarios. In the BS scenario, the CN2 parameter is tightly constrained with the best value being equal to 94, a curve number magnitude that more closely represents urban areas with impervious land cover (Curve Number = 98, USDA-NRCS, 2004) than agricultural areas that characterize the ICB. In contrast, the best parameter value of CN2 under the S2 and S3 corresponds to CN2 values of 76 and 73, which is closer to curve number values that can be expected for this watershed given soil type and predominant land-use. Based on USDA-NRCS (2004), the average runoff curve number value, for soil hydrologic group B, which covers 97% of agricultural lands in the study area, and agricultural row crops under multiple residue cover treatments, corresponds to 76. Thus, even though the BS scenario led to a more tightly constrained CN2 estimate, it led to a hydrologically unrealistic estimate of CN2 compared to the other two scenarios.

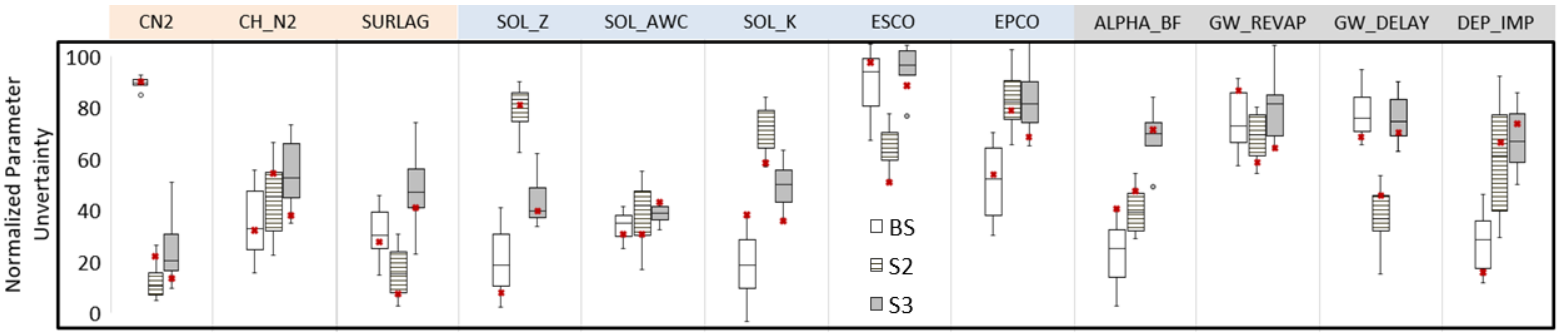

Figure 3.7. Normalized parameter uncertainty scores of the calibration parameters for the Baseline, S2, and S3 scenarios. The red marker on each box plot indicates the positioning of the normalized best parameter value. Increase in the inter-quartile range of the normalized scores implies an increase in parameter uncertainty. Parameters CN2 and DEP_IMP show an increase in uncertainty, CH_N2, SOL_Z, SOL_AWC, SOL_K, ESCO, EPCO, APPHA_BF, GW_REVAP show a decrease in uncertainty, while SURLAG and GW_DELAY show no significant change in uncertainty between the BS and the S2 and S3 scenarios

3.4.8 Prediction Uncertainty and Equifinality

Model refinement led to a decrease in prediction uncertainty. Specifically, the p-factor in model predictions decreased from 0.39 in BS to 0.26 in S2 and 0.31 in S3, while the *r* factor decreased from 0.44 in the BS scenario to 0.16 in S2 and 0.14 in S3. Achieving a low r-factor also reduces the p-factor, and thus, there should be a reasonable trade-off between these two factors (Yang *et al.,* 2008; Ekstrand *et al.,* 2010; Abbaspour., 2012; Bouda *et al.,* 2012; Zuo *et al.,* 2015). The results indicate that while almost the same amount of observed streamflow variability is captured within the 95 PPU band for all three scenarios (39% of observed data in BS versus 31% in S3), a narrower uncertainty band was achieved in scenario S3, with flow partitioning and crop yield inclusion, compared to the baseline scenario (0.44 in BS compared to 0.14 in S3). This demonstrates that the inclusion of flow partitioning and crop yield constraints in calibration reduced the prediction uncertainty (**Table 3.4**).

Table 3.4. Prediction Uncertainty Estimation for three scenarios (BS, S2, and S3)

	p - factor			r - factor		
Stations	**BS**	**S2**	**S3**	**BS**	**S2**	**S3**
Charles City	0.35	0.27	0.32	0.35	0.15	0.14
New Providence	0.34	0.27	0.26	0.64	0.24	0.19
Marshalltown	0.43	0.29	0.29	0.52	0.18	0.15
Cedar Rapids	0.40	0.28	0.36	0.45	0.16	0.15
Iowa City	0.38	0.24	0.29	0.42	0.16	0.13
Lone Tree	0.37	0.22	0.32	0.33	0.15	0.12
Old Man's Creek	0.40	0.24	0.30	0.40	0.15	0.12
Wapello	0.47	0.29	0.33	0.45	0.16	0.14
Overall	**0.39**	**0.26**	**0.31**	**0.44**	**0.16**	**0.14**

* Values are calculated for the period 1993-2002

We further evaluated whether model improvement led to a reduction in equifinality by analyzing the simulations that led to the top 2.5% KGE estimates (behavioral solutions) for both BS and S3 scenario. The analysis revealed that the baseline scenario had 56 behavioral solutions, while both S2 and S3 had only 19 behavioral solutions. The reduction in the number of behavioral solutions due to the inclusion of additional crop yield and flow partitioning constraints indicates a reduction in equifinality of the model simulations.

3.4.9 Model Predictive Ability at Daily Time-scale

The model was calibrated and validated at the monthly timescale. To further evaluate the effect of developing a more hydrologically consistent model on streamflow statistics, the ability of BS, S2, and S3 scenarios to predict daily streamflow were estimated. The BS and S2 scenarios were not able to capture the daily streamflow statistics (**Table 3.5**) despite being able to describe the monthly streamflow (**Table 3.1**). The overall KGE improved from -0.46 (-0.75) in BS to -0.06 (-0.36) in S2 and 0.73 (0.66) in S3 during the calibration (validation) periods (**Table 3.5**). The overall RSR reduced from 2.16 (2.48) in BS to 1.69 (2.03) in S2 and 0.69 (0.80) in S3 during the calibration (validation) periods (**Table 3.5**). There was no significant improvement in the PBIAS metric between the different scenarios. The improvement achieved in the S3 scenario is also clearly visible in the daily hydrographs (**Figure 3.8**).

Improvement in daily streamflow statistics from BS to S2 and S3 is attributed primarily to the increase in flow through the subsurface pathway. Modification of the evapotranspiration method from BS to S2 did lead to an increase in the subsurface flow contribution from 2% of water yield to 26% of water yield, but the increase was not substantial enough to generate adequate daily streamflow metrics, although it generated adequate monthly metrics. A substantial increase in flow through the subsurface pathway (88% of total water yield) was achieved in S3 due to change of the flow partitioning method, and this led to a substantial improvement in the daily streamflow statistics. Such increased water availability in the subsurface system could have triggered the drain tile lag time (GDRAIN) and baseflow recession constant parameter (ALPHA_BF), which has the potential to affect the hydrograph at the daily time step. **Figure 3.7** reveals that ALPHA_BF's interquartile range under S2 and S3 scenarios have reduced by 20% and 50%, respectively when compared with BS, which in-turn indicates that ALPHA_BF was constrained more in S3 than S2. This shows that improvement in daily streamflow statistics could be attributed to the inclusion of flow partitioning constraints in the S3 scenario. Generally, there is no guarantee for a monthly calibrated model to provide reasonable daily statistics since the parameter values are aligned towards matching the monthly flow values which could suppress the errors at the daily time step (Sudheer *et al.,* 2007). The ability of the refined model to capture daily streamflow statistics, despite being calibrated at the monthly time scale, demonstrate the increase of the hydrologic consistency of the model by the modifications.

Table 3.5. Comparison of daily streamflow statistics (KGE, RSR, and PBIAS) of all eight discharge calibration targets for BS, S2, and S3

Daily streamflow statistics	**KGE**		
Stations	**BS**	**S2**	**S3**
Charles City	-0.26 (-1.12)	0.26 (-0.54)	0.65 (0.61)
New Providence	-0.70 (-0.30)	-0.06 (0.17)	0.80 (0.74)
Marshalltown	-0.29 (-0.52)	0.15 (-0.08)	0.87 (0.81)
Cedar Rapids	-0.59 (-0.96)	-0.05 (-0.43)	0.77 (0.72)
Iowa City	-0.61 (-0.85)	-0.30 (-0.56)	0.64 (0.56)
Lone Tree	-0.15 (-0.26)	-0.07 (-0.13)	0.70 (0.66)
Old Man's Creek	-0.52 (-0.84)	-0.26 (-0.60)	0.69 (0.60)
Wapello	-0.59 (-1.14)	-0.18 (-0.68)	0.72 (0.59)
Overall	**-0.46 (-0.75)[a]**	**-0.06 (-0.36)[a]**	**0.73 (0.66)[a]**

Daily streamflow statistics	**RSR**		
Stations	**BS**	**S2**	**S3**
Charles City	1.99 (2.82)	1.37 (2.18)	0.73 (0.88)
New Providence	2.34 (1.93)	1.62 (1.37)	0.59 (0.66)
Marshalltown	1.96 (2.22)	1.42 (1.69)	0.50 (0.59)
Cedar Rapids	2.36 (2.78)	1.74 (2.17)	0.63 (0.75)
Iowa City	2.36 (2.66)	1.99 (2.33)	0.87 (0.98)
Lone Tree	1.70 (1.90)	1.58 (1.72)	0.70 (0.80)
Old Man's Creek	2.24 (2.61)	1.94 (2.32)	0.80 (0.90)
Wapello	2.35 (2.96)	1.86 (2.43)	0.73 (0.88)
Overall	**2.16 (2.48)[a]**	**1.69 (2.03)[a]**	**0.69 (0.80)[a]**

Daily streamflow statistics	**PBIAS**		
Stations	**BS**	**S2**	**S3**
Charles City	-13.9 (-25.1)	0.2 (-16.2)	3.9 (-11.6)
New Providence	-11.9 (-0.1)	-1.0 (8.5)	-5.7 (5.2)
Marshalltown	0.7 (-6.7)	-0.6 (5.2)	1.6 (-5.3)
Cedar Rapids	3.4 (-4.4)	7.5 (-0.6)	10.9 (1.6)
Iowa City	3.9 (9.0)	-1.8 (3.5)	6.3 (7.0)
Lone Tree	4.0 (5.1)	-10.8 (-8.5)	7.7 (0.3)
Old Man's Creek	5.6 (8.0)	-3.1 (0.5)	7.8 (5.4)
Wapello	8.5 (2.6)	7.1 (1.4)	13.7 (5.0)
Overall	**6.32 (7.51)[b]**	**4.0 (5.5)[b]**	**7.02 (5.18)[b]**

[a] Average of KGE / RSR values of individual stations

[b] Average of absolute PBIAS values of individual stations

Values outside (inside) parentheses are for the period 1993-2002 (2003-2012)

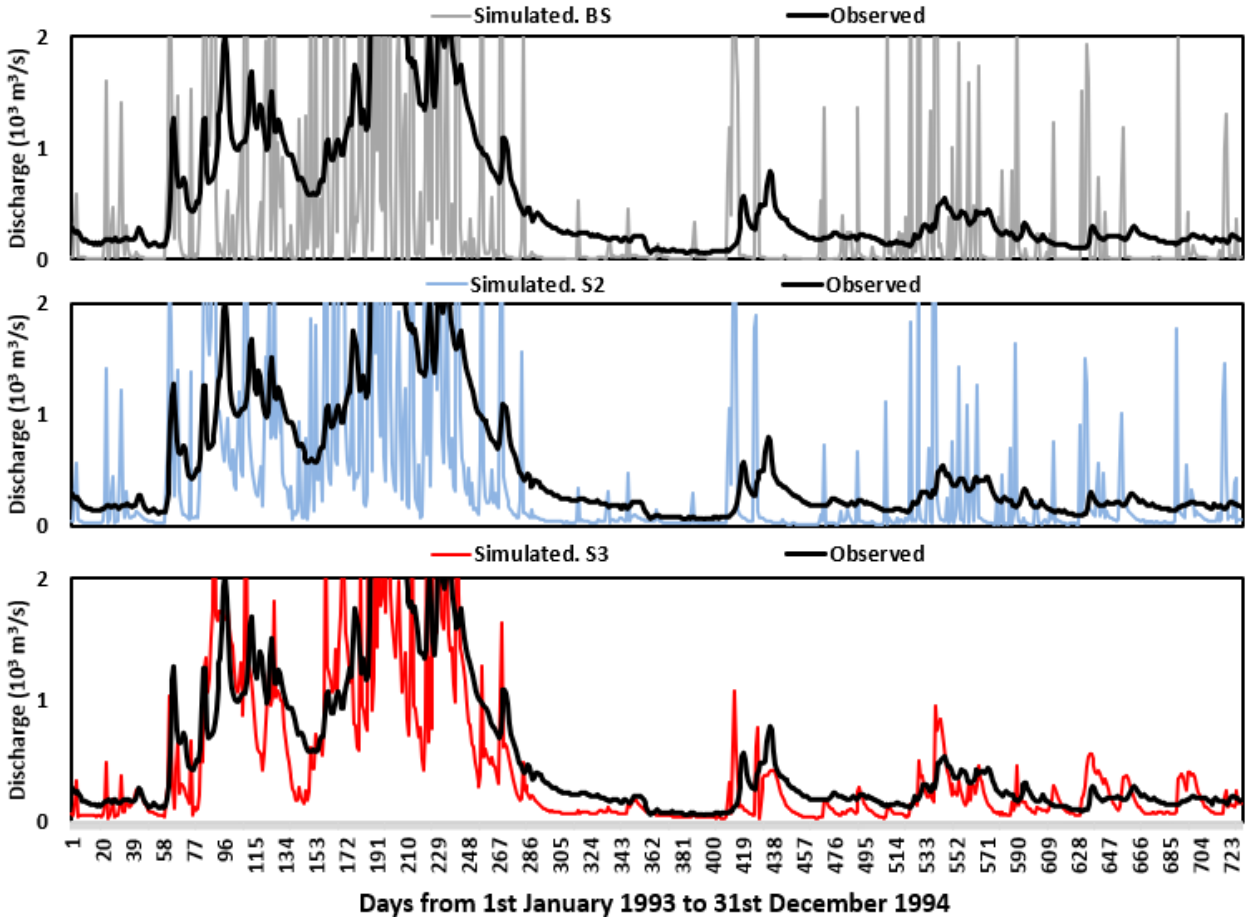

Figure 3.8. Comparison of daily discharge at Wapello outlet for Baseline Scenario (grey line), Scenario S2 (blue line) and Scenario S3 (red line) during 1993-1994. Observed data is shown as a black line. Simulated discharge of Scenario S3 corresponds well with the observed discharge data (black line) than the simulated discharge of BS and S2 Scenario

3.4.10 Model predictive ability for Nitrogen Fluxes

The ability of the model to predict annual nitrate loads without any calibration was also evaluated. The baseline scenario and S2 scenario showed significant underprediction (PBIAS = 61% for BS and 28%) of nitrate loads whereas PBIAS was only equal to -10% without any calibration for S3 (**Figure 3.9**). The capability of the S3 model setting to predict nitrate loads similar to that of observed values is attributed to both proper simulations of crop yield and appropriate flow partitioning. In S3, more water is diverted to the subsurface flow pathway that

accesses nitrogen stores, leading to an increase in the nitrate flux values closer to the measured values. Thus, the hydrologic consistency of models increases their ability to describe solute transport.

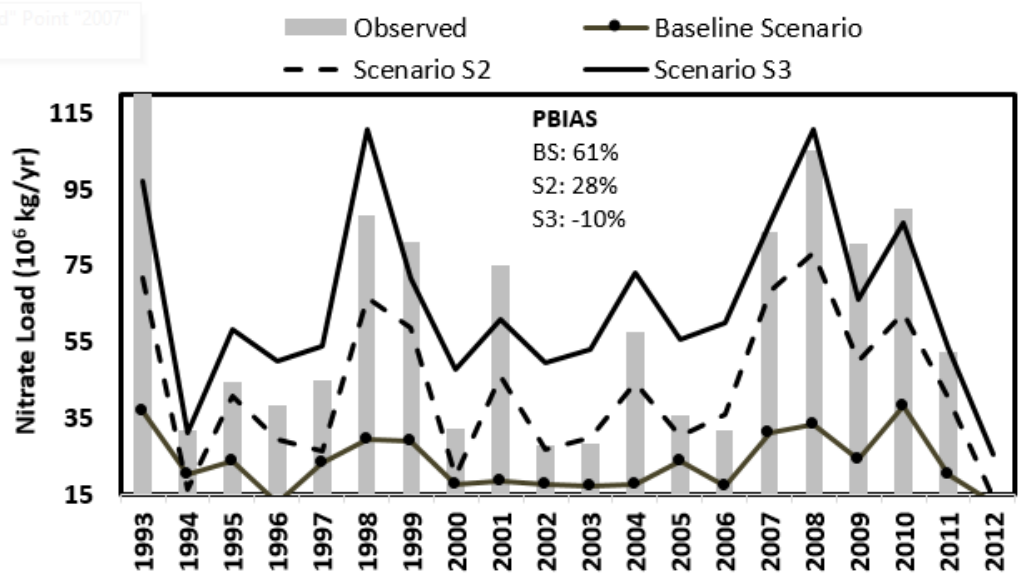

Figure 3.9. Comparison of annual nitrate loads at Wapello outlet for Baseline Scenario (BS), Scenario S2, and Scenario S3 during 1993-2012. S3 predicts nitrate loads closer to observed values even when the model is not calibrated for nitrate loads

3.5 Summary and Conclusions

Hydrologic models are most commonly only calibrated for streamflow at one or multiple stations within the watershed. These calibrated models are then used to predict future streamflow and water quality trends. It is well established now that large, heavily parametrized, hydrologic models are often subject to issues of equifinality where multiple parameter combinations can lead to similar streamflow prediction. It has been argued that this issue can be somewhat addressed using a diagnostic model evaluation with ancillary data (e.g., soil moisture) and sometimes soft data to detect structural model deficiencies. One of the most commonly available datasets for hydrological models in agricultural areas is information on crop yield that is routinely collected and archived. Here, we show, using a case study of a 32,660 km^2 large

agricultural watershed in the Midwestern US how the inclusion of crop yield data and soft data (flow partitioning) for model calibration increases the hydrological consistency of the model, and thus its predictive ability.

A hydrologic model was first developed using the Soil and Water Assessment Tool (SWAT) and was able to reproduce very well the monthly streamflow statistics at eight stations within the watershed (KGE, RSR, and PBIAS). However, when the crop yield estimates from the model were compared with available crop yield data from the agricultural census, the model severely underestimated crop yield (PBIAS corn = 26%, and PBIAS soybean = 61%). This low crop yield was the product of a landscape where the soil water content was low, and the corn and soybean crops were water stressed for 27 and 33 days respectively, during the 150 days growing period. This is an unrealistic scenario for a humid Iowa landscape, except maybe for some very dry years. The next step of model refinement (scenario S1) involved performing a multi-objective calibration by adding crop yield as a calibration target. While this led to a slight improvement in crop yield (PBIAS corn = 27%, and PBIAS soybean = 52%) and a reduction in water stress (corn:14 days and soybean: 28 days), the results remained unsatisfactory.

A diagnostic model evaluation allowed us to identify high potential evapotranspiration (PET) estimated by the most commonly used Penman-Monteith method to be the underlying cause of the model deficiency. Altering the PET method to Hargreaves method (scenario S2) decreased the PET, and thus led to excellent crop yield statistics (PBIAS corn = 2%, and PBIAS soybean = 9%), while not significantly altering the streamflow statistics. Although PM-PET is the most commonly used PET formulation in hydrologic models (Schneider *et al.,* 2007; Earls and Dixon, 2008), recent study has shown that they lead to consistent overestimation (Milly and Dunne, 2016) and alternate methods like the Hargreaves, Makkink and Priestley-Taylor PET methods can often lead to more reasonable estimates (Wang *et al.,* 2006; Schneider *et al.,* 2007; Earls and Dixon, 2008; Sperna Weiland *et al.,* 2012; Alemayehu Tadesse *et al.,* 2016; Samadi, 2016). Indeed, in the Milly and Dunne (2016) study, it was found that the continental drying projected by most global studies is merely a methodological artifact of the PM-PET method. Sperna-Weiland *et al.* (2012) argued against using PM-PET for future climate scenarios, due to its higher data requirement and sensitivity towards input data. These studies imply that the use of the most common PM-PET method does not always guarantee reasonable PET estimates, and

this study also confirm these findings. What is interesting is that despite such an overestimation of PET, the model was able to capture the discharge statistics adequately by reducing the actual evapotranspiration to realistic values by allowing the crops to die, such that actual evapotranspiration and thus, streamflow is similar for all three scenarios -- a classic example of getting the right streamflow but for the wrong reasons.

The final stage of model refinement involved exploring the partitioning of flow between the surface and subsurface flow pathways. In the model scenario S2, only 17% of the flow was routed through the tiled pathway, despite the watershed being 68% tile drained. To address this issue, the flow partitioning method in SWAT was changed from the more traditional soil moisture based curve number method to the evapotranspiration based curve number method. This structural change and manual calibration contributed to 67% of the flow to be transmitted through the tiled pathway, in accordance with values estimated for nearby watersheds. A more rigorous calibration could be done if measured values of tile flow are available at the site. However, the use and value of such "soft data" for model calibration are increasingly being recognized as critical for increasing the consistency of hydrologic models (Seibert and McDonnell, 2002; Arnold *et al.,* 2015; Pfannerstill *et al.,* 2017; Shafii *et al.,* 2017).

Increasing the consistency of the hydrological model by incorporating crop yield information, and soft data on flow partitioning had multiple benefits. First, it led to a reduction in model predictive uncertainty by reducing the 95% prediction interval of the model predictions, and also reduced parameter uncertainty and equifinality in model predictions. Second, the modified model proved to be superior in predicting daily flows, despite being calibrated at the monthly timescale. And finally, increasing the hydrologic consistency of the model increased its ability to predict nitrate fluxes without any calibration. The study highlights the value of using soft data and ancillary datasets like crop yield information to improve the consistency of hydrologic models.

Chapter 4: A Race against Time: Modelling Time Lags in Watershed Response

4.1 Abstract

Land-use change and agricultural intensification have increased food production but at the cost of polluting surface and groundwater. Best management practices implemented to improve water quality have met with limited success. Such lack of success is increasingly attributed to legacy nutrient stores in the subsurface that may act as sources after reduction of external inputs. However, current water quality models lack a framework to capture these legacy effects. This study uses a modified Soil Water Assessment Tool (SWAT) model to capture the effects of nitrogen (N) legacies on water quality under multiple land-management scenarios. The new SWAT-LAG model includes (1) a modified carbon-nitrogen cycling module to capture the dynamics of soil N accumulation, and (2) a groundwater travel time distribution module to capture a range of subsurface travel times. Using a 502 km^2 Iowa watershed as a case study, we found that between 1950 and 2016, 25% of the total watershed N surplus (N Deposition + Fertilizer + Manure + N Fixation – Crop N uptake) had accumulated within the root zone, 14% had accumulated in groundwater, while 27% was lost as riverine output, and 34% was denitrified. In future scenarios, a 100% reduction in fertilizer application led to a 79% reduction in stream N load, but the SWAT-LAG results suggest that it would take 84 years to achieve this reduction, in contrast to the two years predicted in the original SWAT model. The framework proposed here constitutes a first step towards modifying a widely used modeling approach to assess the effects of legacy N on time required to achieve water quality goals.

4.2 Introduction

Human modification of the nitrogen (N) cycle has resulted in a twofold increase in the fixation of reactive N compared to pre-industrial levels (Galloway *et al.,* 1995). This increase can be primarily attributed to emissions from burning fossil fuels, fertilizer production, and leguminous crop production (Galloway *et al.,* 2004; Vitousek *et al.,* 1997). It is estimated that around 50% of the total inorganic N used thus far has been applied in the last 15 years (Howarth *et al.,* 2002; Townsend *et al.,* 2003), and food produced as a result of inorganic N fertilizer now

feeds more than 45% of the world's population (Smil, 2011). High levels of N fertilizer use have significantly perturbed the global N cycle, and it has been argued that planetary boundaries for maintaining human and ecosystem health have been exceeded (Rockström *et al.,* 2009). Increased N flux to coastal and inland waters has accelerated eutrophication, reduced biodiversity through species loss, and significantly reduced the coastal fish catch (Vitousek *et al.,* 1997). The inputs are expected to increase even further in the future to meet the food demands of a growing global population (Vitousek *et al.,* 1997).

Recognition of the detrimental effects of agricultural intensification has led to the adoption of various best management practices (BMPs) for improving water quality. However, these interventions have, in many cases, not led to expected improvements. For example, attempts have been made to reduce inorganic fertilizer inputs in the United Kingdom since the 1980s; however, no substantial decrease has been observed in riverine N concentrations (Howden *et al.,* 2010). In the Susquehanna River Basin, while fertilizer application rates were constant between 1971 and 2002, the riverine nitrate load continued to increase (Van Meter *et al.,* 2017). A recent study in the Yongan river watershed of China shows that stream N concentrations have been increasing consistently, despite reductions in inorganic fertilizer inputs since 1999 (Chen *et al.,* 2014). Similarly, in a review study, Grimvall *et al.,* (2000) show that despite reductions in fertilizer application since the 1990s, the majority of Eastern European rivers have failed to show any reduction in riverine N loads.

The time lags, defined as the time between implementation of agricultural BMPs and improvements in stream water quality, are increasingly recognized as an important factor behind the "apparent failure" of BMPs (Fenton *et al.,* 2011; Meals *et al.,* 2010; Van Meter & Basu, 2015). Meals *et al.* (2010), in a data synthesis study, found that time lags can range from five to more than 50 years and are a function of watershed size, soil type, climate, and management practices. Van Meter and Basu (2017) have estimated watershed lag times to be between 12 and 34 years in the Grand River Watershed in Southern Ontario.

Van Meter and Basu (2015) conceptualized time lags in nitrate response as the sum of two components: (a) a hydrologic time lag that arises from accumulation of dissolved nitrate in the vadose zone and groundwater reservoirs, and (b) a biogeochemical time lag that arises due to

accumulation of soil organic N in the root zones of agricultural soils. While the existence of hydrologic time lags is well accepted, the recognition of biogeochemical time lags for N is relatively recent (Burt *et al.,* 2010; Chen *et al.,* 2014; Van Meter & Basu, 2015). In a recent study, Van Meter *et al.,* (2016) analyzed soil core data from 61 agricultural sites across Iowa that were sampled in 1959 and again in 2007 and observed a net 14% increase in soil N (1478±547 kg/ha) over a depth of 0 to 100 cm.

Despite recognition that the buildup of nutrient legacies can lead to time lags in watershed response, there has until recently been no modeling framework that can predict the time lags. Most watershed models, like the Soil Water Assessment Tool (SWAT) that are used to predict the impact of BMPs can predict the magnitude of the concentration reduction that might be finally achieved, but not how long it will take to achieve that reduction. For policymakers, however, knowing the time required to meet concentration reduction goals is critical to making informed choices.

Recognizing the need to model time lags, Van Meter and Basu (2015) developed a parsimonious, travel time-based approach to quantify time lags, and this method was further refined by adding a simplified biogeochemistry module in Van Meter *et al.* (2016). The model thus developed, also referred to as the ELEMeNT model (Exploration of Long Term Nutrient Trajectories), was able to describe time lags at the outlet of the Mississippi River Basin (Van Meter *et al.,* 2018). However, while the ELEMeNT model can capture long-term trends in soil and stream N, it is not designed to simulate complex agroecosystem dynamics, including the variations in crop type and nutrient management that are routinely handled in agricultural models like SWAT. Accordingly, the present study has two primary objectives: (1) to modify the existing SWAT model to capture time lags in watershed response, and (2) to use the modified model to quantify N time lags under various management scenarios. Specifically, this chapter focuses on two aspects of SWAT modification: (i) refining the ability of SWAT to describe N accumulation in soils that lead to the creation of biogeochemical legacy and time lags, and (ii) coupling SWAT with a travel time distribution model to capture time lags due to slow groundwater flow pathways.

4.3 Modeling Framework: Development of SWAT-LAG to represent Time Lags

A new version of SWAT, SWAT-LAG, was developed by integrating a travel time distribution model into the existing SWAT model. The new SWAT-LAG model accounts for time lags arising from legacy nutrient accumulation in both soil and groundwater reservoirs. In the following sections, the background on the SWAT model, the travel time distribution model, and the model coupling were provided.

4.3.1 SWAT Model: Background and Limitations

SWAT is a watershed-scale, process-based, continuous simulation model that works at a daily time step. In this model, a watershed is divided into sub-basins that are further subdivided into Hydrologic Response Units (HRUs), characterized by the unique soil, slope, land-use, and management attributes. Each HRU is vertically discretized into three compartments, the soil profile (0-2 m), the shallow aquifer (2-20 m), and the deep aquifer (>20 m) (Narula and Gosain, 2013). Runoff and nutrients generated by each HRU are aggregated at the top of the reach specific to the subbasin and then routed through that reach towards the watershed outlet.

One of the most critical model components for adequate representation of nutrient fluxes is the carbon-nitrogen (C-N) cycling module within the soil profile. The most commonly used SWAT formulation for C-N cycling (hereafter referred to as SWAT), tracks five different N pools in the soil: two inorganic N pools (ammonia and nitrate), and three organic N pools (fresh, stable and active). Nitrogen dynamics are driven by water, temperature, soil moisture conditions, and plant uptake. It has been argued that this formulation overlooks several key factors controlling organic carbon dynamics in the soil, including the movement of organic carbon with water and the loss of organic C through soil erosion (Zhang *et al.,* 2013). Recognizing this limitation, Zhang *et al.* (2013) integrated more rigorous C-N cycling equations into the SWAT framework that are adapted from a more complex field-scale agroecosystem model, the CENTURY model. The modified model hereafter referred to as SWAT-M, can accurately capture greenhouse gas emissions from agricultural sites under different soil, climate, and management practices (Zhang *et al.,* 2013).

The other major limitation of the SWAT model is its ability to accurately describe nitrate transport component through the subsurface (Bouraoui *et al.,* 2005; Ekanayake and Davie.,

2005). While SWAT considers a lag time in modeling lateral flow and groundwater flow, the magnitude of this lag time is generally of the order of a few days and represents the recession behaviour of the hydrograph, but not the slow groundwater pathways that have been implicated in longer-term delays in nitrate response (McDonnell and Beven, 2014; Van Meter *et al.,* 2016). Or, in other words, while the parameters GW_DELAY, LAT_TTIME and SURLAG provide information on the celerity of water in the watershed, they do not describe the velocity of water (McDonnell and Beven, 2014). Thus, while SWAT (default SWAT model) can predict what will be the final streamflow nitrate concentration many years after the land-use change (after the system has reached a steady state), it provides no information on the time required to achieve that change in concentration, information that is critical for policymakers and managers.

4.3.2 SWAT-LAG: SWAT coupled with a Travel Time Distribution (TTD) model

To address the issues identified in the above section, the SWAT-LAG model was developed by coupling the SWAT-M model (Zhang *et al.,* 2013) with a travel time distribution model, which includes simulation of N transport through slower groundwater pathways. The new SWAT-LAG model describes the groundwater mass loading $J_{b,lagged}$ (t) (M/T) at the watershed outlet as a function of the groundwater load through the baseflow pathway simulated in SWAT-M, $J_b(t)$, and the travel time distribution $f(\tau)$ as

$$J_{b,lagged}(t) = \int_0^\infty J_b\,(t-\tau)\,f(\tau)\;d\tau \qquad \textbf{(Eq. 4.1)}$$

The modeled nitrate flux at the watershed outlet J(t) is then calculated as the sum of the nitrate flux through surface flow ($J_{surfaceflow}$), lateral flow ($J_{lateralflow}$), tile flow ($J_{tileflow}$), and lagged baseflow ($J_{b,lagged}$) (estimated from **Eq. 4.1**) (**Figure 4.1)**. The outlet nitrate flux is calibrated against the measured stream nitrate data using the Dynamically Dimensioned Search (DDS) algorithm (Tolson and Shoemaker, 2007), in OSTRICH calibration tool (Matott, LS. 2017). In the present study, the coupling of SWAT and the Travel Time Distribution (TTD) model was performed externally using MATLAB (MATLAB, 2018) where for each calibration run, MATLAB extracted Jb(t) from SWAT-M output files and estimated $J_{b,lagged}(t)$ and J(t) (**Figure B5**). Modifications to SWAT-M source code to capture nitrogen legacies were described in Appendix Section B3 (Zhang *et al.,* 2013), while details on assumptions regarding biogeochemical losses are presented in Appendix Section B4.

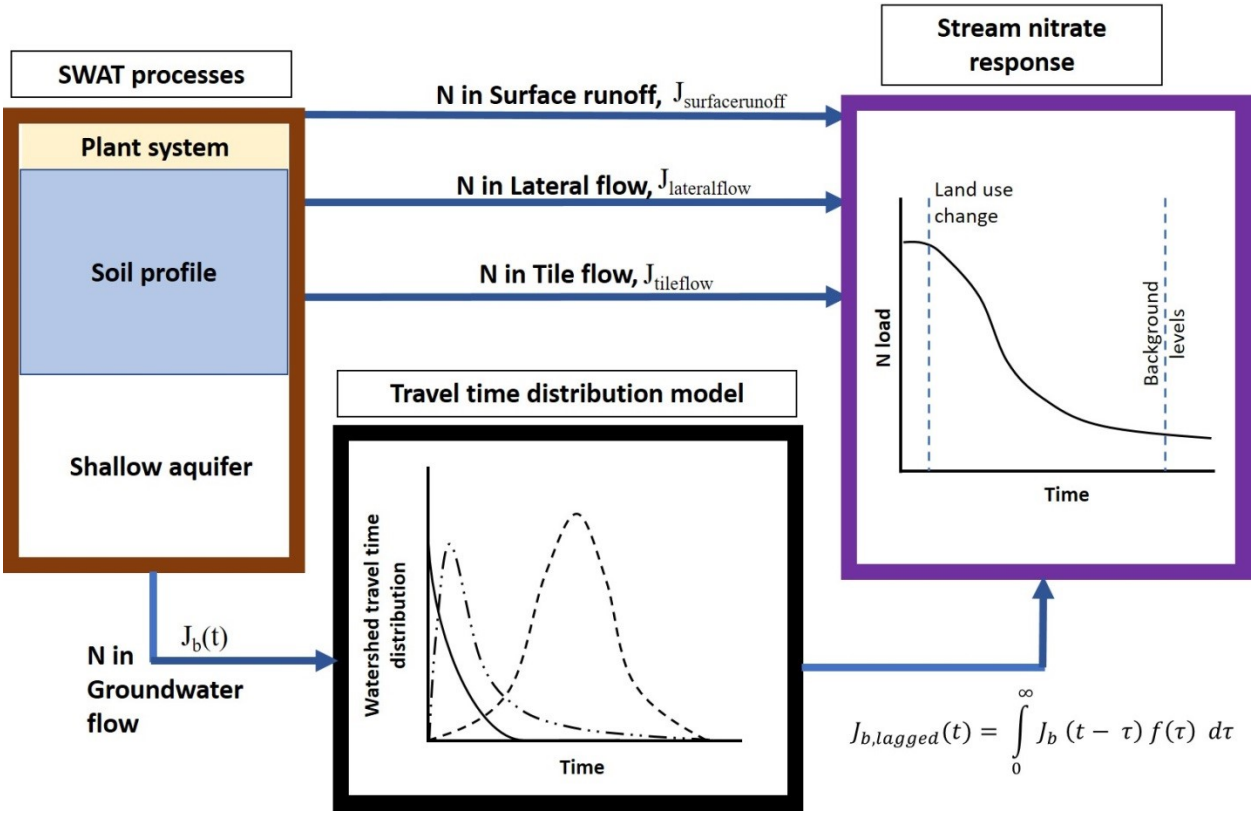

Figure 4.1. Conceptual modeling framework showing the coupling of SWAT-M with the travel time distribution model to create SWAT-LAG model

4.4 Materials and Methods

4.4.1 Study Site

The South Fork Iowa River Watershed (SFIRW), a 502 km^2 predominantly agricultural watershed that is a part of the Iowa-Cedar basin in the Midwestern U.S (**Figure 4.2**), was used in the present study to evaluate the role of legacy nitrogen on time lags in watershed response. The South Fork is representative of typical watersheds in the Midwestern US that contribute significant N loads to the Mississippi River, and thus was a good candidate for analysis. The mean annual rainfall over this watershed is 83 cm, and the mean monthly temperature varies between -7.7 ^{0}C and 23.4 ^{0}C. The watershed lies in the Des Moines Lobe in Iowa, which is characterized by poorly drained soils with low relief and is drained by subsurface tile drains (Green *et al.,* 2006; Tomer *et al.,* 2008). The dominant soil type is Clarion (fine loam), which

makes up 73.8% of the watershed. Land-use in the watershed is dominated by row-crop agriculture (86% of the area under corn-soybean rotations), followed by urban (6.59%) pasture (4.09%), and forest (2.47%).

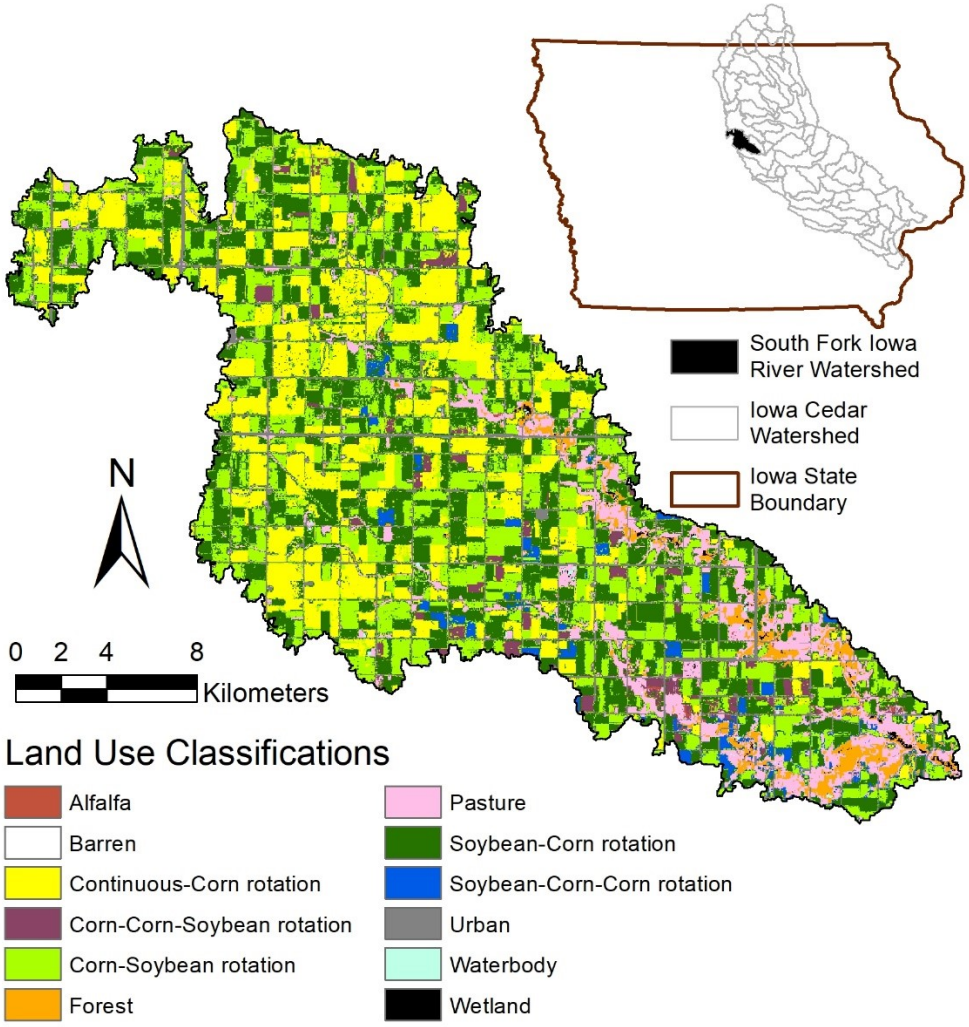

Figure 4.2. Site map showing the location of South Fork Iowa River watershed (SFIRW) and the current land-use (depicting crop rotations) obtained by overlaying 9-year (2004-2012) Crop Data Layers (CDLs) in ArcGIS

4.4.2 SWAT Input Datasets and Model Parameters

Streamflow and nitrate concentration data from 1996 to 2015 were obtained for the gauging station ID 05454300 at the outlet of SFIRW from USGS (2016). Streamflow data were available at the daily timescale, while N concentration data were available at the monthly frequency. The

Weighted Regression on Time, Discharge and Season (WRTDS) model was used to estimate the monthly stream nitrate flux from the sparse data, and these monthly values were used for model calibration and validation (Hirsch *et al.,* 2010; Corsi *et al.,* 2015). Monthly stream nitrate fluxes simulated using WRTDS corresponded well with the observed nitrate flux values with a percent bias (PBIAS) of 2%. The watershed has only one weather station for which daily rainfall and temperature data were obtained from the US National Weather Service (NWS), n.d., United States Environmental Protection Agency (US-EPA, 2013) and Iowa Environmental Mesonet, n.d. for the period 1950 to 2016. SWAT's weather generator was used to simulate solar radiation, relative humidity, and wind speed. Evapotranspiration was estimated using the Hargreaves Potential Evapotranspiration method (Nair *et al.,* 2011). Soil characteristics were obtained from the SWAT's State Soil Geographic Dataset (STATSGO) soil database. We defined 5 slope classes as 0-0.5%, 0.5-1.45%, 1.45-2%, 2-3.5% and >3.5%. The soil, land-use, and slope layers were intersected to create 395 unique HRUs with distinct attributes. The STATSGO soil database was used instead of the finer-resolution Soil Survey Geographic Database (SSURGO) database since increasing the number of HRUs beyond 395 would significantly increase the computational burden of the model. SWAT models that use the SSURGO database often reduce the number of HRUs by focusing on the most dominant HRUs and neglecting the contribution of the others. In this model, we needed a spatially distributed grid of HRUs to couple with the grid scale travel times, and thus the "dominant HRU" option was not feasible. A brief review of studies that compared nitrate flux estimates from STATSGO versus SSURGO inputs revealed mixed conclusions -- while Chaplot (2005) observed improved predictability when using SSURGO data, Geza and McCray (2008) and Bhandari *et al.* (2018) did not observe significant differences between STATSGO and SSURGO predictions. Also, the watershed was assumed to have only one sub-basin. Given the dynamic land use that had to be simulated in the model, adding more subbasins would have significantly increased the computational burden. Furthermore, a larger number of sub-basins is more important for routing that is relevant for daily predictions, while our focus was on decadal lag times.

All the agricultural HRUs with slopes less than 2% were assumed to have tiles (Green *et al.,* 2014) since site-specific tile drain data were not available. This assumption led to 58% of the watershed area (67% of the cropped area) being tile-drained. Depth to sub-surface drain (DDRAIN), time to drain soil to field capacity (TDRAIN) and drain tile lag time (GDRAIN)

values were set to 1000 mm, 48 h and 96 h respectively based on Green *et al.* (2006) and Nair *et al.* (2011). Initial soil N and C mass in 1949 were estimated at the HRU scale based on the regression equations developed by Van Meter *et al.* (2016), in which soil C and N is described as a function of soil type (% sand, silt, and clay). These calculations led to an area-weighted average initial organic N mass estimate of 16,347 kg/ha/yr across the SFIRW, which is close to the range 16,744 - 17,485 kg/ha/yr estimated by Van Meter *et al.* (2016).

Annual crop yield data were estimated using the methods outlined in Appendix Section B1 (Gassman, 2008; Hong *et al.,* 2013; USDA-Agricultural Census, 2012; USDA-Agricultural Survey, 2012). Mineral fertilizer applications rates, estimated using fertilizer sales data (Alexander and Smith, 1990 and USGS, 2012), varied between 2 kg/ha/yr and 211 kg/ha/yr across different years. Estimation of mineral fertilizer application rates was detailed in Appendix **Section B1** (Alexander and Smith, 1990; Sawyer, 2015; USGS, 2012). Manure application rates were estimated using the animal data in the USDA-Agricultural Census (2012) and nitrogen in animal excretion information from Hong *et al.,* (2011) (Appendix **Section B1**). The watershed has a large number of Concentrated Animal Feeding Operation (CAFO) lots (Tomer *et al.,* 2008), and manure produced in these CAFOs is known to be one of the major sources of fertilizer (McCarthy et al.,2012). The typical manure N application rates varied between 37 kg/ha/yr and 105 kg/ha/yr. HRUs under corn, oats, and hay received N fertilizer (inorganic and organic) while soybean and alfalfa HRUs were supplied with P_2O_5 at rates of 45 kg/ha/yr and 73 kg/ha/yr respectively based on Iowa State University's recommendation guide (Mallarino *et al.,* 2013).

4.4.3 Estimation of Travel Time Distribution

The travel time distribution, $f(\tau)$, was estimated using the GIS approach that was proposed by Schilling and Wolter (2007) and Basu *et al.* (2012) and that has been shown to capture groundwater travel times in Iowa landscapes adequately. In this methodology, the travel time τ corresponding to each point in the landscape is described by:

$$\tau = \frac{\text{length}}{\text{average linear velocity}} = \frac{L}{(K * i)/n} \qquad \textbf{(Eq. 4.2)}$$

Where L is the flow path length from each cell in the landscape to the nearest stream (m), K is the hydraulic conductivity (m/s), i is the hydraulic gradient, and n is the aquifer porosity. The primary assumption of this approach is that the water table follows the topography (Schilling and Wolter, 2007; Basu *et al.,* 2012), and thus the hydraulic gradient can be approximated as the ratio of the elevation difference (as estimated from the Digital Elevation Map, DEM) and the flow path distance L between the cell of interest and the nearest outlet.

Using the hydrology toolset in ArcGIS 10.4.1, the 30 m DEM (USGS, 2013) was filled to get the flow direction and flow accumulation raster. The stream network was created by applying a stream initiation threshold of 100 acres on the flow accumulation raster. Using the flow direction and the stream network raster, flow path length (L) (routed value along the flow direction network, towards the stream) was computed for each 30-m cell using the "Flow Length" tool. The hydraulic gradient was estimated using the DEM and the stream network. Saturated hydraulic conductivity (K) was extracted from SWAT's STATSGO soil database. Aquifer porosity was assumed to be equal to 0.3, following Schilling and Wolter (2007) and Basu *et al.* (2012). Average linear velocity was estimated for each 30-m cell in the watershed using K, i, and n as inputs, using the "Darcy Velocity" tool. Using "L" and average linear velocity rasters, the travel time for each 30-m cell in the watershed was computed. The mean travel time τ of each HRU was obtained by averaging the travel time of all cells inside each HRU.

4.4.4 Model Calibration, Validation and Uncertainty Estimation

The modified SWAT model (SWAT-LAG) was calibrated to simulate monthly discharge and nitrate loads, and annual crop yield. Parameters sensitive to hydrology, nitrate flux, and crop yield were selected based on extensive literature review (Baumgart, 2005; Green *et al.,* 2006; Hu *et al.,* 2007; Jha *et al.,* 2007; Kannan *et al.,* 2007; Le, 2015; Faramarzi *et al.,* 2009; Nair *et al.,* 2011), and a One-at-a-time (OAT) sensitivity analysis that was done manually. Fifty-two parameters were selected for calibration, and suitable upper and lower bounds were fixed based on literature values (**Table 4.1 and Table B2**). The model was calibrated from 1996 to 2008 and validated from 2009 to 2015 for monthly streamflow and nitrate flux (**Equation 4.4; Figure B2**).

Annual crop yields were calibrated from 1950 to 2008 and validated from 2009 to 2015 (**Equation 4.4**).

The OSTRICH calibration tool - a model-independent, flexible optimization program with a multi-objective calibration environment, was used for model calibration and validation. Multi-objective calibration was performed by assigning seven calibration targets (discharge, nitrate flux, corn yield, soybean yield, oats yield, alfalfa yield, and hay yield). The Dynamically Dimensioned Search (DDS) algorithm was used to calibrate the KGE values simultaneously in OSTRICH. Specifically, the KGE values of all seven calibration targets were aggregated to obtain the overall objective function (KGE*overall* in **Equation 4.4**) by assuming equal weights for all the calibration targets. Also, the DDS algorithm allowed for the PBIAS for the seven calibration targets to be constrained within ±10%. The DDS algorithm optimized the parameter solutions based on two conditions (i) increase the KGEoverall value towards 1 and (ii) constrain the PBIAS of all the seven calibration targets to be within ±10%. Multiple iterations were performed sequentially with 250 runs per iteration. OSTRICH provided an optimal solution at the end of each iteration, and the calibration parameter ranges were narrowed down manually with each iteration until no further improvement in results was observed. The KGE and PBIAS values were estimated using the optimal solution obtained in the final iteration. Acceptance criteria for KGE was formulated by synthesizing eleven studies as explained in Appendix **Section B2** (Formetta *et al.,* 2014; Hoch *et al.,* 2017; Hublart *et al.,* 2015; Kuentz *et al.,* 2013; Pechlivanidis *et al.,* 2010; Pechlivanidis and Arheimer, 2015; Rajib *et al.,* 2016; Revilla-Romero *et al.,* 2015; Thiemig *et al.,* 2013; Trautmann, 2016; Yang *et al.,* 2016) and **Table B3**. Moreover, the calibration methodology follows the findings of Chapter 3, i.e., consideration of crop yield as additional calibration targets, selection of appropriate PET estimation method (HG-PET), and inclusion of flow partitioning constraints.

$$\mathrm{KGE} = 1 - \sqrt{(r-1)^2 + (\alpha-1)^2 + (\beta-1)^2} \qquad \textbf{(Eq. 4.3)}$$

where r is the linear coefficient between the simulated and measured time series

$\alpha = \frac{\sigma_s}{\sigma_m}$; σ_s and σ_m are the standard deviation of simulated and measured series

$\beta = \frac{\mu_s}{\mu_m}$; μ_s and μ_m are the mean of simulated and measured time series

$$\text{KGE}overall = \frac{1}{n}[KGE_{streamflow} + KGE_{nitrate\ flux} + \frac{1}{x}\sum_{i=1}^{x} KGE_{crop\ yield}] \quad \textbf{(Eq. 4.4)}$$

where n = 3 and x = 5 (watershed scale crop yield for 5 crops)

$$\text{PBIAS} = 100 * \frac{\sum(Q_m - Q_s)}{\sum Q_m} \quad \textbf{(Eq. 4.5)}$$

where Q_m and Q_s are measured, and simulated data and PBIAS of all seven calibration targets were constrained to be within ±10%

The model prediction uncertainty was estimated as a function of both parameter uncertainty and input uncertainty. Parameter uncertainty was estimated by considering all the 250 parameter sets from the 250 DDS runs. In addition to parameter uncertainty, input uncertainty due to rainfall, fertilizer application rates and travel time were also estimated. Specifically, the rainfall, fertilizer application rates, and travel time magnitudes were varied by ±25% and created 281 parameter sets for estimation of input uncertainty. The input uncertainty was considered in conjunction with the parameter uncertainty to estimate the 95% prediction uncertainty (95 PPU) (Beven and Binley, 1992; Beven and Freer, 2001; Beven, 2006; Abbaspour. K. C., 2012) for discharge and nitrate load at a monthly time step.

4.4.5 Developing temporally varying land-use maps (crop rotations) in SWAT

As the final set of input parameters, time-varying land-use maps for the study were developed. One of the challenges in simulating a long trajectory of land-use change and nitrogen accumulation in SWAT is related to the appropriate representation of land-use change and crop rotation patterns over time. Capturing these trajectories is important, as the exact sequence of land-use change and rotation impacts legacy accumulation and depletion. As described below, to effectively simulate crop rotations and land-use change in SWAT, two different methodologies were used, dependent on data availability across the simulation period. Only agricultural census data was available before 2004, while more detailed crop data layers were available in the later period as described below.

For the period 1950–2003, the county (a subdivision of states in the U.S) scale information on annual cropped areas from USDA-Agricultural survey (2012) was used in conjunction with USDA-Agricultural Census (2012) data to estimate the annual area under each crop (**Figure B1**). Given the difficulty in reassigning HRUs continuously in time as a function of land-use change, the period was split into two time-blocks (1950-1960, 1961–2003) and maintained the land-use and crop rotation constant within each time block. The time-blocks were chosen based on land-use trends, as indicated by the survey data. Specifically, there was a dramatic shift in land-use between 1961-1964, with large increases in the area under soybean and decreases in the area under oats and hay. Average crop acreages within each time block were calculated as the mean of the time series of the cropped area within that block (**Figure B1**). The rotation history for each block was estimated based on prior knowledge regarding crop rotations in the Midwest (Anderson, 2005; Bruns, 2012). The resulting crop rotations and land-use data are presented in **Table B1**.

The methodology followed for the 2004-2012 period is based on Srinivasan et al.,(2010) and Teshager et al.,(2016) and involved using Crop Data Layers (CDL) from the National Agricultural Statistics Service (USDA-CDL, 2012). These CDL layers were intersected with the watershed and classified to identify the crop rotations. For example, if a CDL cell had corn from 2004 to 2012, it was considered to be continuous corn. Based on this analysis, the following rotation types were estimated in the study area: continuous corn (CC): 20.2%, soybean-corn (SC): 33.12%, corn-soybean (CS): 28.46%, corn-corn-soybean (CCS): 2.54%, soybean-corn-corn (SCC): 2.06%, continuous alfalfa (0.14%). Other land-use types included: forest (2.47%), pasture (4.09%), urban (6.59%), waterbody (0.1%) and wetland (0.23%) (**Table B1**). Since corn and soybean yields have been increasing since the 1950s due to the introduction of hybrid crop varieties, three different corn and soybean crop varieties were used in the three time-blocks to replicate the observed yield trends.

4.4.6 Model Runs and Scenario Formulation

The effect of model conceptualization on time lags was evaluated by comparing the default SWAT model with two modifications of SWAT that explicitly consider lag times in the landscape. The first modification, SWAT-M, involves the use of modified C-N cycling equations

to capture the accumulation of soil organic N. In the second modification, SWAT-LAG, SWAT-M was coupled with the travel time distribution model to capture hydrologic and biogeochemical time lags. All three model versions (SWAT, SWAT-M, and SWAT-LAG) were compared to evaluate differences in performance.

For future projections, only SWAT-LAG model was used and simulated four nutrient management scenarios and three land-use change scenarios for 84 years (2017-2100). Daily rainfall and temperature data corresponding to average rainfall year during the simulation period (1950-2016) was used to simulate the climate, following Muenich *et al.* (2016). The actual future climate scenarios were not used as the goal was to isolate the effects of landscape legacies and time lags. For the business-as-usual (BAU) scenario, the land-use and management practices from 2004-2016 were maintained from 2017 to 2100. We considered four nutrient management scenarios in which land-use was kept the same as BAU, but the fertilizer application on corn HRUs was reduced by 25% (NM1), 50% (NM2), 75% (NM3) and 100% (NM4). Also, three land-use change scenarios were considered, in which agricultural land was converted to land under switchgrass production. These scenarios were based on the U.S Renewable Fuel standard mandate that sets a goal of producing more than half of biofuel from cellulose-based sources (primarily switchgrass and miscanthus) by 2022. We used the Shawnee switchgrass (upland cultivar) and adopted the plant growth parameters outlined in Cibin *et al.* (2010) and Trybula *et al.* (2014), and a fertilization rate of 30 kg/ha/yr to maintain switchgrass yields. The three scenarios included planting switchgrass in all agricultural HRUs (LU1), planting switchgrass only in agricultural HRUs with slopes greater than 0.5% (LU2) or greater than 1.45% (LU3).

4.5 Results and Discussion

4.5.1 Groundwater Travel Time Distribution for the South Fork Iowa Watershed

Modeled groundwater travel times in the South Fork Iowa watershed ranged from 36 days in some areas of the watershed to more than 50 years in others (**Figure 4.3a**). Approximately 8% of the watershed has a travel time > 50 years, which corresponds to an area of poorly drained clayey soils. Travel times are much smaller (< 10 years) around the stream network where the soil is sandier and has a greater hydraulic conductivity. The distribution of travel times was described well by an exponential distribution (**Figure 4.3b**) with a mean travel

time of 13 years, which is similar to the mean travel time of 10 years estimated for the Walnut Creek Watershed in Northern Iowa (Schilling and Wolter, 2007; Basu *et al.,* 2012). The travel time distribution obtained from this analysis was convoluted with the nitrate fluxes generated in SWAT-M to generate lagged nitrate concentrations at the catchment outlet.

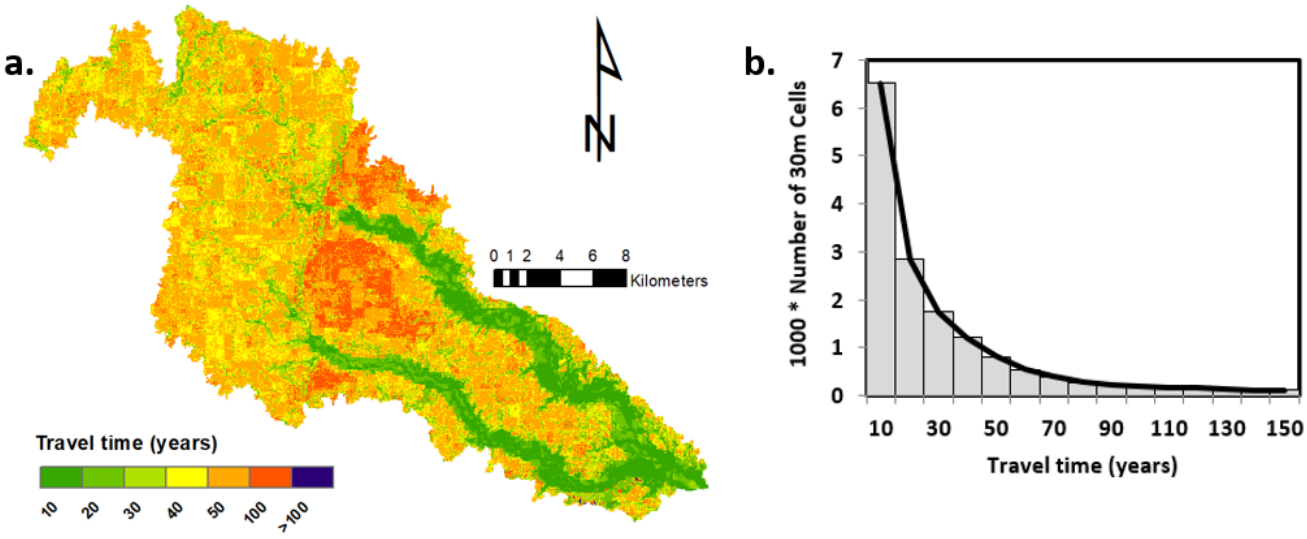

Figure 4.3. Groundwater Travel Time (a) map and (b) histogram for the South Fork Iowa River Watershed (SFIRW)

4.5.2 Model Calibration and Validation

We calibrated three model versions (SWAT, SWAT-M, and SWAT-LAG) and found the calibrated parameters to be not significantly different with respect to current and past predictions of crop yield, discharge, and nitrate flux. Similarities between the three approaches are most likely due to the water quality time series of 20 years being too short of capturing legacy effects. Since the calibrated parameters were not significantly different, to ensure consistency across model versions, we used the calibrated parameters from SWAT-LAG in SWAT and SWAT-M to evaluate the goodness of fit metrics for streamflow, nitrate flux, and crop yield. All three model versions (SWAT, SWAT-M, and SWAT-LAG) performed adequately, with KGE values for streamflow and nitrate flux ranging from 0.45 to 0.77, and PBIAS varying from -11.2% to 20.2%, respectively (**Figure B2, Figure B6, Figure B7** and **Table 4.2**). PBIAS values for crop

yield were also good, ranging from -7.6% to 14.9% (**Table 4.3**). For comparison, we have also presented model simulations from the individual calibrated models, and the statistics are not significantly different (Appendix **Figure B8** and **Figure B9**). For the remainder of this chapter, we have used SWAT-LAG's parameters to ensure a more accurate comparison of the three model versions. Despite the similarity in predicting the current loads, the models varied in their ability to predict future scenarios and time lags, which is addressed in **Section 4.5**. The final calibrated parameters are presented in **Table 4.1** and **Table B2**. Also, the evaluation of the monthly calibrated SWAT-LAG model to simulate the daily discharge from 1996 through 2016, revealed a satisfactory performance with a KGE value of 0.5 and a PBIAS value of 1% (**Figure B10**).

Table 4.1. Hydrology and nitrate flux calibration variables, descriptions, ranges and final calibrated parameter values

Variables	Description	Range	Calibrated Values
Hydrology			
CN2_1	Runoff curve number 1	59 - 73.7	61.6
CN2_2	Runoff curve number 2	66 - 82.5	73.9
CN2_3	Runoff curve number 3	69 - 86.3	85.2
CN2_4	Runoff curve number 4	77 - 96.3	84.9
CN2_5	Runoff curve number 5	78 - 97.5	83.1
CN2_6	Runoff curve number 6	86 - 100	94.6
CN2_7	Runoff curve number 7	92 - 100	96.4
ESCO	Soil evaporation compensation coefficient	0.8 - 1.0	0.92
DEP_IMP	Depth to impervious layer, mm	3250-3650	3502
GWQMN	Threshold water content in shallow aquifer before groundwater can flow, mm	75 - 175	104
REVAPMN	Threshold depth of water in the shallow aquifer for REVAP (movement of water from shallow aquifer into the overlying unsaturated zone) to occur, mm	75 - 175	105
CNCOEFF	Plant ET curve number coefficient	0.1 - 0.3	0.21
Nitrate Flux			
HLIFE_NGW	Half-life of nitrate in groundwater, day	5 - 75	71
BIOMIX	Biological mixing efficiency	0.18 - 0.22	0.18
CDN	Soil denitrification rate coefficient	0.1 - 1	0.53
NPERCO	Nitrogen percolation coefficient	0.2 - 1	0.95

(i) CN2_1to7: The study area has seven different types of curve numbers which were treated as individual calibration parameters in OSTRICH calibration tool and

(ii) Crop calibration parameters are provided in Table S2

4.5.3 Nitrogen Stores and Fluxes over Time

The SWAT-LAG model was used to explore how N stores and fluxes have changed over the last 67 years (1950-2016) in the South Fork Iowa Watershed. During this period, application rates for N fertilizer and N fixation rates increased consistently from 1960–1970 and then stabilized (**Figure 4.4a**). This was accompanied by a concomitant increase in the crop N uptake rates, leading to an approximately constant N surplus value since the 1980s (**Figure 4.4a and Figure B3).** Nitrogen surplus in agricultural landscapes is often used for evaluating the efficiency of the agricultural practices – an N surplus of zero indicates that the N added to the landscape has been utilized efficiently by the crops. The analysis indicates 4-year average N surplus values ranging between 39 and 122 kg/ha/yr from 1950 to 2016. The magnitude of the N surplus is significant considering that it is 79–101% of the sum of fertilizer and manure addition (which varies from 43 to 143 kg/ha/yr) to the watershed over this period.

A fraction of this N surplus is denitrified and lost as riverine N, while the remaining, what we hereafter refer to as legacy N, is stored in soil and groundwater (Howden *et al.,* 2011; Worrall *et al.,* 2015, Van Meter *et al.,* 2016). The exact magnitudes of the denitrification flux are a challenge to estimate at the landscape scale (David *et al.,* 2008, 2010), making it difficult to quantify magnitudes of legacy stores. In this modeling study, the magnitudes of riverine N and denitrification flux has increased from 1950 through the 1980s, concurrent with increases in the N surplus (**Figure 4.4b**). Nitrogen accumulation in soil and groundwater has also been increasing over this period. While the rate of accumulation of the biogeochemical legacy (soil organic N) appears to have plateaued since the last decade, the hydrologic legacy continues to increase (**Figure 4.4b**).

On a cumulative basis, over the 67 years (1950-2016) simulated in this study, the total N surplus over the South Fork Iowa River watershed was 6181 kg/ha (92 kg/ha/yr), of which 2111 kg/ha (34%) was denitrified, 1688 kg/ha (27%) was lost as riverine output, 1588 kg/ha (25%) accumulated in the root zone, while 859 kg/ha (14%) accumulated in groundwater (**Figure 4.4c and 4.4d**). Our estimates of 27% of the total N surplus exported as riverine output is very close to Boyer *et al.* (2002) estimates (25%). The estimated values for soil N accumulation (1588 kg/ha) fell within the range of values (931-2025 kg/ha) reported by Van Meter *et al.* (2016), in

which they synthesized soil core data at multiple sites in Iowa. Also, our numbers for groundwater N accumulation (859 kg/ha) were close to groundwater nitrogen accumulations reported for the Susquehanna River Basin (390–655 kg/ha) and within the same order of magnitude for Thames River Basin (503-950 kg/ha) (Worrall *et al.,* 2015). It is interesting to note that the overall magnitude of accumulation of biogeochemical legacy is greater than the magnitude of accumulation of hydrology legacy.

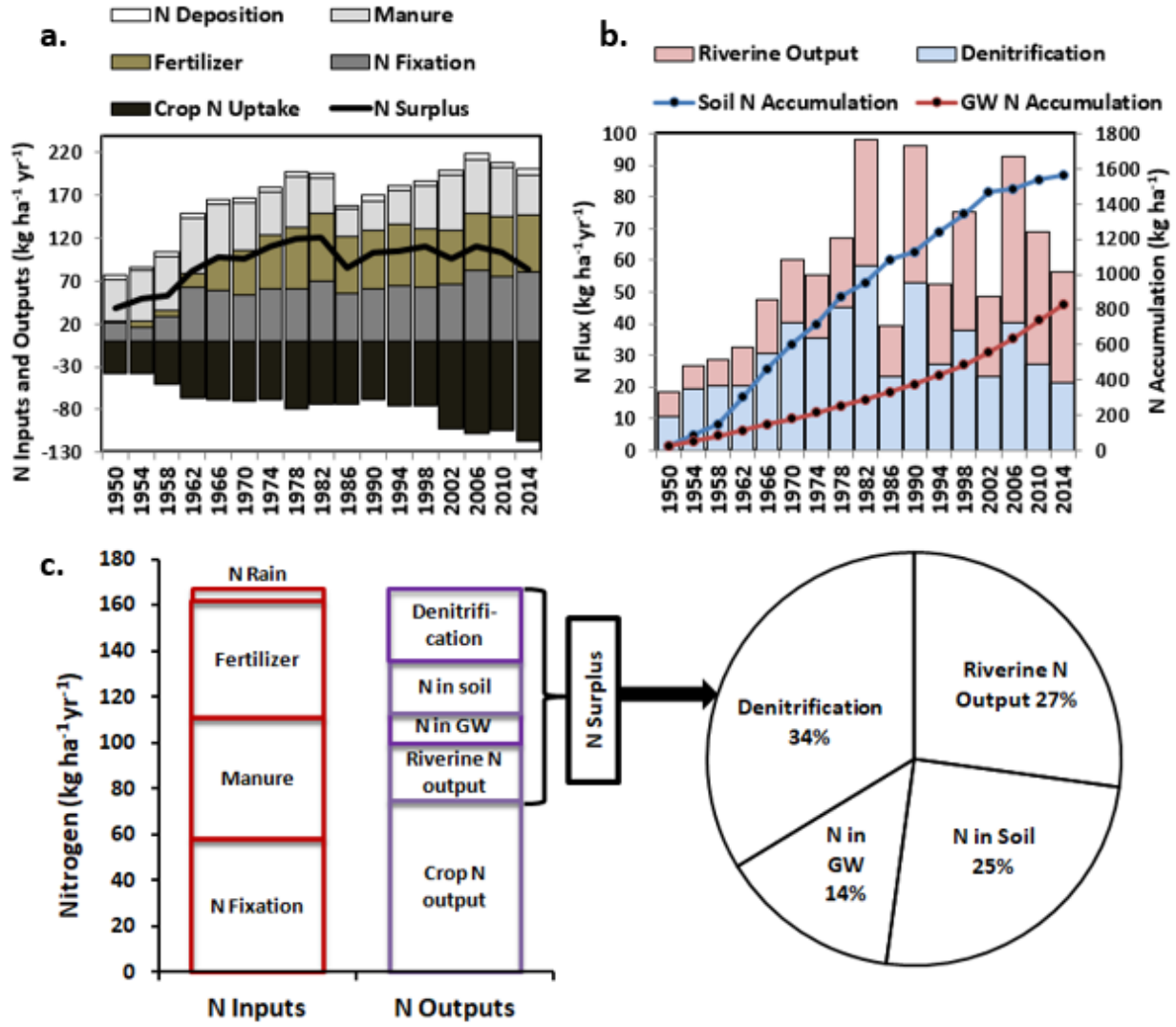

Figure 4.4. (a) Temporal trends in nitrogen surplus and its components (N deposition, fertilizer, manure, fixation, and crop N output), (b) Trends in riverine output and denitrification, soil and groundwater N accumulation and (c) Watershed-scale cumulative mass balance from 1950 to 2016 across SFIRW. Note that each stacked bar and data point represents a four-year averaged value

4.5.4 Spatial Patterns in Soil Nitrogen Accumulation

We next evaluated the spatial patterns of soil nitrogen accumulation and how topography and land-use characteristics contributed to accumulation. Initial Soil Organic Nitrogen (SON) levels in the watershed followed a predictable pattern, with higher SON levels along the river network and lower values in the upland (**Figure 4.5a**). Patterns of accumulation (**Figure 4.5b**), however, were found to vary as a function not just of landscape position, but numerous factors, including cropping patterns, soil type, and slope. To explore this further, we explicitly compared the effect of cropping choices (Continuous Corn and Corn-Soybean rotation), soil type (Canisteo with 26% clay and Clarion with 21% clay) and topography (<3% and >3% slope), on soil N accumulation. As land-use was temporally varying over the study period, we selected the last decade (2004-2016), during which land-use remained constant, for this analysis.

We found that under the Continuous Corn (CC) rotation, clayey Canisteo soils accumulated 4 kg/ha/yr (< 3% slope) and 6 kg/ha/yr (> 3% slope) more SON than sandy Clarion soils **(Figure 4.5c)**. Similarly, under the Corn-Soybean (CS) rotation, clayey soils accumulated 3 kg/ha/yr (for both slope categories) more than sandy soils. The greater accumulation of organic nitrogen in clayey soils is consistent with existing literature that reports greater organic content, and slower organic matter decomposition rates in clays (Legg., n.d; Six *et al.,* 2002; McLauchlan, 2006). Also, the land under CC accumulates 7 kg/ha/yr (< 3% slope category) and 8 kg/ha/yr (> 3% slope category) more SON than land under a CS rotation in clayey soils, and 6 kg/ha/yr (< 3% slope category) and 5 kg/ha/yr (> 3% slope category) more than land under CS in sandy soils **(Figure 4.5c)**. This phenomenon is consistent with findings of Varvel (1994) and Jagadamma *et al.* (2007), where Continuous Corn (CC) rotation led to a greater increase in the soil total nitrogen concentrations. This most likely arises due to (i) high fertilizer application rates in CC, (ii) high C/N ratio of corn residue (Jagadamma *et al.,* 2007; DeJong Hughes and Coulter, 2009) which has more resistance towards microbial decomposition and (iii) more residue contribution in Continuous Corn rotation than in Corn-Soybean rotation (Varvel, 1994; DeJong Hughes and Coulter, 2009). Finally, the flatter areas of the landscape (slope < 3%) accumulated more organic nitrogen, possibly due to lower slopes leading to less N loss to the stream.

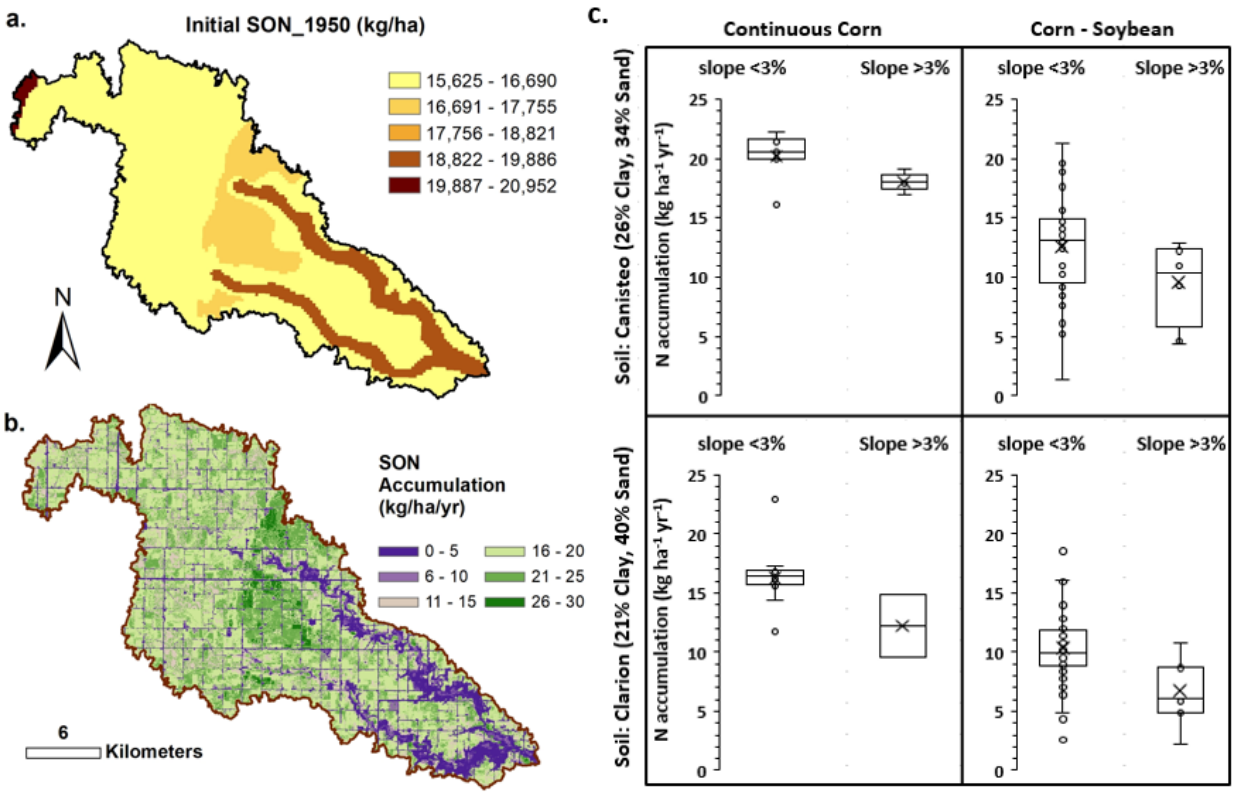

Figure 4.5. Soil organic N in SFIRW: a) Initial SON (1950), (b) Soil nitrogen accumulation (SON) rates between 1950 and 2016, and (c) SON accumulation rates between 2004-2016 as a function of soil type (clayey Canisteo soil and sandy Clarion soil), crop rotation (Continuous Corn and Corn-Soybean) and slope

4.5.5 Time Lags in Watershed Response

There was no significant difference in performance between the three models for current and past simulations (**Table 4.2 and Table 4.3**). It is important to note that even though baseline model performance is not different between the model versions, getting the time lags correct is important when the model is used to predict future scenarios of water quality due to land management. It is important for policymakers to know these time lags to be able to set realistic policy goals. Indeed, when a management change was implemented in SWAT-LAG for the forecast period (2017-2100), the three models responded differently (**Figure 4.6**). The management scenario implemented was a 100% reduction in fertilizer application rate. The original SWAT model (SWAT) responded by predicting a 46% reduction in nitrate load within one year of the change (**Figure 4.6a**), while the N loads generated by the SWAT-M and SWAT-LAG models remained consistently high for multiple decades. The lag times to achieving a 50%

N load reduction were, respectively, 1 year for SWAT, 4 years for SWAT-M, and 19 years for SWAT-LAG (**Figure 4.6b**), while the times to achieving a 70% N load reduction were 2 years for SWAT, 22 years for SWAT-M, and 62 years for SWAT-LAG. However, regardless of the different lag times, all models predicted an approximately 75% nitrate load reduction by the year 2100 (84 years after the land-use change) (**Figure 4.6b**). Significant uncertainty lies in the estimation of these time lags, given the uncertainty in parameters like the travel time, as well as inputs like fertilizer application rates. This is captured in the 95 PPU band predicted around the lag time (**Figure 6c**) that shows, for example, that in 2025 that N load predicted by SWAT-LAG can vary between 277 to 1354 tons/year, with the median value being equal to 827 tons/year. For comparison, nitrate load reduction for a 100% fertilizer reduction scenario for the individually calibrated models (SWAT, SWAT-M, and SWAT-LAG) is reported in Appendix (Figure B11).

SWAT showed the greatest load reduction soon after the land management change, as the C-N module in SWAT is not sophisticated enough to capture how the organic matter responds to changes in management practices. Addition of the more sophisticated organic matter dynamics in SWAT-M leads to a greater lag time than that obtained with SWAT – this is what has been referred to before as the "biogeochemical time lag" (Hamilton Stephen K., 2011; Van Meter *et al.,* 2016). Finally, the greatest lag time is observed in SWAT-LAG due to the additional consideration of the nutrient buildup in the groundwater reservoir – this has been referred to "hydrologic time lag" (Schilling *et al.,* 2008; Meals *et al.,* 2010). The time lag predicted by SWAT-LAG, which includes both the hydrologic and biogeochemical time lag, is critical for predicting changes in water quality after changes in management, making it possible for policymakers to make appropriate decisions and also to manage expectations among stakeholders.

Table 4.2. Monthly calibration (1996-2008) and validation statistics (2009-2015) for streamflow and nitrate flux for three model versions (SWAT, SWAT-M, and SWAT-LAG)

Variables	KGE	Performance	PBIAS (%)	Performance
SWAT				
Streamflow	0.61 (0.63)	Moderate (Moderate)	20.2 (8.8)	- (Good)
Nitrate flux	0.68 (0.45)	Good (Moderate)	-6.5 (-7.8)	Very good (Very good)
SWAT-M				
Streamflow	0.72 (0.68)	Good (Good)	5.8 (-4.2)	Good (Good)
Nitrate flux	0.72 (0.62)	Good (Moderate)	-11.2 (-9.1)	Good (Very good)
SWAT-LAG				
Streamflow	0.72 (0.68)	Good (Good)	5.8 (-4.2)	Good (Good)
Nitrate flux	0.77 (0.58)	Good (Moderate)	9.7 (8.0)	Very good (Very good)

(i) KGE performance criteria were based on an extensive literature review (refer **Sect. S.2**)
(ii) PBIAS performance was based on (Moriasi *et al.,* 2015)

Table 4.3. Annual calibration (1950-2008) and validation statistics (2009-2015) for crop yields for three model versions (SWAT, SWAT-M/LAG)

Variables	SWAT	SWAT-M/LAG
	PBIAS (%)	PBIAS (%)
Corn yield	4.7 (14.9)	3.1 (8.0)
Soybean yield	5.6 (2.8)	5.0 (1.4)
Alfalfa yield	-7.4 (-)	-7.4 (-)
Oats yield	0.7 (-)	-0.0 (-)
Other hay yield	-4.1 (-)	-7.6 (-)

Note. (i) PBIAS <±15% is considered to be good based on Srinivasan *et al.* (2010)
(ii) KGE values were not reported since they were poor, due to the difficulty in matching the crop yield at the annual time-step

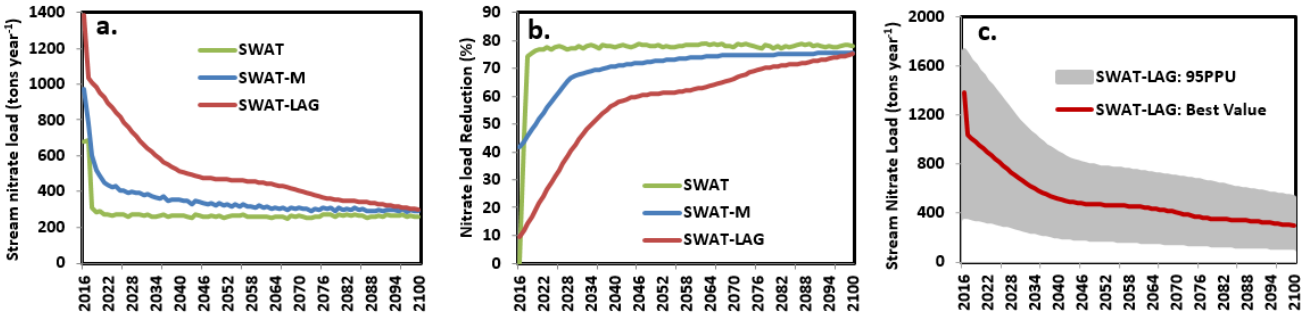

Figure 4.6. (a) Stream N load and (b) N load reduction as a function of time, simulated by SWAT, SWAT-M and SWAT-LAG for NM4 (100% fertilizer reduction in Corn HRUs). (c) Uncertainty in stream N load prediction quantified by SWAT-LAG, as captured by the 95% prediction band (95 PPU). The stream nitrate load reduction trajectory was obtained by subtracting N load for the NM4 scenario from that of the BAU scenario. Longer lag times are observed for the SWAT-LAG and SWAT-M scenarios, compared to the SWAT scenario

4.5.6 Effects of Land Management on Nitrogen Time Lags

The effects of different land-use and land management on time required to see reductions in N loads at the catchment outlet was evaluated using the modified SWAT-LAG model. In the first set of scenarios, NM1, NM2, NM3, and NM4, fertilizer application on all corn HRUs was reduced by 25%, 50%, 75%, and 100%, respectively, which corresponded to 26%, 44%, 63%, and 80% decreases in the N surplus at the watershed scale. These reductions led to reductions in the stream nitrate load in all cases; however, time lags between the reductions in input and subsequent load reductions at the outlet differed across the different fertilizer reduction scenarios (**Figure 4.7a**). The relationship between reductions in fertilizer application rates and N load reductions was linear, but the slope of the relationship increased over time indicating that for the more extreme scenario (NM4), waiting for longer leads to proportionally greater benefits compared to a less extreme scenario like NM2 (**Figure 4.7b**). For the 25% reduction in fertilizer application rate scenario, the N load reduction is ~ 14% in 2025, while it is 23% in 2050. For a 100% reduction in fertilizer application rates, the N load reduction is ~ 45% in 2025, while it is 70% in 2050. A 40% reduction in N load can be achieved by a 100% reduction in fertilizer application within seven years after implementation; whereas if one is willing to wait 30 years the same load reduction can be achieved with only 50% reduction in fertilizer application rates.

In the second set of scenarios, switchgrass was planted in the agricultural HRUs, thus reducing both the N surplus (LU1- 86%, LU2- 52% and LU3- 37%) and N loads at the catchment outlet (**Figure 4.7c** and **Figure 4.7d**). Much greater magnitudes of N reduction were evident under the switchgrass scenario, as switchgrass is actively harvested and removed from the system, thus reducing the amount of residue in the field that would serve as a source of mineralizable N. While corn was also harvested, corn yields were poor under the extreme fertilizer reduction scenarios, thus decreasing their effectiveness as an N-sink. Under LU1, when all agricultural HRUs were planted with switchgrass, 67% N load reduction was achieved in 2025, while an 81% reduction in N load was attained in 2050 (**Figure 4.7d**). As can be seen in the figure, the relationship between percent land-use change and N load reduction is linear, and the slope increases over time.

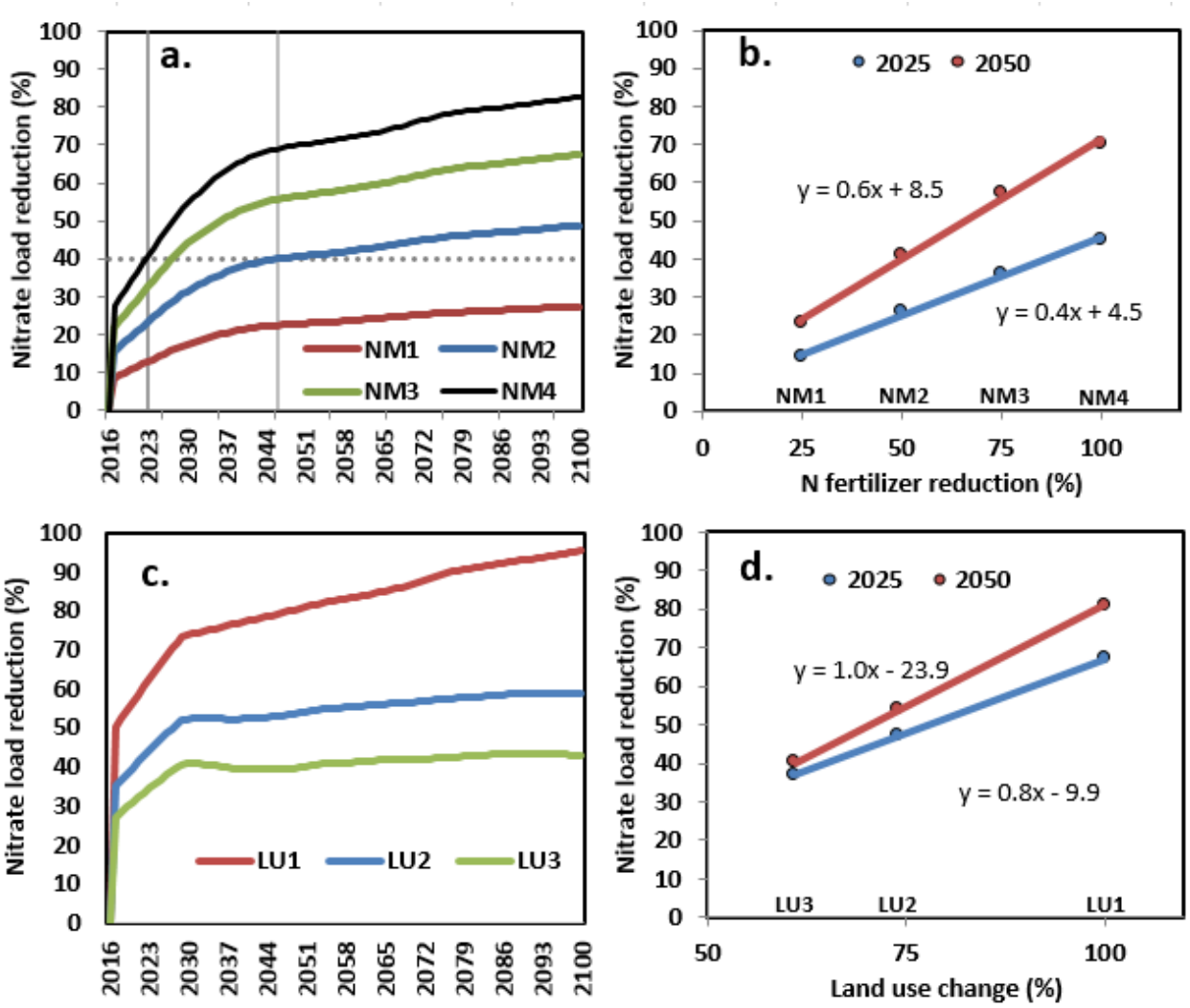

Figure 4.7. Effect of land-use and land management on time lags: (a) Percent N load reduction trajectories for four management scenarios where nitrogen fertilizer application rates on Corn HRUs were reduced by 25% (NM1), 50% (NM2), 75% (NM3) and 100% (NM4), (b) Percent N load reduction as a function of % fertilizer reduction in 2025 and 2050, (c) Percent N load reduction trajectories for three land management scenarios where 100% (LU1), 74% (LU2) and 61% (LU3) of agricultural lands were planted with switchgrass and the rest of row crop HRUs followed BAU, (d) Percent N load reduction as a function of percent land-use change in 2025 and 2050.

The above two paragraphs highlight that there are fundamental tradeoffs between the time required to achieve a given N load reduction and the magnitude of the N surplus reduction. For example, the Watershed Nutrient Task Force (WNTF) set a goal to reduce the 5-yr average area of the hypoxic zone in the gulf to less than 5,000 km^2 by 2035, which corresponds to N load

reduction of 60% for the Mississippi River Watershed (Scavia *et al.,* 2017). The results indicate that in the SFIRW it would theoretically be possible to achieve the target loads by 2035 with N fertilizer reductions of 100% (red line in Fig. 8a), or with the conversion of 86% of land under row crop to switchgrass (**Figure 4.8**). However, if the target year were extended by another 32 years to 2067, less drastic reductions in fertilizer application (75%) or changes in land-use (77%) would be necessary. In other words, if we are willing to wait longer to achieve water quality goals, less aggressive measures to improve nutrient management can be pursued. Conversely, the more we reduce nutrient inputs now, the faster we can reduce nitrate concentrations to desired levels.

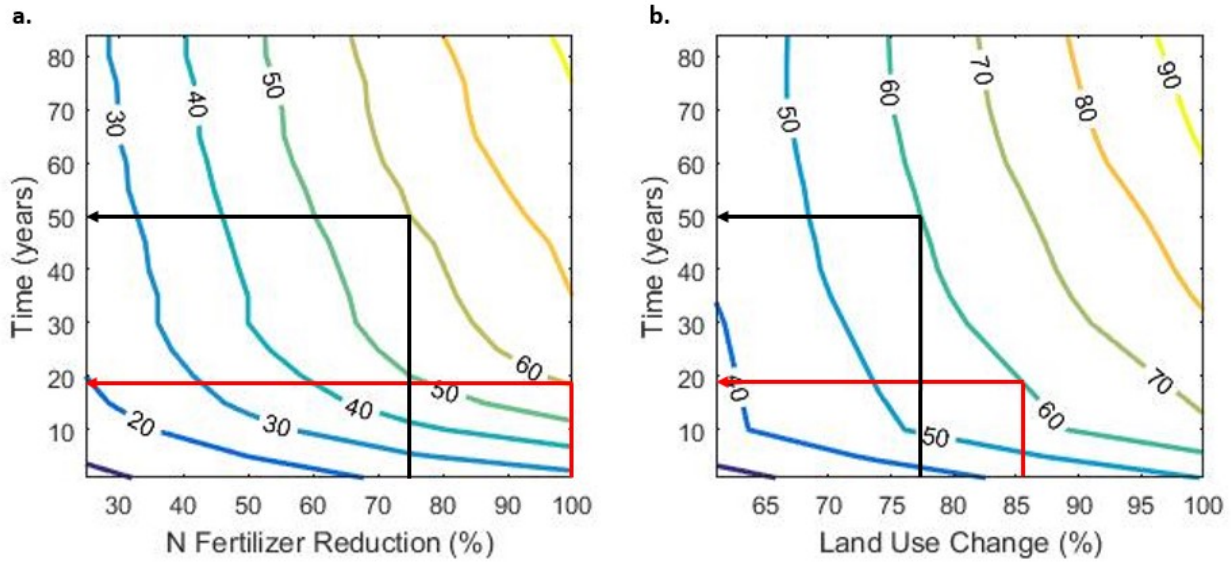

Figure 4.8. Cost- time tradeoffs in achieving reductions in N loads as a function of (a) reduction in fertilizer application, and (b) conversion of land under row crop agriculture to switchgrass. The contour lines represent percent reductions in N loading at the watershed outlet. The red and black arrows in (a) show that it may take between 18 and 50 years to achieve a 60% reduction in N loading, depending upon the magnitude of fertilizer reduction. The red and black arrows in (b) show that it may take between 18 and 50 years to achieve a 60% reduction in N loading as a function of the magnitude of land-use conversion

4.6 Conclusion

The buildup of nitrogen legacies in agricultural landscapes has been linked to time lags between changes in land management and measurable improvements in stream water quality (Chen *et al.,* 2015; Van Meter & Basu, 2015; Van Meter *et al.,* 2016, 2017). However, current watershed models do not explicitly consider the accumulation and depletion of legacies and the corresponding time lags in water quality improvement (Van Meter *et al.,* 2016 and Van Meter *et al.,* 2017). The water quality model SWAT was modified to capture time lags in water quality response that arise from the accumulation of legacy nitrogen. The new SWAT-LAG includes (1) a modified carbon-nitrogen cycling module to capture the accumulation and depletion of soil organic N, and (2) a groundwater travel time distribution module to capture the dynamics of the groundwater nitrate store. While the focus of this paper is on the modification of the SWAT model, a similar approach could be used to modify any spatially distributed watershed model to account for legacies.

A 502 km^2 agricultural watershed in North-Central Iowa was used as a case study, and the model was run from 1950 to 2016 to capture the build-up of legacy nitrogen in the landscape. The results show that over the 67 years simulated in the study, the cumulative N surplus in the landscape was 6181 kg/ha, of which 2111 kg/ha (34%) was denitrified, and 1688 kg/ha (27%) was lost as riverine output, while 1588 kg/ha (25%) accumulated in the root zone, and 859 kg/ha (14%) accumulated in the groundwater as *legacy* N. The SWAT-LAG model was able to describe the time lag in the landscape response – a 100% reduction in fertilizer application led to a 79% reduction in stream N load, and reduction was achieved in 84 years in SWAT-LAG, while it took only 2 years in the original SWAT model. Varying land-use and land management practices impacted both the final reduction in N load that could be achieved, as well as the time taken to achieve the load reduction. It is thus important to recognize the trade-offs between costs incurred for a particular land-use change and the water quality benefits achieved. Larger changes in land-use or greater implementation of new management practices come with a greater cost but can lead to a faster rate of achievement of water quality benefits. Of course, other routes to faster achievement of water quality goals may exist. More specifically, it has been shown that when the implementation of conservation measures is spatially targeted to areas identified as having faster travel times to the catchment outlet, stream concentrations are reduced more quickly (Van Meter and Basu, 2015). Alternatively, "end-of-pipe" solutions, such as restoration of riverine

wetlands that can intercept legacy nitrate loads before they enter the stream, could be used to reduce legacy-related loads via denitrification directly.

It is important to note that there is significant uncertainty in the actual magnitude of lag times estimated by my model, given a lack of long-term datasets for model validation. While nitrogen surplus information is available for longer periods, water quality data is often available for < 20 years. In a recent paper, Van Meter *et al.* (2018) modeled water quality in the Mississippi River Basin (MRB) over the past 100 years, and used sediment core information, preserved in the Gulf, for model validation. Furthermore, the water quality data available at the outlet of MRB is for 40 years and demonstrates the effect of legacy stores. Specifically, data at the outlet of the MRB shows that inputs have been decreasing since the 1970s, but water quality has remained stable, which is clearly due to the presence of legacy (Van Meter *et al.,* 2018). A similar effect was also observed at the Wapello outlet of Iowa cedar River Basin (**Figure B4**). Unfortunately, such long-term datasets are not most commonly available.

Furthermore, even when such datasets are available, equifinality in model predictions makes it difficult to identify lag times only through model fits. Often information content in the output time series is not enough to distinguish between models considering lag times and models not including lag times. It should be noted, however, that the groundwater travel times estimated in the current model are based on calculated travel times for a similar Iowa watershed (Basu *et al.,* 2012).

Despite such uncertainties, lag time models like SWAT-LAG must be developed to provide policymakers and regulators with realistic time frames for recovery of water quality. To constrain such models, one needs to use ancillary datasets, like soil nitrogen accumulation, and sediment records. Given the lack of data, uncertainty in model predictions is a function of uncertainty in the estimation of groundwater travel times, and reaction rates. Future work would thus include using various tracers to constrain groundwater travel time distributions, as well as using various ancillary datasets like sediment cores for model validation.

Chapter 5: Intensive Agriculture, Nitrogen Sequestration, and Water Quality: Intersections and Implications

5.1 Abstract

The field-scale biogeochemical model CENTURY was used to quantify SON accumulation and depletion trends using climate and soil type gradients characteristic of the Mississippi River Basin. The model was validated using field-scale data, from field sites in north-central Illinois that had SON data over the 100 years. The study revealed that across the climate gradient typical of the MRB, SON accumulation was greater in warmer areas due to greater crop yield with an increase in temperature. The accumulation was also higher in drier areas due to less N lost by leaching. Finally, the analysis revealed an interesting hysteretic pattern, where the same levels of SON in the 1930s contributed to a lower mineralization flux compared to current.

5.2 Introduction

Since the early 1800s, much of the North American landscape has been converted to agricultural land. In many parts of Iowa and Illinois, key agricultural states in the intensively cultivated Upper Mississippi River basin, as much as 75-80% of all land is planted in commodity crops such as corn and soybeans. This extensive conversion of the midwestern U.S. landscape from pristine prairie and grassland to cropland has been accompanied by the widespread use of commercial fertilizers as well as increases in livestock densities and the number of concentrated animal feeding operations. With this intensification of agriculture, we have seen troubling increases in nutrient pollution, both in groundwater and surface water. Across the U.S., the EPA estimates that greater than 40% of all stream miles suffer from nutrient pollution (EPA), and problems of hypoxia and eutrophication are increasingly arising in coastal zones (USEPA, 2017). In the Gulf of Mexico, the summer “dead zone,” driven primarily by nitrogen (N) runoff from the Mississippi River Basin commonly covers an area larger than the state of New Jersey (Action Plan, 2001).

Many attempts have been made to address the problems of nutrient pollution in intensively farmed areas. Millions of state, federal, and individual farmer dollars have been spent on implementing a range of conservation measures, from straightforward reductions in fertilizer use to the planting of cover crops and the creation of riparian buffers (Van Meter et al., 2018). While some small-scale improvements in water quality have been observed in response to these efforts, in general, the results have been disappointing. The Gulf of Mexico hypoxic zone continues to grow to 2-3 times the target size set by policy groups, and in 2018, Chesapeake Bay water quality received a failing grade for nitrogen (N) pollution in the Chesapeake Bay Program's biennial "State of the Bay" report (State of the Bay, 2018).

The clear difficulties in meeting water quality goals are increasingly understood to be due, at least in part, to the often long lag times between implementation of new management practices and measurable improvements in water quality (Meals *et al.,* 2010; Van Meter and Basu, 2015; Vero *et al.,* 2018). For nitrate, it is generally well understood that such lags can be attributed to long groundwater transit times, leading to increases in groundwater nitrate concentrations and potentially large accumulations of N mass in the subsurface (hydrologic N legacy). Less understood, however, is the potential for N to accumulate within soil organic matter and the likelihood that this biogeochemical N legacy can also lead to increased leaching of N to surface and groundwater.

It has typically been assumed that with intensive agricultural production, soil organic N is depleted from the soil profile and must be annually replenished with manure or commercial fertilizers for the soil to remain productive. First, it is well-documented that large losses of soil carbon (C) and soil organic N occurred after initial cultivation of nutrient-rich soil of the North American prairie region (Arrouays and Pelissier, 1994; Murty *et al.,* 2002; Van Meter *et al.,* 2016), largely due to a loss of physical protection provided by soil aggregates (Six *et al.,* 2002). Also, it is clear that soil fertility can be lost if high rates of agricultural production are not accompanied by sufficient application of mineral fertilizers or manure to replenish lost nutrients—a problem that still exists in Africa today (Sanchez, 2002). However, with regular fertilizer use as well as implementation of management practices leaving higher fractions of crop residues in the field, it has been observed that agricultural fields can operate with a positive mass balance for both C and N, opening the opportunity for C sequestration as well as for the

accumulation of legacy N (Lal, 2015; Van Meter *et al.,* 2016). For example, within the Mississippi River Basin, Van Meter *et al.* (2016) have found, since 1980, accumulation rates of soil organic N on the order of 3.8 Mt/year.

Although simple modeling frameworks have been developed to explain increases in soil N under intensive agriculture (Van Meter *et al.,* 2016, 2017), it remains unclear the ways in which coupled C-N dynamics as well, variations in soil type and climate, and different cropping patterns may impact accumulation and depletion trajectories for N in agricultural landscapes or the ultimate impacts on water quality. The present work has three primary objectives:

1. Using CENTURY, a detailed, C-N cycling model, test the hypothesis that nitrogen will accumulate in agricultural soils under conditions of a positive N surplus, residue management, and conservation tillage practices
2. Explore the impacts of climate, soil type, and management on accumulation and depletion rates for soil nitrogen
3. Explore the linkages between soil organic nitrogen and the leaching of nitrate to the subsurface to answer the question "does legacy soil N serve as a long-term source to groundwater and surface water"?

5.3 Methods

5.3.1 Model Description

CENTURY is an ecosystem model that simulates major processes associated with the cycling of Carbon (C), Nitrogen (N), Phosphorous (P) and Sulphur (S) in grassland, forest, and cropland systems (Parton *et al.,* 1988, 1993). The model runs at a monthly time step and includes sub-models that represent soil water and temperature dynamics, crop growth, litter chemistry, soil organic matter (SOM) decomposition, land-atmosphere gaseous exchange, and C and N leaching mechanisms (Del Grosso *et al.,* 2002; Adler *et al.,* 2007). The model simulates C and N stocks which are described by two litter pools (structural and metabolic litter) and three soil organic pools, namely active, slow, and passive, which differ in size and turnover rates. The active pool has turnover rates of a few years (1 to 5 years) while the slow and the passive pools have turnover rates varying from 20 to 50 years and 200 to 1500 years respectively (Begum *et*

al., 2017). The flow of carbon and nitrogen between pools is controlled by the sizes of the pools, C/N ratios and lignin content of the pools, soil water/temperature factors and soil texture (Adler *et al.,* 2007; Davis *et al.,* 2010). Transformation of SOC/SON between pools involves respiration of CO_2 or nitrogen gases. Mineralized nitrogen from SON pools and mineral N inputs from atmospheric deposition, symbiotic, and non-symbiotic N fixation enter mineral N pool where it is susceptible to leaching and volatilization (Metherell *et al.,* 1993). CENTURY and its daily version DAYCENT has been successfully used to study SOC and SON dynamics in grasslands, forest and agricultural lands (Parton *et al.,* 1988, 1993; Del Grosso *et al.,* 2002; Evans *et al.,* 2011), predict greenhouse gas emissions (Del Grosso *et al.,* 2002, 2005, 2008, 2009, 2011; Adler *et al.,* 2007; Davis *et al.,* 2012; Field *et al.,* 2016), and to explore the climate and edaphic controls on SOC and SON dynamics (Burke *et al.,* 1989; Evans *et al.,* 2011; Follett *et al.,* 2012).

5.4 Illustrative Case Study for SON Accumulation

5.4.1 Model Inputs

The field data from Champaign County, Illinois was used as a case study in the CENTURY model to explore dynamics in SON depletion following plowing in the 1875-1950 and then the subsequent build-up of organic matter under intensive agriculture (David *et al.,* 2009). The David *et al.* (2009) study consisted of five field sites that were maintained under corn-soybean rotation since the 1950s, and soil organic nitrogen levels were measured during 1957 and 2002. This study was selected since it is one of the very few studies that have SON data across such long timescales.

We modeled four different phases to represent the anthropogenically induced evolution of the landscape: (1) native grassland, pre-cultivation (warmup period of 10,000 years before 1875); (2) post-cultivation, low-input agriculture (1875 - 1924); (3) post-cultivation, low-input agriculture (1925–1950); (4) post-cultivation, high input agriculture (1951–2014). Information on land-use and land management for the field plots was obtained from David *et al.* (2008, 2009) for 1950-2014 (**Table 5.1**). For the earlier period (1875-1950), we used general management practices followed in the Mid-Western US based on literature values and databases (Huggins *et al.,* 1998; Manies *et al.,* 2000; USDA-Agricultural Census, 2012). We used Corn–Oats–Hay

(COH) crop rotation from 1875 to 1925 and Corn-Soybean (CS) from 1925 to 2014. To account for the difference in the start of different rotation types, six scenarios were formulated and aggregated to represent ensemble model behavior. For example, for the 1875-1924 period, which involves Corn–Oats–Hay (COH) rotation, three rotations were formulated, i.e., COH, OHC, and HCO. From 1925-2014, Corn-Soybean (C-S) and Soybean-Corn (S-C) rotation were developed for each of the three scenarios (COH, OHC, and HCO), resulting in six scenarios namely COH-CS, COH-SC, OHC-CS, OHC-SC, HCO-CS, and HCO-SC. Thus, the base model represents the aggregated responses of all of the above six scenarios.

Crop residues were not returned to the field till 1950 and returned after that based on David *et al.* (2009) and Huggins *et al.* (1998). Conventional tillage was considered from 1875 to 1980s, and No-till was done after that based on Manies *et al.* (2000) and David *et al.* (2009). Manure application was considered from 1875 to 1950 at a rate of 20 kg/ha/yr based on the animal count in Champaign county (USDA-Agricultural Census, 2012) and N content in animal excretion (Hong *et al.,* 2013). Mineral N application estimates from 1951 to 2014 were obtained from Alexander and Smith (1990) and USGS (2012) for Champaign County. Fertilizer application rates for corn increased over time from approximately 15 kg/ha/yr in 1950 to 187 kg/ha/yr in 2014.

Nitrogen deposition was estimated over the timeframe of analysis (1875 - 2014) using a combination of National Atmospheric Deposition Data (NADP, 2014) and a global study on N deposition (Dentener, 2006). From 1978 to 2014 N deposition data was obtained from the NADP dataset for the Bondville station, located in Champaign County. Nitrogen deposition information for the earlier years was obtained by linear interpolation between NADP data in 1978, and the Denterner (2006) study that provided global N deposition maps in 1860. Nitrogen deposition data for the time-blocks 1875-1924, 1925-1966, and 1967-2014 were estimated as 3, 7, and 11 kg/ha/yr, respectively.

Monthly precipitation and temperature data for the Champaign station were obtained for the period 1890s to 2014 from the cli-MATE online tool (cli-MATE, 2019). The study sites were located one Drummer soil, and the soil texture information was obtained from STATSGO soil map (9% sand, 63% silt and 28% clay) (Soil Survey Staff., n.d.).

Table 5.1. Land-use and management practices for the study area, obtained through literature review

Timeframe	Land-use	Fertilizer	Tillage	Residue return	Sources
1875-1924	Corn-Oats-Alfalfa Hay	Manure	Conventional	No	David *et al.,* (2008, 2009); Huggins *et al.,* (1998);
1925-1950	Corn-Soybean	Manure	Conventional	No	Manies *et al.,* (2000);
1951-1980	Corn-Soybean	Mineral N	Conventional	Yes	USDA-Agricultural
1981-2014	Corn-Soybean	Mineral N	No-Tillage	Yes	Census, (2012)

5.4.2 Model Outputs and Parameterization:

Rigorous model calibration and validation were not done due to a lack of site-specific field data. However, the model parameters were adjusted so that the modeled time-varying crop yields, SON accumulation, nitrate leaching fluxes, N fixation rates, and denitrification losses matched observed or literature values. This step ensured the consistency of model runs.

One of the key factors that contribute to SON buildup is the return of crop residue, which is impacted by crop yields that change over time. Since crop yield information was not available for the specific field plots, we used crop yield values for Champaign County, obtained from the USDA Agricultural Census (2012) and USGS Agricultural Survey (2012) databases. To account for the fact that crop yields have increased over time, multiple crop varieties were simulated to match the observed crop yield patterns. This was achieved by modifying model parameters PRDX (Potential aboveground monthly production for crops, g-C/m^2), and HIMAX (Maximum harvest index for crops) intermittently (**Table C1**). Also the model parameters VLOSSE (fraction per month of excess N left in the soil after nutrient uptake by the plant, which is volatilized) and VLOSSG (fraction per month of gross mineralization which is volatilized) were adjusted so that crop N uptake (119 kg/ha/yr) and gaseous N loss (12 kg/ha/yr) were comparable with the values reported by David *et al.* (2008) (129 kg/ha/yr - N uptake and 11 kg/ha/yr - gaseous N loss).

Soil organic nitrogen levels reported for five of the five field plots (Ogden, Manteno, Onarga, Roseville, and Sheldon), during 1957 and 2002, were aggregated to compare with modeled values. The study also reported SON values of native prairie sites, adjacent to the agricultural field plots, which were considered as surrogate for initial SON levels for the year 1875. The other critical component of the nitrogen budget is N fixation by leguminous crops. The model parameter SNFXMX, representing the maximum symbiotic N fixation was adjusted so that the N fixation rates for alfalfa and soybean fell within the ranges proposed by Russelle and Birr (2004) and David *et al.* (2008) (**Table C1**). Finally, since site-specific information on N leaching was not available, the parameters MINLCH (critical water flow depth for leaching of minerals, cm of H_2O leached below 30 cm soil depth) and FLEACH (slope and intercept values for a normal month to compute the fraction of mineral N which will leach to the next layer when there is a saturated water flow) were adjusted so that the mean N leaching flux (22 kg/ha/yr) over 1951 - 2014 was similar to 26 kg/ha/yr for the Embarrass River Watershed (David *et al.*, 2008) and falling within the range 14 to 38 kg/ha/yr, measured by Mitchell *et al.* (2000) in the East-Central Illinois agricultural field sites

5.4.3 Effect of Climate and Soil Type on SON Accumulation:

One of the objectives of this study is to evaluate the effect of variations in soil texture and climate on SON accumulation. For climate scenarios, we focused on the Mississippi River Basin (MRB) as a case study and used precipitation and temperature data across MRB. MRB has 179 climate regions for which Mean Annual Precipitation (MAP) and Mean July Temperature (MJT) data were obtained for 30 years (1985-2014) from Midwestern Regional climate Centre's (MRCC) cli-MATE online portal (cli-MATE, 2019). The CENTURY model was then run for MAP values between 536 and 1290 mm (Mean ± 1 Standard Deviation, covering 83% of the observed values) and MJT values between 17-30 C (Mean ± 2 Standard Deviation, covering 98% of the observed values). By choosing 4 MAP values (equally spaced between the 536-1290 mm range) and 6 MJT values (equally spaced between 17-30 ^{o}C range), 24 unique climate scenarios were created, and these mean values were then scaled to the baseline precipitation time series to create monthly precipitation values. We used only one crop rotation type (COH-CS) with soil, fertilizer inputs, land-use, and management details, same as the baseline scenario explained

in **Section 5.4.1**. Each of the 24 unique scenarios was subject to a 10,000-year warm-up period to simulate SOC and SON levels in soil in the 1850s under different climate conditions. For the soil scenarios, we had created 11 different soil texture combinations between the extreme ranges 0% Sand & 100% (Silt+Clay) and 100% Sand & 0% (Silt+Clay). The soil scenarios have been executed only for one crop rotation type (COH-CS) with the weather, fertilizer inputs, land-use, and management data, same as the baseline scenario.

5.5 Results and Discussion

5.5.1 Crop Yield and Soil Organic Nitrogen:

The model was able to capture crop yields for corn, and soybean from 1925 to 2014, with PBIAS values of 20% and -1% for corn and soybean, respectively (**Figure 5.1**). There was a significant increase in the yields of corn and soybean over this time frame, with corn yields increasing from 1 to 10 t/ha/yr, and soybean yields increasing from 1 to 4 t/ha/yr. The parameters PRDX and HIMAX were modified intermittently to capture (potential aboveground monthly production for crops, g-C/m^2), and HIMAX (maximum harvest index for crops) over the entire time frame (**Table C1**). The model was also able to capture the crop yield values over the earlier period, from 1875-1924, with PBIAS of 3%, -15% and -0.2% for corn, oats, and hay respectively. Realistic representation of crop growth is critical to appropriately simulating trends in SOC and SON accumulation.

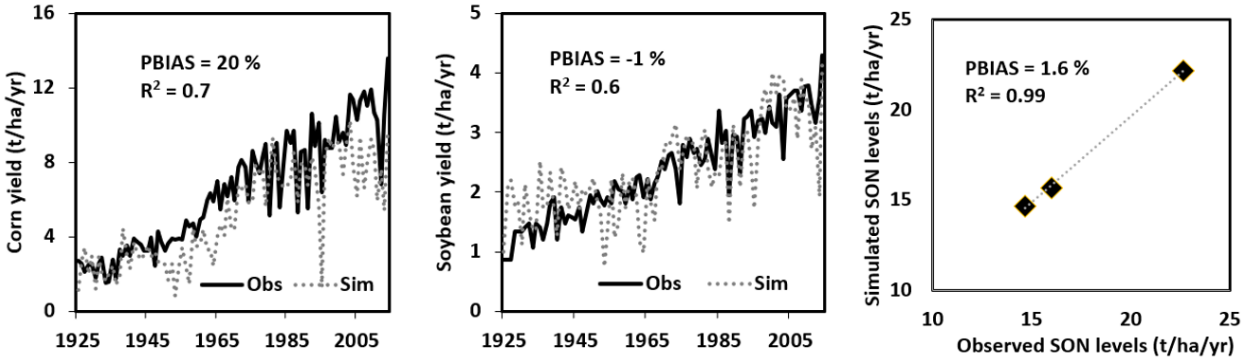

Figure 5.1. (a) Corn yield and (b) Soybean yield validation from 1925 to 2014. Note that the simulation involves multiple crop varieties mimicking the usage of hybrid crop traits (Edgerton, 2009; Brekke *et al.,* 2011) and (c) Comparison of observed and simulated SON levels (t/ha/yr)

The decomposition rates for the slow and the passive pools were adjusted such that SON levels in the soil matched the observed values. Specifically, we had three points in time when SON levels were measured in the soil, and the model was able to capture all three points in time adequately. The first point in time is pre-cultivation SON levels (before 1875) that were the highest values observed and equal to 22.6 ± 1.5 t/ha/yr. This value was matched by running the model for a warm-up period of 10,000 years and adjusting the decomposition rates of the slow and the passive pools to simulate lower decomposition rates in more stable prairie soils (**Table 5.2**). The decomposition rates were increased post-1875 to represent the increase in soil organic matter oxidation during plowing. This led to a decrease in SON levels to 14.7 ± 0.6 t/ha/yr in the 1950s. The landscape saw two major changes after 1950 -- crop residue return post-1950 and change from conventional tillage to no-till in the 1980s. The change to no-till agriculture in the 1980s was simulated by a slight lowering of the decomposition rates to match the observed SON level of 16 ± 0.6 t/ha/yr in 2014. The model was thus able to capture measured SON values over the entire time frame with an R^2 of 1 and a PBIAS value of 1.6%. Also, the rate of SON accumulation (22.6 kg/ha/yr) was closer to the SON accumulation rate (24 kg/ha/yr) reported by Ilampooranan *et al.* (2019) for the SFIRW in Iowa.

Table 5.2. CENTURY parameters used for calibration/validation of SON levels, N Leaching and Atmospheric N Depletion, along with final calibrated values

Parameter	Warm-up period	1875-1980	1981-2014
DEC5	0.1	0.216	0.146
DEC4	0.003	0.006	0.004

DEC5: Maximum decomposition rate of surface organic matter with intermediate turnover (slow pool);
DEC4: Maximum decomposition rate of soil organic matter with slow turnover (passive pool)

5.5.2 Nitrogen Stores and Fluxes from 1875 to 2014

The model results were then used to understand how nitrogen stores and fluxes changed in this landscape over the last 140 years, from 1875 to 2014 **(Figure 5.2a)**. Before the introduction of commercial fertilizers in the 1950s, the primary N input to the system was through biological fixation (alfalfa hay - 99 kg/ha/yr), followed by atmospheric deposition (5 kg/ha/yr) and manure N (13 kg/ha/yr). The primary output from the system is N removed in grain and stover. Average N removal in stover during 1875-1925 was 158 kg/ha/yr (C-O-H rotation), while during 1925-1950, it was 45 kg/ha/yr (C-S rotation). Such higher stover N

removal magnitude during 1875-1925 was due to higher production of alfalfa hay that has a higher N content. We assumed that stover was removed in this earlier period based on literature that state that stover removal for bedding and fodder was in practice from 1875 - 1950, while post-1950 crop residues were returned to the soil. This led to N deficit in the system from 1875 - 1950, with mineralization of SON and biological N fixation supplying most of the N needs of the crops again.

The system dynamics changed significantly since the 1950s, with the introduction of commercial fertilizers and the return of crop residue to the soil. The dominant N input from the 1950s has been commercial fertilizer followed by biological N fixation and atmospheric deposition. Atmospheric N deposition has increased from 4 kg/ha/yr in 1875 to 11 kg/ha/yr in 2014 but is a small component of the overall N budget. The amount of N removed in grain has increased since 1875, from 50 kg/ha/yr in 1875 to 142 kg/ha/yr in 2014, reflecting the periodic introduction of high yielding crop traits that have higher grain production. This led to a build-up of N surplus in the system from 12 kg/ha in 1950 to 83 kg/ha in 2014 **(Figure 5.2a)**. These N surplus values are of similar magnitudes to those observed for the Midwest by Van Meter *et al.* (2016).

A portion of the N surplus leaves the system via denitrification or leaching, while the remaining build up as soil organic N. N leaching has increased from 1875-2014, with higher leaching magnitudes observed during 1966-2014 **(Figure 5.2b)**, a period involving higher mineral N fertilizer application and higher mineralization rates. The denitrification loss rate was approximately constant over the entire time frame (15 kg/ha/yr). During 1966-2014, when the system was under N accumulation phase, 22 kg/ha/yr (30% of N Surplus) and 14 kg/ha/yr (20% of N Surplus) was lost through N Leaching and denitrification, respectively, while a significant portion (38 kg/ha/yr, which is 51% of the N surplus) **(Figure 5.2b)** remains in the system as soil organic N, and could contribute to leaching losses even when fertilizer application has ceased.

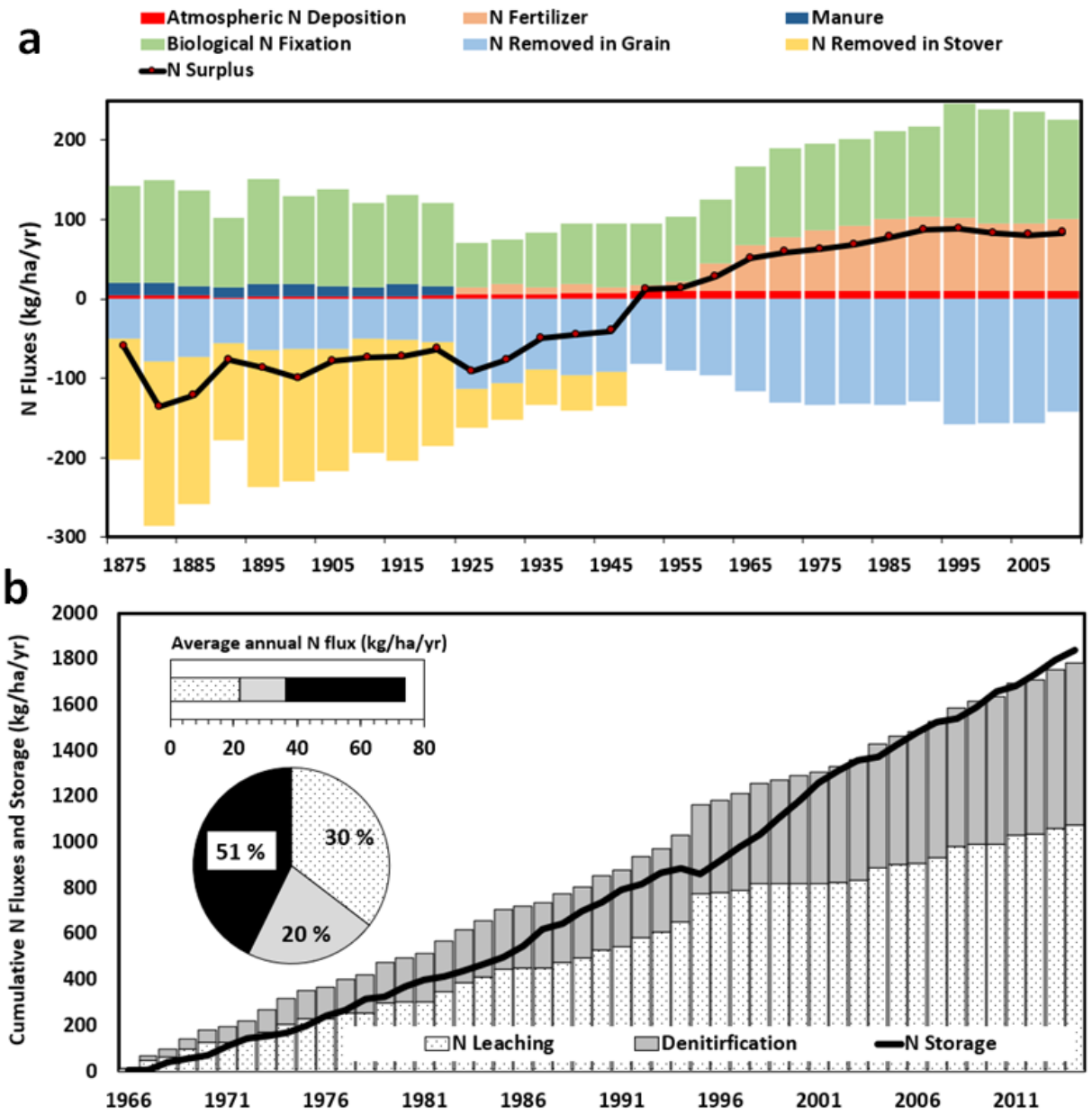

Figure 5.2. (a) Temporal trend of N Inputs (Biological Nitrogen Fixation, Atmospheric Nitrogen Deposition, Fertilizer Nitrogen Application), N Outputs (Crop N Uptake) and N Surplus (N Inputs - N Outputs) from 1875 to 2014. Note that each stacked bar in (a) represents a five-year averaged value; (b) Cumulative N Leaching, Denitrification and Soil N Storage from 1966 to 2014. The bar graph inside the subplot (b) denotes average annual N Leaching, Denitrification, and Soil N Storage, and the Pie-chart indicates the percentage of N Surplus lost through N Leaching and Denitrification and percent N Surplus stored in the soil, during 1966-2014

5.5.3 Soil Organic Nitrogen (SON) dynamics from 1875 - 2014:

The Century model was able to capture both the depletion of SON following plowing in the 1900s and the accumulation of SON since the 1950s (**Figure 5.3).** We observed a 34% decline in SON between 1875-1950s, and this is attributed to plowing that led to breakup and oxidation of organic aggregates. Furthermore, during this period the soil received minimal N inputs, manure at a rate of 13 kg/ha/yr, N fixation by alfalfa hay at a rate of 99 kg/ha/yr and N in atmospheric deposition at 5 kg/ha/yr, and this was not sufficient to sustain the crop N uptake (194 kg/ha/yr) leading to a depletion of SON. This changed dramatically since the 1950s, with mineral fertilizer application rates increasing from 8 kg/ha/yr in 1950 to 90 kg/ha/yr in 2014. Furthermore, crop residues were returned to the soil after 1950, and no-till practices were adopted after 1980. During this period, N inputs exceeded N outputs creating an N surplus that led to an increase in soil organic nitrogen levels at a rate of ~ 25 kg/ha/yr. Increase in soil organic nitrogen levels over time occurred due to the introduction of mineral fertilizers, increased crop yield, and incorporation of the residue with high N content into the soil matrix. The model was able to capture both the earlier declining trend in SON and the later increase in SON over time **(Figure 5.3)**.

It is also interesting to note the different temporal dynamics of the active, slow, and passive SON pools. Specifically, the passive recalcitrant pool with a turnover time of 200-1500 years, gets depleted through the entire timeframe of the simulation (1875-2014), while the active and slow pools start accumulating nitrogen since the 1960s. This is important since it implies that although intensive agriculture led to an increase in SON, the accumulation occurred in the two pools that had faster decay kinetics. This has implications, as shown in **Section 5.5.5**, for the ability of this pool to mineralize and supply N fluxes through leaching to downstream waters.

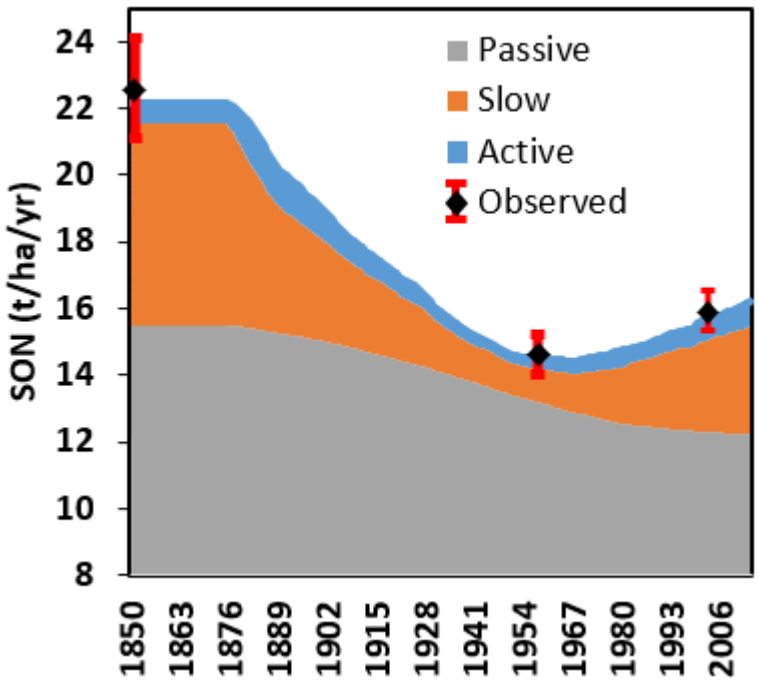

Figure 5.3. Soil organic nitrogen dynamics from 1850 to 2014. The CENTURY model simulates three SON pools, the active pool (blue), the slow pool (orange) and the passive pool (grey). The symbols with the error bars represent measured SON values by David *et al.* (2009)

5.5.4 Climate and Soil Texture Controls on SON Accumulation:

Soil organic nitrogen levels during the 1850s were simulated for the different climate scenarios by running the model for 10,000 years under each scenario. SON values decreased with plowing and intensive agriculture between 1875 to 1950, and then again increased over time from 1950 to 2014 due to no-till agriculture and the return of crop residue **(Figure 5.4)**. Overall, higher SON levels were associated with lower temperatures, consistent with the understanding that there is less decomposition, and thus greater accumulation in a colder climate (Cole, 1988). SON levels were the maximum for moderately wet areas (750 mm to 1150 mm) but decreased at both higher and lower precipitation values. Lower SON in a more arid climate is possibly due to greater aerobic degradation rates in these landscapes, while lower SON at very high rainfall values is possibly due to greater N leaching rates at higher rainfall.

Soil organic nitrogen accumulation magnitudes, over 1951 - 2014, varied from 0.3 to 2.4 t/ha (4.7 kg/ha/yr to 37.5 kg/ha/yr) for precipitation and temperature gradients relevant to the MRB. While this is a small amount in comparison to existing SON levels, it is a large component

of the soil N budget, given croplands receive around 67 kg/ha/yr of fertilizer. The patterns of SON accumulation are however counter to existing paradigms, with lower accumulation in colder temperatures and accumulation increases with an increase in the mean July temperature. We argue that this is likely because lower temperatures are associated with lower crop yields that translate to lower crop residue and thus less SON accumulation. Indeed, average annual crop yields increased by 22% for corn (**Figure C1.a**), and 60% for soybean (**Figure C1.b**) over the temperature gradient analyzed in the current study. It is also interesting to note that accumulation decreases with an increase in rainfall, again contrary to existing paradigms. We argue that at higher rainfall more nitrogen is lost through leaching leading to lower accumulation (refer **Figure C1.c** for the dependence of N leaching on mean annual rainfall). Others have argued it before that SOC and SON accumulation is a complex function of rainfall and temperature patterns (Smith, 2008; Gottschalk *et al.,* 2012). However, what we see here is an interesting example of how human landscape management changes these patterns from what would be expected in a more natural landscape.

Also, we explored the pattern of variation in SON accumulation magnitudes as a function of soil texture in **Figure 5.5**. The SON accumulation increased with increase in silt and clay fraction in soils, possibly because clay particles offer physical and biochemical protection against decomposition (Six *et al.,* 2002; Müller and Höper, 2004), leading to accumulation of soil organic nitrogen. Also, the plots under continuous corn had more accumulation than the plots under corn-soybean rotation, possibly due to the greater application rates of fertilizers and residue incorporation.

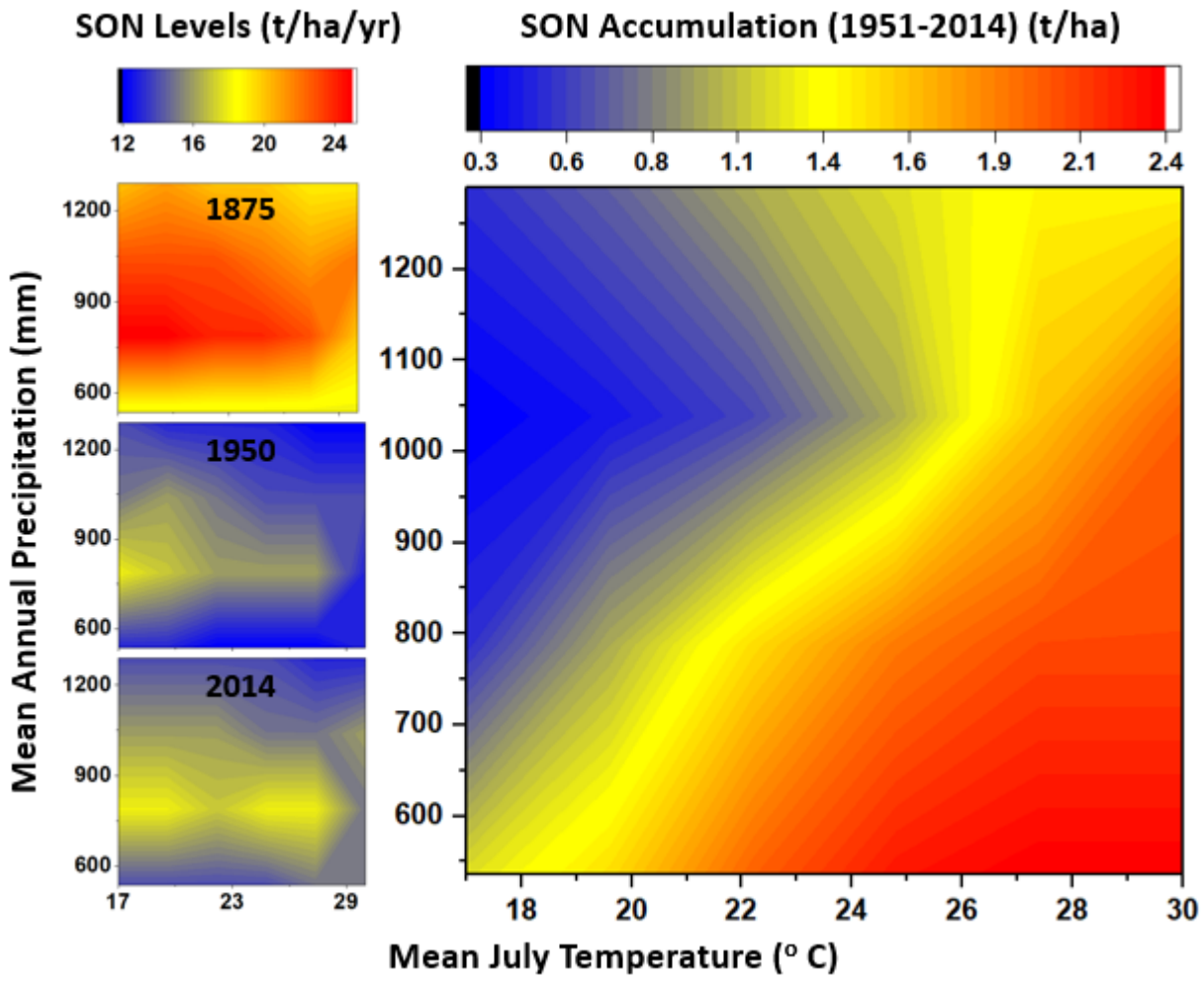

Figure 5.4. Soil Organic Nitrogen (SON) levels (t/ha/yr) as a function of precipitation and temperature gradients in the MRB, for the years 1875, 1950 and 2014; Soil Organic Nitrogen accumulation from 1951 to 2014 (t/ha)

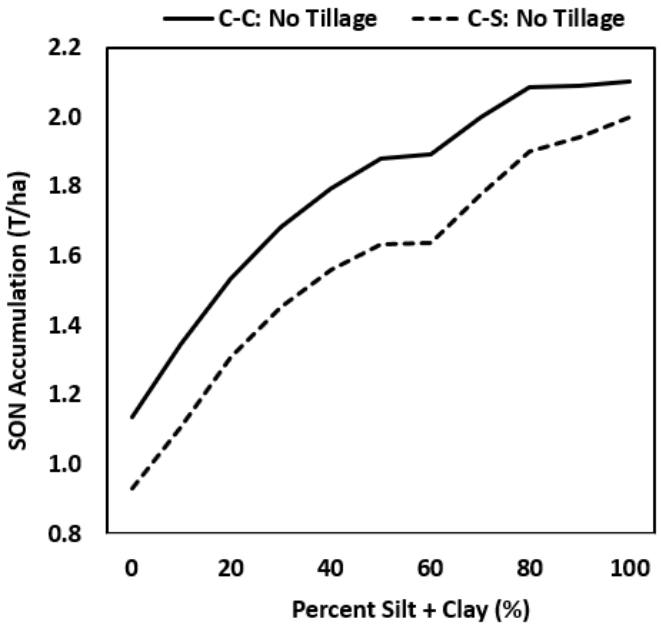

Figure 5.5. Soil Organic Nitrogen accumulation as a function of soil texture for Continuous Corn (C-C) and Corn-Soybean (C-S) rotations, under no-tillage condition. SON accumulation increases with increase in Silt+Clay fractions in soil and SON accumulation is higher under Continuous Corn (C-C) rotation

5.5.5 Soil Organic Nitrogen and Mineralization Fluxes

Finally, we ask the question: what is the role of increased N sequestration with intensive agriculture on N leaching fluxes to the stream? Given that current SON levels of ~ 16 t/ha/yr are still significantly less than the SON levels of the 1900s (19 t/ha/yr), is there any increased risk that SON accumulation poses to the environment? If organic matter rich prairie soils leached much lower levels of nitrate to the aquatic environment, would current nitrate leaching rates go back to those pristine values once fertilizer application is ceased? Or in other words, is the relationship between SON levels in soils and N mineralization rates linear and reversible?

To explore this question, we looked at both time trajectories of SON and N mineralization rates and the relationship between N mineralization and soil quality. It is apparent from **Figure 5.6a** that mineralization is a function of SON levels and an increase in SON levels contributes to increasing mineralization fluxes. This is somewhat unsurprising given that

mineralization is modeled as a first-order process. What is surprising and interesting, however, is the relationship between SON levels in soil and N mineralization fluxes (**Figure 5.6b**). Specifically, we observed a hysteretic response, where N mineralization fluxes are higher currently (1981-2014) compared to the fluxes in the early period (1905-1950), for the same SON level in the soil. For example, soil N level of 16 t/ha in 1930-1940 time frame corresponds to a mineralization flux of 125 kg/ha/yr, while the same soil N level in 2004-2014 corresponds to a flux of 190 kg/ha/yr. We hypothesize that this hysteretic response occurs due to change in the forms of SON that accumulate under intensive agriculture (**Figure 5.6c**). For example, in the current times, there is a much greater proportion of N in the active and slow pools (24%) compared to the 1950s (8%) or the 1900s (19%), and this is what possibly contributes to the higher mineralization fluxes (**Figure 5.6a and b**)

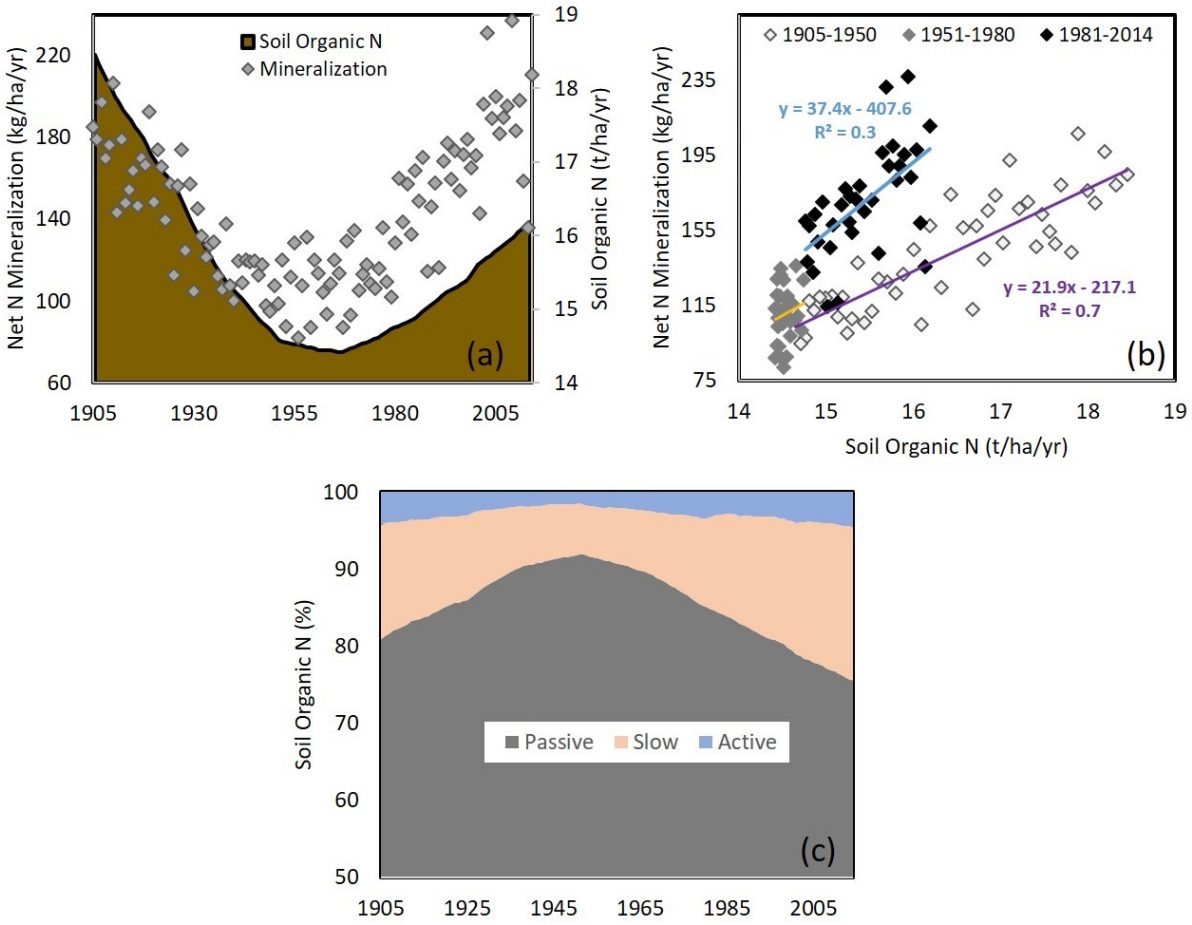

Figure 5.6. Temporal changes in Soil Organic N levels and Net N Mineralization flux from 1905-2014, (b) Comparison of Soil Organic N Levels and Net N Mineralization fluxes indicating a hysteric relationship and (c) Proportions (%) of Soil Organic N in active, slow and passive soil pools from 1905-2014. Increase in Soil Organic N levels has increased Net N mineralization flux during 1905-1950 and 1981-2014; however, for the same soil organic N, the mineralization flux is greater in the 1981 - 2014 period compared to the earlier period. Higher Net N Mineralization rates during 1981-2014 are attributed to the higher proportion of the N in active and slow pools compared to the passive pool.

5.6 Conclusion:

A process-based C-N cycling model, CENTURY, was used to test the hypothesis that N will accumulate in agricultural soils under conditions of a positive N surplus, residue management, and conservation tillage practices. Using realistic temporal trajectories of land-use and management practices, the model was able to capture the SON depletion that occurred in the 1870s during conversion of prairie grassland to low-input agriculture, as well as the accumulation of SON that has been observed since the 1950s with intensive use of mineral fertilizer, and return of crop residues to the soil.

The magnitude of SON accumulation as a function of climate and soil type characteristic of the Mississippi River Basin was then explored. Contrary to the consensus that SON accumulation increases with an increase in precipitation and decreases with an increase in temperature, we found that SON accumulation was more in warmer and drier areas. We argue that such a higher accumulation in a warmer climate can be attributed to an increase in crop yield with a temperature that contributes to increasing crop residue and thus, SON accumulation. The lower accumulation at higher rainfall can be attributed to greater nitrate leaching at higher rainfall.

Finally, we explored the effect of SON accumulation on N mineralization fluxes and found an interesting hysteretic response between SON magnitudes and N mineralization rates, where mineralization rates are higher in 2005-2014 compared to 1930-1940 for the same SON level in the soils. Increasing mineralization rates were attributed to changing composition of the SON that was dominated by the more recalcitrant, passive pool in the 1950s, compared to the slow and active pools in the current day SON. Future work would involve measuring SON composition across a land-use gradient to understand how land-use and management impact changes in SON composition.

Chapter 6: Summary and Conclusions

6.1 Summary

Previous research has shown that legacy nitrogen accumulates in agricultural watersheds due to decades of fertilizer application, and contributes to lag times between implementation of watershed conservation measures and water quality improvement. Legacy nitrogen can accumulate as soil organic N in the root zone of agricultural soils, also referred to as biogeochemical legacy, or nitrate dissolved in soil water and groundwater, also referred to as hydrological legacy. The overall goal of this thesis was to understand and quantify hydrological and biogeochemical legacies at the watershed scale using commonly used watershed and field-scale models.

As a first step (**Chapter 2**), a mass balance approach was used to quantify the magnitude of legacy stores in a large (32,660 km^2) agricultural watershed in the Iowa corn belt, the Midwestern U.S. The long term (64 years) data synthesis revealed that net inputs (NANI) to the system has increased from the 1950s to 1980s, and decreased since 1980s, following crop yield and N fertilizer application patterns. The magnitude of subsurface legacy nitrogen accumulation was estimated as 33.3 kg/ha/yr, which accounts for 48% of the N surplus in the landscape.

My next major objective was to modify the SWAT model to predict N legacies and time lags. However, before predicting nutrient dynamics, we needed to develop a robust hydrology model. Since crop growth plays such a key role in nutrient accumulation, the ability of the SWAT model to simultaneously predict water flow and crop growth was evaluated using the 32,660 km^2 Iowa Cedar Basin as a case study (**Chapter 3**). The calibration of the model using only streamflow led to a solution in which the crop yield was severely underestimated to match observed streamflow patterns. Thus, good calibration metrics for the hydrology model were achieved with poor representation of internal watershed partitioning of water, a great example of getting the right answer for the wrong reasons. The crop yield and flow partitioning calibration targets were then used, and the PET method in SWAT was changed so that the model was able to capture streamflow, crop yield, and percent flow through the tiled pathway. The modified model was hydrologically more robust, with lower prediction uncertainty and better ability to predict nitrate

loads without calibration. Based on the findings, we would recommend that SWAT modelers routinely use crop yield as a calibration target in addition to streamflow. Crop yield data is easily available and would increase the hydrologic consistency of the models. Currently, less than 1.5% of SWAT studies use crop yield information.

In Chapter 4, the focus was on modifying SWAT to include nitrogen legacies and time lags. Note that modification of the SWAT model is not necessary to predict the observed nitrate concentration patterns at the outlet. As others have noted before, SWAT can adequately capture N concentrations at the catchment outlet without adequate considerations of lag times. This is because of the information content of the nitrate time series is not enough to differentiate between legacy fluxes and current day fluxes. However, it has also been noted that models like SWAT cannot appreciably capture lag times in the landscape. In this chapter, we focused on a small (502 km^2) sub-watershed of the Iowa Cedar Basin, the South Fork Iowa River Watershed (SFIRW), and developed a new model SWAT-LAG to predict lag times to watershed response. The model was developed by using the more complex carbon-nitrogen cycling model in SWAT to capture biogeochemical legacies and coupling it to a travel time distribution model to estimate hydrologic legacies. The SON accumulation in soil stores (biogeochemical legacy) and groundwater stores (hydrological legacy) was estimated as 24 and 13 kg/ha/yr from 1950 to 2016, respectively. The C-N cycling model was modified such that the biogeochemical legacy store magnitude was compatible with independent estimates from Van Meter *et al.* (2016). This is another example of using internal watershed data to increase model robustness. Between 1950 and 2016, 25% of the total watershed N surplus (N Deposition + Fertilizer + Manure + N Fixation – Crop N uptake) had accumulated within the root zone, 14% had accumulated in groundwater, while 27% was lost as riverine output, and 34% was denitrified. Also, the SON accumulation was greater for fields under continuous corn compared to corn-soybean rotation), and in more mildly sloping clayey soils. Finally, SWAT-LAG model was used to predict time lags under various management scenarios. For a 100% fertilizer reduction scenario, the default SWAT mode, showed approximately 74% of the reduction in stream nitrate reduction within two years, while the SWAT-LAG model needed 84 years to achieve the same reduction. The framework proposed here constitutes a first step towards modifying a widely used modeling approach to assess the effects of legacy N on time required to achieve water quality goals.

The analysis in Chapter 4 highlighted a significant uncertainty in the prediction of biogeochemical legacies -- to address this uncertainty in Chapter 5, the field scale model CENTURY was used to quantify SON accumulation and depletion trends using climate and soil type gradients characteristic of the Mississippi River Basin. We first used field-scale data from field sites in north-central Illinois that had SON data over 140 years (1875-2014). Specifically, there was SON data collected in a set of field sites in the 1950s and current, as well as SON data in neighboring prairie sites as a control. We showed that the CENTURY model was able to capture the SON depletion (1875-1950) and accumulation (1951-2014) dynamics due to changes in agricultural practices over time. The SON accumulation during 1951-2014 was estimated as 25 kg/ha/yr. The study revealed that across the climate gradient typical of the MRB, SON accumulation was greater in warmer areas due to greater crop yield with an increase in temperature. The accumulation was also higher in drier areas due to less N lost by leaching. Finally, the analysis revealed an interesting hysteretic pattern, where the same levels of SON in the 1930s contributed to a lower mineralization flux compared to current. We argue that this is because the newer SON is associated with, the more easily degradable pools of N, while the older SON was in more recalcitrant pools. This analysis highlights how humans have changed the nature of soil organic matter and its implications for riverine fluxes.

6.2 Major contributions

The thesis has four significant contributions. First, a 64-year mass balance approach was used to document the presence of legacy N stores in a midwestern US watershed. Second, a novel modeling framework was developed by coupling the well-established SWAT model with a travel time distribution framework, to describe nutrient legacies and time lags in an intensively managed watershed in the midwestern US. The modeling framework developed can be used by others that are trying to address legacy issues in agricultural watersheds. Third, it was demonstrated that the use of crop yield as a calibration target in watershed models significantly improves hydrologic consistency and predictability. We recommend, based on our findings, that crop yield could be routinely used in hydrologic model calibration. Finally, we showed how human intervention could completely alter trends and forms of soil organic nitrogen accumulation in anthropogenic landscapes.

6.3 Limitations and future works

The study of nutrient legacies is fraught with uncertainties. Most of the time, the data available is limited, leading to large error bounds on legacy estimates. However, despite this, it is important to understand and quantify legacy accumulations and time lags to be able to guide policy. The following are some of the key limitations:

1. The groundwater travel time used in Chapter 3, is based on simplified assumptions of the water table following the topography. Future work would involve using numerical groundwater solvers like MODFLOW and couple it to SWAT to quantify lag times. It would also be valuable to have site-specific tracer data for validation of groundwater data.

2. Another major limitation is the lack of long term water quality data for model validation. Such data are relatively scarce; however, as shown by Van Meter *et al.* (2018), sediment core data in lakes or estuaries can be used to evaluate long term patterns. Further work can also involve using additional data sources like soil nitrogen accumulation or groundwater accumulation as additional data sources for model validation.

3. A major limitation of using the field scale model across climate and land-use gradients in the MRB is the cross-correlation between soil and climate factors in the region. Future work will include more accurate constraining of soil type and climate combinations to capture accumulation patterns. Future work will also include the estimation of SOC and SON stocks and lag times at the U.S and global scale.

References

Abbaspour KC. Abbaspour, K. C. 2012. SWAT-CUP4: SWAT calibration and uncertainty programs. A User Manual. Eawag 2014, Dübendorf, Switzerland.: 100

Abbaspour KC, Yang J, Maximov I, Siber R, Bogner K, Mieleitner J, Zobrist J, Srinivasan R. 2007. Modeling hydrology and water quality in the pre-alpine/alpine Thur watershed using SWAT. Journal of Hydrology 333 (2–4): 413–430 DOI: 10.1016/j.jhydrol.2006.09.014

Action Plan, 2001. Action Plan for Reducing, Mitigating, and Controlling Hypoxia in the Northern Gulf of Mexico. Mississippi River / Gulf of Mexico Watershed Nutrient Task Force. Available at: https://www.epa.gov/sites/production/files/2015-03/documents/2001_04_04_msbasin_actionplan2001.pdf [Accessed 22 February 2019]

Adler PR, Grosso SJD, Parton WJ. 2007. LIFE-CYCLE ASSESSMENT OF NET GREENHOUSE-GAS FLUX FOR BIOENERGY CROPPING SYSTEMS. Ecological Applications 17 (3): 675–691 DOI: 10.1890/05-2018

Alazzy AA, Lü H, Chen R, Ali AB, Zhu Y, Su J. 2017. Evaluation of Satellite Precipitation Products and Their Potential Influence on Hydrological Modeling over the Ganzi River Basin of the Tibetan Plateau. Advances in Meteorology DOI: 10.1155/2017/3695285

Alemayehu Tadesse, Griensven Ann van, Bauwens Willy. 2016. Evaluating CFSR and WATCH Data as Input to SWAT for the Estimation of the Potential Evapotranspiration in a Data-Scarce Eastern-African Catchment. Journal of Hydrologic Engineering 21 (3): 05015028 DOI: 10.1061/(ASCE)HE.1943-5584.0001305

Alexander, R. B. and R. A. Smith. 1990. County-level estimates of nitrogen and phosphorus fertilizer use in the United States, 1945 to 1985, U.S. Geological Survey Open-File Report 90-130. Data downloaded from <http://pubs.usgs.gov/of/1990/ofr90130/data.html>.

Alexander RB, Johnes PJ, Boyer EW, Smith RA. 2002. A Comparison of Models for Estimating the Riverine Export of Nitrogen from Large Watersheds. Biogeochemistry 57/58: 295–339

Alexander RB, Böhlke JK, Boyer EW, David MB, Harvey JW, Mulholland PJ, Seitzinger SP, Tobias CR, Tonitto C, Wollheim WM. 2009. Dynamic modeling of nitrogen losses in river networks unravels the coupled effects of hydrological and biogeochemical processes. Biogeochemistry 93 (1): 91–116 DOI: 10.1007/s10533-008-9274-8

Andersen J, Dybkjaer G, Jensen KH, Refsgaard JC, Rasmussen K. 2002. Use of remotely sensed precipitation and leaf area index in a distributed hydrological model. Journal of Hydrology 264 (1): 34–50 DOI: 10.1016/S0022-1694(02)00046-X

Anderson J. 2005. Industrializing the Corn Belt: Iowa farmers, technology and the Midwestern landscape, 1945-1972. Retrospective Theses and Dissertations Available at: http://lib.dr.iastate.edu/rtd/1827

Arnold JG, Fohrer N. 2005. SWAT2000: current capabilities and research opportunities in applied watershed modeling. Hydrological Processes 19 (3): 563–572 DOI: 10.1002/hyp.5611

Arnold JG, Youssef MA, Yen H, White MJ, Sheshukov AY, Sadeghi AM, Moriasi DN, Steiner JL, Amatya D, Skaggs RW, et al.,2015. Hydrological processes and model representation: impact of soft data on calibration. American Society of Agricultural and Biological Engineers 58 (6): 1637–1660 DOI: 10.13031/trans.58.10726

Arrouays D, Pelissier P. 1994. Changes in carbon storage in temperate humic loamy soils after forest clearing and continuous corn cropping in France. Plant and Soil 160 (2): 215–223 DOI: 10.1007/BF00010147

Baker LA, Hope D, Xu Y, Edmonds J, Lauver L. 2001. Nitrogen Balance for the Central Arizona–Phoenix (CAP) Ecosystem. Ecosystems 4 (6): 582–602 DOI: 10.1007/s10021-001-0031-2

Balkovič J, Schmid E, Skalský R, Nováková M. 2011. Modeling soil organic carbon changes on arable land under climate change – a case study analysis of the Kočín farm in Slovakia. Soil and Water Research 6 (No. 1): 30–42 DOI: 10.17221/29/2010-SWR

Basu NB, Destouni G, Jawitz JW, Thompson SE, Loukinova NV, Darracq A, Zanardo S, Yaeger M, Sivapalan M, Rinaldo A, et al.,2010. Nutrient loads exported from managed catchments reveal emergent biogeochemical stationarity. Geophysical Research Letters 37 (23): L23404 DOI: 10.1029/2010GL045168

Basu NB, Jindal P, Schilling KE, Wolter CF, Takle ES. 2012. Evaluation of analytical and numerical approaches for the estimation of groundwater travel time distribution. Journal of Hydrology 475: 65–73 DOI: 10.1016/j.jhydrol.2012.08.052

Basu NB, Rao PSC, Thompson SE, Loukinova NV, Donner SD, Ye S, Sivapalan M. 2011. Spatiotemporal averaging of in-stream solute removal dynamics: SOLUTE REMOVAL IN STREAM NETWORKS. Water Resources Research 47 (10) DOI: 10.1029/2010WR010196

Beaulieu JJ, Tank JL, Hamilton SK, Wollheim WM, Hall RO, Mulholland PJ, Peterson BJ, Ashkenas LR, Cooper LW, Dahm CN, et al.,2011. Nitrous oxide emission from denitrification in stream and river networks. Proceedings of the National Academy of Sciences 108 (1): 214–219 DOI: 10.1073/pnas.1011464108

Begum K, Kuhnert M, Yeluripati J, Glendinning M, Smith P. 2017. Simulating soil carbon sequestration from long term fertilizer and manure additions under continuous wheat using the DailyDayCent model. Nutrient Cycling in Agroecosystems 109 (3): 291–302 DOI: 10.1007/s10705-017-9888-0

Beven K. 1993. Prophecy, reality, and uncertainty in distributed hydrological modeling. Advances in Water Resources 16 (1): 41–51 DOI: 10.1016/0309-1708(93)90028-E

Beven K. 2006. A manifesto for the equifinality thesis. Journal of Hydrology 320 (1): 18–36 DOI: 10.1016/j.jhydrol.2005.07.007

Beven K, Binley A. 1992. The future of distributed models: Model calibration and uncertainty prediction. Hydrological Processes 6 (3): 279–298 DOI: 10.1002/hyp.3360060305

Beven K, Freer J. 2001. Equifinality, data assimilation, and uncertainty estimation in mechanistic modeling of complex environmental systems using the GLUE methodology. Journal of Hydrology 249 (1): 11–29 DOI: 10.1016/S0022-1694(01)00421-8

Bicknell BR, Imhoff JC, Kittle JL, Donigian AS. 1996. HYDROLOGICAL SIMULATION PROGRAM - FORTRAN USER'S MANUAL FOR RELEASE 1: 880

Bieger K, Hörmann G, Fohrer N. 2015. Detailed spatial analysis of SWAT-simulated surface runoff and sediment yield in a mountainous watershed in China. Hydrological Sciences Journal 60 (5): 784–800 DOI: 10.1080/02626667.2014.965172

Bingner RL, Drive M, Theurer FD, Yuan Y, Taguas EV. 2018. AnnAGNPS TECHNICAL PROCESSES: 207

Boscarello L, Ravazzani G, Mancini M. 2013. Catchment Multisite Discharge Measurements for Hydrological Model Calibration. Procedia Environmental Sciences 19: 158–167 DOI: 10.1016/j.proenv.2013.06.018

Bouda M, Rousseau AN, Konan B, Gagnon P, Gumiere SJ. 2012. Bayesian Uncertainty Analysis of the Distributed Hydrological Model HYDROTEL. Journal of Hydrologic Engineering 17 (9): 1021–1032 DOI: 10.1061/(ASCE)HE.1943-5584.0000550

Bouraoui F, Grizzetti B. 2014. Modeling mitigation options to reduce diffuse nitrogen water pollution from agriculture. Science of The Total Environment 468–469: 1267–1277 DOI: 10.1016/j.scitotenv.2013.07.066

Bouraoui F, Benabdallah S, Jrad A, Bidoglio G. 2005. Application of the SWAT model on the Medjerda river basin (Tunisia). Physics and Chemistry of the Earth, Parts A/B/C 30 (8–10): 497–507 DOI: 10.1016/j.pce.2005.07.004

Bouwman AF ; Drecht G van ; Hoek KW van der. (2005), Global and regional surface nitrogen balances in intensive agricultural production systems for the period of 1970-2030, Pedosphere 2005; 15(2):137-55, http://www.pbl.nl/en/publications/2005/Global_and_regional_surface_nitrogen_balances_in_intensive_agricultural_production_systems.

Boyer EW, Goodale CL, Jaworski NA, Howarth RW. 2002. Anthropogenic nitrogen sources and relationships to riverine nitrogen export in the northeastern U.S.A. Biogeochemistry 57–58 (1): 137–169 DOI: 10.1023/A:1015709302073

Brekke B, Edwards J, Knapp A. 2011. Selection and Adaptation to High Plant Density in the Iowa Stiff Stalk Synthetic Maize (L.) Population. Crop Science 51 (5): 1965 DOI: 10.2135/cropsci2010.09.0563

Bruns HA. 2012. Concepts in Crop Rotations DOI: 10.5772/35935

Burke IC, Yonker CM, Parton WJ, Cole CV, Schimel DS, Flach K. 1989. Texture, Climate, and Cultivation Effects on Soil Organic Matter Content in U.S. Grassland Soils. Soil Science Society of America Journal 53 (3): 800–805 DOI: 10.2136/sssaj1989.03615995005300030029x

Burt TP, Howden NJK, Worrall F, Whelan MJ. 2010. Long-term monitoring of river water nitrate: how much data do we need? Journal of Environmental Monitoring 12 (1): 71–79 DOI: 10.1039/B913003A

Butts M, Graham D. 2005. Flexible Integrated Watershed Modeling with MIKE SHE. In Watershed Models, Frevert D, Singh V (eds).CRC Press; 245–271. DOI: 10.1201/9781420037432.ch10

Cao P, Lu C, Yu Z. 2018. Historical nitrogen fertilizer use in agricultural ecosystems of the contiguous United States during 1850–2015: application rate, timing, and fertilizer types. Earth System Science Data 10 (2): 969–984 DOI: 10.5194/essd-10-969-2018

Cao W, Bowden WB, Davie T, Fenemor A. 2006. Multi-variable and multi-site calibration and validation of SWAT in a large mountainous catchment with high spatial variability. Hydrological Processes 20 (5): 1057–1073 DOI: 10.1002/hyp.5933

Causarano HJ, Doraiswamy PC, McCarty GW, Hatfield JL, Milak S, Stern AJ. 2008. EPIC Modeling of Soil Organic Carbon Sequestration in Croplands of Iowa. Journal of Environment Quality 37 (4): 1345 DOI: 10.2134/jeq2007.0277

Chameides WL, Kasibhatla PS, Yienger J, Levy H. 1994. Growth of Continental-Scale Metro-Agro-Plexes, Regional Ozone Pollution, and World Food Production. Science 264 (5155): 74–77 DOI: 10.1126/science.264.5155.74

Chen D, Guo Y, Hu M, Dahlgren RA. 2015. A lagged variable model for characterizing temporally dynamic export of legacy anthropogenic nitrogen from watersheds to rivers. Environmental Science and Pollution Research 22 (15): 11314–11326 DOI: 10.1007/s11356-015-4377-y

Chen D, Hu M, Dahlgren RA. 2014a. A dynamic watershed model for determining the effects of transient storage on nitrogen export to rivers. Water Resources Research 50 (10): 7714–7730 DOI: 10.1002/2014WR015852

Chen D, Huang H, Hu M, Dahlgren RA. 2014b. Influence of Lag Effect, Soil Release, And Climate Change on Watershed Anthropogenic Nitrogen Inputs and Riverine Export Dynamics. Environmental Science & Technology 48 (10): 5683–5690 DOI: 10.1021/es500127t

Cherry KA, Shepherd M, Withers PJA, Mooney SJ. 2008. Assessing the effectiveness of actions to mitigate nutrient loss from agriculture: A review of methods. Science of The Total Environment 406 (1): 1–23 DOI: 10.1016/j.scitotenv.2008.07.015

Cibin R, Sudheer KP, Chaubey I. 2010. Sensitivity and identifiability of streamflow generation parameters of the SWAT model. Hydrological Processes 24 (9): 1133–1148 DOI: 10.1002/hyp.7568

Clair TA, Pelletier N, Bittman S, Leip A, Arp P, Moran MD, Dennis I, Niemi D, Sterling S, Drury CF, et al.,2014. Interactions between reactive nitrogen and the Canadian landscape: A budget approach. Global Biogeochemical Cycles 28 (11): 1343–1357 DOI: 10.1002/2014GB004880

cli-MATE, 2019. cli-MATE: MRCC Application Tools Environment. Available at: https://mrcc.illinois.edu/CLIMATE/ [Accessed 10 October 2018]

Corsi SR, De Cicco LA, Lutz MA, Hirsch RM. 2015. River chloride trends in snow-affected urban watersheds: increasing concentrations outpace urban growth rate and are common among all seasons. Science of The Total Environment 508 (Supplement C): 488–497 DOI: 10.1016/j.scitotenv.2014.12.012

Cunha LK, Mandapaka PV, Krajewski WF, Mantilla R, Bradley AA. 2012. Impact of radar-rainfall error structure on estimated flood magnitude across scales: An investigation based on a parsimonious distributed hydrological model. Water Resources Research 48 (10) DOI: 10.1029/2012WR012138

Cusack GA, Hutchinson MF, Kalma JD. 1997. Remotely Sensed Vegetation Data for Hydrological Applications: Calibrating Airborne and Satellite Data With Biomass. In Subsurface Hydrological Responses to Land Cover and Land-use Changes, Taniguchi M (ed.).Springer US: Boston, MA; 205–220. DOI: 10.1007/978-1-4615-6141-5_14

David MB, Gentry LE. 2000. Anthropogenic Inputs of Nitrogen and Phosphorus and Riverine Export for Illinois, USA. Journal of Environment Quality 29 (2): 494 DOI: 10.2134/jeq2000.00472425002900020018x

David MB, Drinkwater LE, McIsaac GF. 2010. Sources of nitrate yields in the Mississippi River Basin. Journal of Environmental Quality 39 (5): 1657–1667

David MB, Grosso SJD, Hu X, Marshall EP, McIsaac GF, Parton WJ, Tonitto C, Youssef MA. 2008. Modeling denitrification in a tile-drained, corn and soybean agroecosystem of Illinois, USA. Biogeochemistry 93 (1–2): 7–30 DOI: 10.1007/s10533-008-9273-9

David MB, McIsaac GF, Darmody RG, Omonode RA. 2009. Long-Term Changes in Mollisol Organic Carbon and Nitrogen. Journal of Environment Quality 38 (1): 200 DOI: 10.2134/jeq2008.0132

Davis CA, Ward AS, Burgin AJ, Loecke TD, Riveros-Iregui DA, Schnoebelen DJ, Just CL, Thomas SA, Weber LJ, St. Clair MA. 2014. Antecedent Moisture Controls on Stream Nitrate Flux in an Agricultural Watershed. Journal of Environment Quality 43 (4): 1494 DOI: 10.2134/jeq2013.11.0438

Davis SC, Parton WJ, Dohleman FG, Smith CM, Grosso SD, Kent AD, DeLucia EH. 2010. Comparative Biogeochemical Cycles of Bioenergy Crops Reveal Nitrogen-Fixation and Low Greenhouse Gas Emissions in a <Emphasis Type="Italic">Miscanthus</Emphasis> × <Emphasis Type="Italic">giganteus</Emphasis> Agro-Ecosystem. Ecosystems 13 (1): 144–156 DOI: 10.1007/s10021-009-9306-9

Davis SC, Parton WJ, Grosso SJD, Keough C, Marx E, Adler PR, DeLucia EH. 2012. Impact of second-generation biofuel agriculture on greenhouse-gas emissions in the corn-growing regions of the US. Frontiers in Ecology and the Environment 10 (2): 69–74 DOI: 10.1890/110003

DeJong Hughes J, Coulter J. 2009. Considerations for corn residue harvest : Harvest : Corn : University of Minnesota Extension Available at: https://www.extension.umn.edu/agriculture/corn/harvest/considerations-for-corn-residue-harvest/ [Accessed 14 December 2017]

Del Grosso S, Ojima D, Parton W, Mosier A, Peterson G, Schimel D. 2002. Simulated effects of dryland cropping intensification on soil organic matter and greenhouse gas exchanges using the DAYCENT ecosystem model. Environmental Pollution 116: S75–S83 DOI: 10.1016/S0269-7491(01)00260-3

Del Grosso SJ, Halvorson AD, Parton WJ. 2008. Testing DAYCENT model simulations of corn yields and nitrous oxide emissions in irrigated tillage systems in Colorado. Journal of Environmental Quality 37 (4): 1383–1389 DOI: 10.2134/jeq2007.0292

Del Grosso SJ, Mosier AR, Parton WJ, Ojima DS. 2005. DAYCENT model analysis of past and contemporary soil N2O and net greenhouse gas flux for major crops in the USA. Soil and Tillage Research 83 (1): 9–24 DOI: 10.1016/j.still.2005.02.007

Del Grosso SJ, Ojima DS, Parton WJ, Stehfest E, Heistemann M, DeAngelo B, Rose S. 2009. Global scale DAYCENT model analysis of greenhouse gas emissions and mitigation strategies for cropped soils. Global and Planetary Change 67 (1): 44–50 DOI: 10.1016/j.gloplacha.2008.12.006

Del Grosso SJ, Parton WJ, Keough CA, Reyes-Fox M. 2011. Special Features of the DayCent Modeling Package and Additional Procedures for Parameterization, Calibration, Validation, and Applications. Methods of Introducing System Models into Agricultural Research advancesinagric (methodsofintrod): 155–176 DOI: 10.2134/advagricsystmodel2.c5

Dentener, F. J. 2006. Global Maps of Atmospheric Nitrogen Deposition, 1860, 1993, and 2050. Data set. Available on-line [http://daac.ornl.gov/] from Oak Ridge National Laboratory Distributed Active Archive Center, Oak Ridge, Tennessee, U.S.A. doi:10.3334/ORNLDAAC/830.

Ding X, Shen Z, Hong Q, Yang Z, Wu X, Liu R. 2010. Development and test of the Export Coefficient Model in the Upper Reach of the Yangtze River. Journal of Hydrology 383 (3): 233–244 DOI: 10.1016/j.jhydrol.2009.12.039

Drinkwater LE, Wagoner P, Sarrantonio M. 1998. Legume-based cropping systems have reduced carbon and nitrogen losses. Nature 396 (6708): 262–265 DOI: 10.1038/24376

Duarte CM, Conley DJ, Carstensen J, Sánchez-Camacho M. 2008. Return to Neverland: Shifting Baselines Affect Eutrophication Restoration Targets. Estuaries and Coasts 32 (1): 29–36 DOI: 10.1007/s12237-008-9111-2

Earls J, Dixon B. 2008. A Comparison of SWAT Model-Predicted Potential Evapotranspiration Using Real and Modeled Meteorological Data. Vadose Zone Journal - VADOSE ZONE J 7 DOI: 10.2136/vzj2007.0012

Edgerton MD. 2009. Increasing Crop Productivity to Meet Global Needs for Feed, Food, and Fuel. Plant Physiology 149 (1): 7–13 DOI: 10.1104/pp.108.130195

Ekanayake, J. and Davie, T., (2005). The SWAT model applied to simulating nitrogen fluxes in the Motueka River catchment, Motueka Integrated Catchment Management Programme Report series, http://icm.landcareresearch.co.nz/knowledgebase/publications/public/SWAT_modelling_N-04-05.pdf#search="swat".

Ekstrand S, Wallenberg P, Djodjic F. 2010. Process Based Modelling of Phosphorus Losses from Arable Land. AMBIO 39 (2): 100–115 DOI: 10.1007/s13280-010-0016-5

Evans SE, Burke IC, Lauenroth WK. 2011. Controls on soil organic carbon and nitrogen in Inner Mongolia, China: A cross-continental comparison of temperate grasslands. Global Biogeochemical Cycles 25 (3): GB3006 DOI: 10.1029/2010GB003945

Faramarzi M, Abbaspour KC, Schulin R, Yang H. 2009. Modeling blue and green water resources availability in Iran. Hydrological Processes 23 (3): 486–501 DOI: 10.1002/hyp.7160

Fenton O, Schulte RPO, Jordan P, Lalor STJ, Richards KG. 2011. Time lag: a methodology for the estimation of vertical and horizontal travel and flushing timescales to nitrate threshold concentrations in Irish aquifers. Environmental Science & Policy 14 (4): 419–431 DOI: 10.1016/j.envsci.2011.03.006

Field JL, Marx E, Easter M, Adler PR, Paustian K. 2016. Ecosystem model parameterization and adaptation for sustainable cellulosic biofuel landscape design. GCB Bioenergy 8 (6): 1106–1123 DOI: 10.1111/gcbb.12316

Follett RF, Stewart CE, Pruessner EG, Kimble JM. 2012. Effects of climate change on soil carbon and nitrogen storage in the US Great Plains. Journal of Soil and Water Conservation 67 (5): 331–342 DOI: 10.2489/jswc.67.5.331

Formetta G, Kampf SK, David O, Rigon R. 2014. Snow water equivalent modeling components in NewAge-JGrass. Geosci. Model Dev. 7 (3): 725–736 DOI: 10.5194/gmd-7-725-2014

Forster DL, Richards RP, Baker DB, Blue EN. 2000. EPIC modeling of the effects of farming practice changes on water quality in two Lake Erie watersheds. Journal of Soil and Water Conservation 55 (1): 85–90

Fowler D, Coyle M, Skiba U, Sutton Mark A., Cape J. Neil, Reis Stefan, Sheppard Lucy J., Jenkins Alan, Grizzetti Bruna, Galloway James N., et al.,2013. The global nitrogen cycle in the twenty-first century. Philosophical Transactions of the Royal Society B: Biological Sciences 368 (1621): 20130164 DOI: 10.1098/rstb.2013.0164

Frana AS. 2012. Applicability of MIKE SHE to simulate hydrology in heavily tile drained agricultural land and effects of drainage characteristics on hydrology: 151

Fry, J. A., G. Xian, S. Jin, J. A. Dewitz, C. G. Homer, L. Yang, C. A. Barnes, N. D. Herold, and J. D. Wickham., (2012). Completion of the 2006 National Land Cover Database Update for the Conterminous United States. Photogrammetric Engineering and Remote Sensing. American Society for Photogrammetry and Remote Sensing, Bethesda, MD, 77:858-864.

Gaiser T, Stahr K, Billen N, Mohammad MA-R. 2008. Modeling carbon sequestration under zero tillage at the regional scale. I. The effect of soil erosion. Ecological Modelling 218 (1): 110–120 DOI: 10.1016/j.ecolmodel.2008.06.025

Galloway JN, Cowling EB. 2002. Reactive nitrogen and the world: 200 years of change. Ambio 31 (2): 64–71

Galloway JN, Dentener FJ, Capone DG, Boyer EW, Howarth RW, Seitzinger SP, Asner GP, Cleveland CC, Green PA, Holland EA, et al.,2004. Nitrogen Cycles: Past, Present, and Future. Biogeochemistry 70 (2): 153–226 DOI: 10.1007/s10533-004-0370-0

Galloway JN, Schlesinger WH, I HL, Michaels A, Schnoor JL. 1995. Nitrogen fixation: Anthropogenic enhancement-environmental response. Global Biogeochemical Cycles: 235–252

Galloway JN, Townsend AR, Erisman JW, Bekunda M, Cai Z, Freney JR, Martinelli LA, Seitzinger SP, Sutton MA. 2008. Transformation of the Nitrogen Cycle: Recent Trends, Questions, and Potential Solutions. Science 320 (5878): 889–892 DOI: 10.1126/science.1136674

Gassman P. 2008. A simulation assessment of the Boone River watershed: baseline calibration/validation results and issues, and future research needs. Retrospective Theses and Dissertations Available at: http://lib.dr.iastate.edu/rtd/15629

Gassman PW, Sadeghi AM, Srinivasan R. 2014. Applications of the SWAT Model Special Section: Overview and Insights. Journal of Environmental Quality 43 (1): 1–8 DOI: 10.2134/jeq2013.11.0466

Gentry LE, David MB, Below FE, Royer TV, McIsaac GF. 2009. Nitrogen Mass Balance of a Tile-drained Agricultural Watershed in East-Central Illinois. Journal of Environment Quality 38 (5): 1841 DOI: 10.2134/jeq2008.0406

Glendining MJ, Powlson DS, Poulton PR, Bradbury NJ, Palazzo D, Ll X. 1996. The effects of long-term applications of inorganic nitrogen fertilizer on soil nitrogen in the Broadbalk Wheat Experiment. The Journal of Agricultural Science 127 (3): 347–363 DOI: 10.1017/S0021859600078527

Glenn EP, Huete AR, Nagler PL, Hirschboeck KK, Brown P. 2007. Integrating Remote Sensing and Ground Methods to Estimate Evapotranspiration. Critical Reviews in Plant Sciences 26 (3): 139–168 DOI: 10.1080/07352680701402503

Glenn EP, Neale CMU, Hunsaker DJ, Nagler PL. 2011. Vegetation index-based crop coefficients to estimate evapotranspiration by remote sensing in agricultural and natural ecosystems. Hydrological Processes 25 (26): 4050–4062 DOI: 10.1002/hyp.8392

Goolsby DA, Battaglin WA, Lawrence GB, Artz RS, Aulenbach BT, Hooper RP, Keeney DR, Stensland GJ. 1999. Flux and Sources of Nutrients in the Mississippi-Atchafalaya River Basin. Technical Report. National Oceanic and Atmospheric Administration National Ocean Service Coastal Ocean Program. Available at: https://repositories.tdl.org/tamug-ir/handle/1969.3/27186 [Accessed 31 July 2015]

Gottschalk P, Smith JU, Wattenbach M, Bellarby J, Stehfest E, Arnell N, Osborn TJ, Jones C, Smith P. 2012. How will organic carbon stocks in mineral soils evolve under future climate? Global projections using RothC for a range of climate change scenarios. Biogeosciences 9 (8): 3151–3171 DOI: 10.5194/bg-9-3151-2012

Grayson RB, Blöschl G, Western AW, McMahon TA. 2002. Advances in the use of observed spatial patterns of catchment hydrological response. Advances in Water Resources 25 (8): 1313–1334 DOI: 10.1016/S0309-1708(02)00060-X

Green CH, Tomer MD, Luzio MD, Arnold JG. 2006. HYDROLOGIC EVALUATION OF THE SOIL AND WATER ASSESSMENT TOOL FOR A LARGE TILE-DRAINED WATERSHED IN IOWA. Transactions of the ASABE 49 (2): 413–422 DOI: 10.13031/2013.20415

Green CT, Bekins BA, Kalkhoff SJ, Hirsch RM, Liao L, Barnes KK. 2014. Decadal surface water quality trends under variable climate, land-use, and hydrogeochemical setting in Iowa, USA. Water Resources Research 50 (3): 2425–2443 DOI: 10.1002/2013WR014829

Grimvall A, Stålnacke P, Tonderski A. 2000. Time scales of nutrient losses from land to sea — a European perspective. Ecological Engineering 14 (4): 363–371 DOI: 10.1016/S0925-8574(99)00061-0

Grizzetti B, Bouraoui F, Marsily GD. 2008. Assessing nitrogen pressures on European surface water. Global Biogeochemical Cycles 22 (4) DOI: 10.1029/2007GB003085

Grizzetti B, Bouraoui F, de Marsily G, Bidoglio G. 2005. A statistical method for source apportionment of riverine nitrogen loads. Journal of Hydrology 304 (1): 302–315 DOI: 10.1016/j.jhydrol.2004.07.036

Groffman PM, Altabet MA, Böhlke JK, Butterbach-Bahl K, David MB, Firestone MK, Giblin AE, Kana TM, Nielsen LP, Voytek MA. 2006. Methods for Measuring Denitrification: Diverse Approaches to a Difficult Problem. Ecological Applications 16 (6): 2091–2122 DOI: 10.1890/1051-0761(2006)016[2091:MFMDDA]2.0.CO;2

Hamilton SK. 2012. Biogeochemical time lags may delay responses of streams to ecological restoration. Freshwater Biology 57: 43–57 DOI: 10.1111/j.1365-2427.2011.02685.x

Hamilton Stephen K. 2011. Biogeochemical time lags may delay responses of streams to ecological restoration. Freshwater Biology 57 (s1): 43–57 DOI: 10.1111/j.1365-2427.2011.02685.x

Han H, Allan JD. 2008. Estimation of nitrogen inputs to catchments: comparison of methods and consequences for riverine export prediction. Biogeochemistry 91 (2–3): 177–199 DOI: 10.1007/s10533-008-9279-3

Haynes RJ. 1986. The decomposition process: mineralization, immobilization, humus formation, and degradation. Mineral nitrogen in the plant soil system Available at: https://eurekamag.com/research/001/703/001703988.php [Accessed 6 March 2019]

Her Y, Chaubey I. 2015. Impact of the numbers of observations and calibration parameters on equifinality, model performance, and output and parameter uncertainty. Hydrological Processes 29 (19): 4220–4237 DOI: 10.1002/hyp.10487

Herzmann DE. Daryl Herzmann, Iowa Environmental Mesonet, 2019. Available at: https://mesonet.agron.iastate.edu/ [Accessed 19 February 2019]

Hirsch RM, Moyer DL, Archfield SA. 2010. Weighted Regressions on Time, Discharge, and Season (WRTDS), with an Application to Chesapeake Bay River Inputs. Journal of the American Water Resources Association 46 (5): 857–880 DOI: 10.1111/j.1752-1688.2010.00482.x

Hoch JM, Neal JC, Baart F, van Beek R, Winsemius HC, Bates PD, Bierkens MFP. 2017. GLOFRIM v1.0 – A globally applicable computational framework for integrated hydrological–hydrodynamic modelling. Geosci. Model Dev. 10 (10): 3913–3929 DOI: 10.5194/gmd-10-3913-2017

Hong B, Swaney DP, Howarth RW. 2011. A toolbox for calculating net anthropogenic nitrogen inputs (NANI). Environmental Modelling & Software 26 (5): 623–633 DOI: 10.1016/j.envsoft.2010.11.012

Hong B, Swaney DP, Howarth RW. 2013. Estimating Net Anthropogenic Nitrogen Inputs to U.S. Watersheds: Comparison of Methodologies. Environmental Science & Technology 47 (10): 5199–5207 DOI: 10.1021/es303437c

Hong Q. 2012. Small-scale watershed extended method for non-point source pollution estimation in part of the Three Gorges Reservoir Region. International Journal of Environmental Science and Technology 9 (4): 595–604

Howarth RW. 1998. An assessment of human influences on fluxes of nitrogen from the terrestrial landscape to the estuaries and continental shelves of the North Atlantic Ocean. Nutrient Cycling in Agroecosystems 52 (2–3): 213–223 DOI: 10.1023/A:1009784210657

Howarth RW, Billen G, Swaney D, Townsend A, Jaworski N, Lajtha K, Downing JA, Elmgren R, Caraco N, Jordan T, et al.,1996. Regional nitrogen budgets and riverine N & P fluxes for the drainages to the North Atlantic Ocean: Natural and human influences. Biogeochemistry 35 (1): 75–139 DOI: 10.1007/BF02179825

Howarth RW, Sharpley A, Walker D. 2002. Sources of nutrient pollution to coastal waters in the United States: Implications for achieving coastal water quality goals. Estuaries 25 (4): 656–676 DOI: 10.1007/BF02804898

Howden NJK, Burt TP, Worrall F, Simon M, Whelan MJ. 2011. Nitrate pollution in intensively farmed regions: What are the prospects for sustaining high-quality groundwater? Water Resources Research 47 (6) DOI: 10.1029/2011WR010843

Howden NJK, Burt TP, Worrall F, Whelan MJ, Bieroza M. 2010. Nitrate concentrations and fluxes in the River Thames over 140 years (1868–2008): are increases irreversible? Hydrological Processes 24 (18): 2657–2662 DOI: 10.1002/hyp.7835

Howe E, Moore J. 2016. 54 West Shore Road Grand Isle, VT 05458: 79

Hu X, McIsaac GF, David MB, Louwers CAL. 2007. Modeling Riverine Nitrate Export from an East-Central Illinois Watershed Using SWAT. Journal of Environment Quality 36 (4): 996 DOI: 10.2134/jeq2006.0228

Hublart P, Ruelland D, García De Cortázar Atauri I, Ibacache A. 2015. Reliability of a conceptual hydrological model in a semi-arid Andean catchment facing water-use changes. In Proceedings of the International Association of Hydrological SciencesCopernicus GmbH; 203–209. DOI: https://doi.org/10.5194/piahs-371-203-2015

Huggins DR, Buyanovsky GA, Wagner GH, Brown JR, Darmody RG, Peck TR, Lesoing GW, Vanotti MB, Bundy LG. 1998. Soil organic C in the tallgrass prairie-derived region of the corn

belt: effects of long-term crop management. Soil and Tillage Research 47 (3): 219–234 DOI: 10.1016/S0167-1987(98)00108-1

Hughes JD, Liu J. 2008. MIKE SHE: Software for Integrated Surface Water/Ground Water Modeling. Groundwater 46 (6): 797–802 DOI: 10.1111/j.1745-6584.2008.00500.x

Hunink JE, Eekhout JPC, Vente JD, Contreras S, Droogers P, Baille A. 2017. Hydrological Modelling using Satellite-Based Crop Coefficients: A Comparison of Methods at the Basin Scale. Remote Sensing 9 (2): 174 DOI: 10.3390/rs9020174

ICRB Report. (2010). Iowa-Cedar River Basin Cedar River Basin, Needs and Capacity Assessment Summary, https://drive.google.com/file/d/0ByWmhV8D9VqVNWRjNGM1ZTktMmJiMS00YWFlLTgwMjYtZmE5OWVkNjRmMTc0/view?ddrp=1&hl=en#.

Ilampooranan I, Van Meter KJ, Basu NB. 2019. A Race Against Time: Modeling Time Lags in Watershed Response. Water Resources Research 0 (0) DOI: 10.1029/2018WR023815

Immerzeel WW, Droogers P. 2008. Calibration of a distributed hydrological model based on satellite evapotranspiration. Journal of Hydrology 349 (3): 411–424 DOI: 10.1016/j.jhydrol.2007.11.017

Iowa Department of Natural Resources (DNR). (2012.). Natural Resources Geographic Information Systems Library. Retrieved from <http://www.igsb.uiowa.edu/nrgislibx/>.

Iowa DNR (2017), Drainage Districts in Iowa, Iowa Geodata. Available at: https://geodata.iowa.gov/dataset/drainage-districts-iowa [Accessed 10 April 2019]

Iowa Environmental Mesonet. Available at: https://mesonet.agron.iastate.edu/ [Accessed 3 December 2018]

Izaurralde RC, Williams JR, McGill WB, Rosenberg NJ, Jakas MCQ. 2006. Simulating soil C dynamics with EPIC: Model description and testing against long-term data. Ecological Modelling 192 (3): 362–384 DOI: 10.1016/j.ecolmodel.2005.07.010

Izaurralde RC, Williams JR, Post WM, Thomson AM, McGill WB, Owens LB, Lal R. 2007. Long-term modeling of soil C erosion and sequestration at the small watershed scale. Climatic Change 80 (1–2): 73–90 DOI: 10.1007/s10584-006-9167-6

J. K. Mitchell, G. F. McIsaac, S. E. Walker, M. C. Hirschi. 2000. NITRATE IN RIVER AND SUBSURFACE DRAINAGE FLOWS FROM AN EAST CENTRAL ILLINOIS WATERSHED. Transactions of the ASAE 43 (2): 337–342 DOI: 10.13031/2013.2709

Jagadamma S, Lal R, Hoeft RG, Nafziger ED, Adee EA. 2007. Nitrogen fertilization and cropping systems effects on soil organic carbon and total nitrogen pools under chisel-plow tillage in Illinois. Soil and Tillage Research 95 (1): 348–356 DOI: 10.1016/j.still.2007.02.006

Jenkinson DS, Stewart William Duncan Paterson, Rosswall T. 1982. The nitrogen cycle in long-term field experiments. Philosophical Transactions of the Royal Society of London. B, Biological Sciences 296 (1082): 563–571 DOI: 10.1098/rstb.1982.0028

Jha MK, Gassman PW, Arnold JG. 2007. Water quality modeling for the Raccoon River watershed using SWAT. Transactions of the ASABE 50 (2): 479–493

Johnes PJ. 1996. Evaluation and management of the impact of land-use change on the nitrogen and phosphorus load delivered to surface waters: The export coefficient modelling approach. Journal of Hydrology 183 (3–4): 323–349 DOI: 10.1016/0022-1694(95)02951-6

Johnson C, Albrecht G, Ketterings Q, Beckman J, Stockin K. 2005. nitrogen-basics-the-nitrogen-cycle.pdf Available at: http://cceonondaga.org/resources/nitrogen-basics-the-nitrogen-cycle [Accessed 2 March 2019]

Kannan N, White SM, Worrall F, Whelan MJ. 2007. Hydrological modelling of a small catchment using SWAT-2000 – Ensuring correct flow partitioning for contaminant modelling. Journal of Hydrology 334 (1–2): 64–72 DOI: 10.1016/j.jhydrol.2006.09.030

Kalcic MM, Frankenberger J, Chaubey I. 2015. Spatial Optimization of Six Conservation Practices Using Swat in Tile-Drained Agricultural Watersheds. JAWRA Journal of the American Water Resources Association 51 (4): 956–972 DOI: 10.1111/1752-1688.12338

Keeney DR, Hatfield JL. 2008. Chapter 1. The Nitrogen Cycle, Historical Perspective, and Current and Potential Future Concerns. Publications from USDA-ARS / UNL Faculty Available at: http://digitalcommons.unl.edu/usdaarsfacpub/262

Kirchner JW. 2006. Getting the right answers for the right reasons: Linking measurements, analyses, and models to advance the science of hydrology. Water Resources Research 42 (3): W03S04 DOI: 10.1029/2005WR004362

Kopáček J, Hejzlar J, Posch M. 2013. Factors Controlling the Export of Nitrogen from Agricultural Land in a Large Central European Catchment during 1900–2010. Environmental Science & Technology 47 (12): 6400–6407 DOI: 10.1021/es400181m

Krysanova V, Arnold JG. 2008. Advances in ecohydrological modelling with SWAT—a review. Hydrological Sciences Journal 53 (5): 939–947 DOI: 10.1623/hysj.53.5.939

Kuentz, A., T. Mathevet, J. Gailhard, C. Perret, and V. Andreassian, 2013: Over 100 years of climatic and hydrologic variability of a Mediterranean and mountainous watershed: The Durance River. Cold and Mountain Region Hydrological Systems under Climate Change: Towards Improved Projections, A. Gelfan *et al.,* Eds., IAHS Publ. 360, 19–25. Available at: https://webgr.irstea.fr/wp-content/uploads/2014/10/an2013-pub00039716.pdf [Accessed 12 July 2017]

Lal R. 2015. A system approach to conservation agriculture. Journal of Soil and Water Conservation 70 (4): 82A-88A DOI: 10.2489/jswc.70.4.82A

Le L. 2015. Modeling stream discharge and nitrate loading in the Iowa-Cedar River basin under climate and land-use change. Theses and Dissertations Available at: http://ir.uiowa.edu/etd/1872

Legg (n.d). Influence of plants on nitrogen transformations in soils. [available at http://images.library.wisc.edu/EcoNatRes/EFacs/NAPC/NAPC04/reference/econatres.napc04.jlegg.pdf, accessed on December 14, 2017]. Available at:

http://images.library.wisc.edu/EcoNatRes/EFacs/NAPC/NAPC04/reference/econatres.napc04.jlegg.pdf [Accessed 15 December 2017]

Leip A, Britz W, Weiss F, de Vries W. 2011. Farm, land, and soil nitrogen budgets for agriculture in Europe calculated with CAPRI. Environmental Pollution 159 (11): 3243–3253 DOI: 10.1016/j.envpol.2011.01.040

Li Z, Liu H-Y, Li Y. 2012. [Review on HSPF model for simulation of hydrology and water quality processes]. Huan Jing Ke Xue= Huanjing Kexue 33 (7): 2217–2223

Li Z, Luo C, Jiang K, Wan R, Li H. 2017. Comprehensive Performance Evaluation for Hydrological and Nutrients Simulation Using the Hydrological Simulation Program–Fortran in a Mesoscale Monsoon Watershed, China. International Journal of Environmental Research and Public Health 14 (12) DOI: 10.3390/ijerph14121599

Liang S, Qin J. 2008. Data Assimilation Methods for Land Surface Variable Estimation. In Advances in Land Remote Sensing, Liang S (ed.).Springer Netherlands: Dordrecht; 313–339. DOI: 10.1007/978-1-4020-6450-0_12

Liu C. 2015. Assessment of the Effects of Riparian Buffer Zones on Water Quality in the Jinghe Catchment Using the AnnAGNPS and REMM Models: 105

Luo C, Li Z, Li H, Chen X. 2015. Evaluation of the AnnAGNPS Model for Predicting Runoff and Nutrient Export in a Typical Small Watershed in the Hilly Region of Taihu Lake. International Journal of Environmental Research and Public Health 12 (9): 10955–10973 DOI: 10.3390/ijerph120910955

Ma L, He C, Bian H, Sheng L. 2016. MIKE SHE modeling of ecohydrological processes: Merits, applications, and challenges. Ecological Engineering 96: 137–149 DOI: 10.1016/j.ecoleng.2016.01.008

Ma X, Li Y, Zhang M, Zheng F, Du S. 2011. Assessment and analysis of non-point source nitrogen and phosphorus loads in the Three Gorges Reservoir Area of Hubei Province, China. Science of The Total Environment 412–413: 154–161 DOI: 10.1016/j.scitotenv.2011.09.034

Madsen H. 2003. Parameter estimation in distributed hydrological catchment modelling using automatic calibration with multiple objectives. Advances in Water Resources 26 (2): 205–216 DOI: 10.1016/S0309-1708(02)00092-1

Mallarino A, Sawyer J, Barnhart S. 2013. A General Guide for Crop Nutrient and Limestone Recommendations in Iowa. Extension and Outreach Publications Available at: http://lib.dr.iastate.edu/extension_pubs/82

Manies KL, Harden JW, Kramer L, Parton W. 2000. Parameterizing century to model cultivated and noncultivated sites in the Loess region of western Iowa. USGS Numbered Series 2000–508. U.S. Geological Survey, Reston, VA. Available at: http://pubs.er.usgs.gov/publication/ofr00508 [Accessed 23 February 2019]

Matott, LS. 2017. OSTRICH: an Optimization Software Tool, Documentation and User's Guide, Version 17.12.19. 79 pages, University at Buffalo Center for Computational Research, www.eng.buffalo.edu/~lsmatott/Ostrich/OstrichMain.html. Available at: http://www.eng.buffalo.edu/~lsmatott/Ostrich/OstrichMain.html [Accessed 24 May 2018]

Mattikalli NM, Richards KS. 1996. Estimation of Surface Water Quality Changes in Response to Land-use Change: Application of The Export Coefficient Model Using Remote Sensing and Geographical Information System. Journal of Environmental Management 48 (3): 263–282 DOI: 10.1006/jema.1996.0077

McCarthy, K.A., Rose, C.E., and Kalkhoff, S.J., 2012, Environmental settings of the South Fork Iowa River basin, Iowa, and the Bogue Phalia basin, Mississippi, 2006–10: U.S. Geological Survey Scientific Investigations Report 2012–5021, 22 p. Available at: https://pubs.usgs.gov/sir/2012/5021/pdf/sir20125021.pdf [Accessed 19 December 2017]

McDonnell JJ, Beven K. 2014. Debates—The future of hydrological sciences: A (common) path forward? A call to action aimed at understanding velocities, celerities and residence time distributions of the headwater hydrograph. Water Resources Research 50 (6): 5342–5350 DOI: 10.1002/2013WR015141

McLauchlan K. 2006. The Nature and Longevity of Agricultural Impacts on Soil Carbon and Nutrients: A Review. Ecosystems 9 (8): 1364–1382 DOI: 10.1007/s10021-005-0135-1

Meals DW, Dressing SA, Davenport TE. 2010. Lag time in water quality response to best management practices: a review. Journal of Environmental Quality 39 (1): 85–96 DOI: 10.2134/jeq2009.0108

Metherell AK, Harding LA, Cole VC, Parton WJ. 1993. CENTURY Soil Organic Matter Model Environment Available at: https://www2.nrel.colostate.edu/projects/century/MANUAL/html_manual/man96.html [Accessed 23 February 2019]

Milly PCD, Dunne KA. 2016. Potential evapotranspiration and continental drying. Nature Climate Change 6 (10): 946–949 DOI: 10.1038/nclimate3046

Mockler EM, O'Loughlin FE, Bruen M. 2016. Understanding hydrological flow paths in conceptual catchment models using uncertainty and sensitivity analysis. Computers & Geosciences 90: 66–77 DOI: 10.1016/j.cageo.2015.08.015

Moriasi, D. N., Gitau, M. W., Pai, N., & Daggupati, P. (2015). Hydrologic and water quality models: Performance measures and evaluation criteria. Trans. ASABE, 58(6), 1763-1785. http://dx.doi.org/10.13031/trans.58.10715. Available at: http://elibrary.asabe.org/azdez.asp?AID=46548&T=2 [Accessed 19 December 2017]

Muenich RL, Kalcic M, Scavia D. 2016. Evaluating the Impact of Legacy P and Agricultural Conservation Practices on Nutrient Loads from the Maumee River Watershed. Environmental Science & Technology 50 (15): 8146–8154 DOI: 10.1021/acs.est.6b01421

Mulholland PJ, Helton AM, Poole GC, Hall RO, Hamilton SK, Peterson BJ, Tank JL, Ashkenas LR, Cooper LW, Dahm CN, et al.,2008. Stream denitrification across biomes and its response to anthropogenic nitrate loading. Nature 452 (7184): 202–205 DOI: 10.1038/nature06686

Müller T, Höper H. 2004. Soil organic matter turnover as a function of the soil clay content: consequences for model applications. Soil Biology and Biochemistry 36 (6): 877–888 DOI: 10.1016/j.soilbio.2003.12.015

Murphy, J.C., Hirsch, R.M., and Sprague, L.A., 2013, Nitrate in the Mississippi River and its tributaries, 1980–2010—An update: U.S. Geological Survey Scientific Investigations Report 2013–5169, 31 p.

Murty D, Kirschbaum MUF, Mcmurtrie RE, Mcgilvray H. 2002. Does conversion of forest to agricultural land change soil carbon and nitrogen? a review of the literature. Global Change Biology 8 (2): 105–123 DOI: 10.1046/j.1354-1013.2001.00459.x

Nair SS, King KW, Witter JD, Sohngen BL, Fausey NR. 2011. Importance of Crop Yield in Calibrating Watershed Water Quality Simulation Tools1. JAWRA Journal of the American Water Resources Association 47 (6): 1285–1297 DOI: 10.1111/j.1752-1688.2011.00570.x

Narula KK, Gosain AK. 2013. Modeling hydrology, groundwater recharge and non-point nitrate loadings in the Himalayan Upper Yamuna basin. Science of The Total Environment 468–469, Supplement: S102–S116 DOI: 10.1016/j.scitotenv.2013.01.022

National Atmospheric Deposition Program (NADP) (2014). Data downloaded from [http://nadp.sws.uiuc.edu/data/].

Neitsch, S. L., J. G. Arnold, J. R. Kiniry, J. R. Williams, and K. W. King. 2011. Soil and Water Assessment Tool: Theoretical documentation, version 2009. TWRI Report TR-406. College Station, Texas: Texas Water Resources Institute.

Parsons E, Thomas DL, Huffman RL. 2004. AGRICULTURAL NON-POINT SOURCE WATER QUALITY MODELS: THEIR USE AND APPLICATION Southern Cooperative Series Bulletin #398.

Parton WJ, Scurlock JMO, Ojima DS, Gilmanov TG, Scholes RJ, Schimel DS, Kirchner T, Menaut J-C, Seastedt T, Moya EG, et al.,1993. Observations and modeling of biomass and soil organic matter dynamics for the grassland biome worldwide. Global Biogeochemical Cycles 7 (4): 785–809 DOI: 10.1029/93GB02042

Parton WJ, Stewart JWB, Cole CV. 1988. Dynamics of C, N, P and S in grassland soils: a model. Biogeochemistry 5 (1): 109–131 DOI: 10.1007/BF02180320

Paul Baumgart. (2005). Lower Green Bay and Lower Fox Tributary Modeling Report, http://www.co.brown.wi.us/i_brown/d/land__water_conservation/lowerfox_tss-p_load-allocation.pdf.

Pechlivanidis IG, Arheimer B. 2015. Large-scale hydrological modelling by using modified PUB recommendations: the India-HYPE case. Hydrol. Earth Syst. Sci. 19 (11): 4559–4579 DOI: 10.5194/hess-19-4559-2015

Pechlivanidis I.G., Jackson B., McMillan H., (2010), The use of entropy as a model diagnostic in rainfallrunoff modelling, in iEMSs 2010: International Congress on Environmental Modelling and Software, 5- 8 July, Ottawa, Canada. Available at: http://www.iemss.org/iemss2010/papers/S20/S.20.10.The%20Use%20of%20Entropy%20as%20a%20Model%20Diagnostic%20in%20Rainfall%20Runoff%20Modelling%20-%20ILIAS%20PECHLIVANIDIS.pdf [Accessed 12 July 2017]

Pfannerstill M, Bieger K, Guse B, Bosch DD, Fohrer N, Arnold JG. 2017. How to Constrain Multi-Objective Calibrations of the SWAT Model Using Water Balance Components. JAWRA

Journal of the American Water Resources Association 53 (3): 532–546 DOI: 10.1111/1752-1688.12524

Pope CA, Burnett RT, Thun MJ, Calle EE, Krewski D, Ito K, Thurston GD. 2002. Lung cancer, cardiopulmonary mortality, and long-term exposure to fine particulate air pollution. JAMA 287 (9): 1132–1141

Preston SD, Alexander RB, Wolock DM. 2011. Sparrow Modeling to Understand Water-Quality Conditions in Major Regions of the United States: A Featured Collection Introduction. Journal of the American Water Resources Association 47 (5): 887–890 DOI: 10.1111/j.1752-1688.2011.00585.x

Qiao L, Herrmann RB, Pan Z. 2013. Parameter Uncertainty Reduction for SWAT Using Grace, Streamflow, and Groundwater Table Data for Lower Missouri River Basin1. JAWRA Journal of the American Water Resources Association 49 (2): 343–358 DOI: 10.1111/jawr.12021

Rajib MA, Merwade V. 2016. Improving soil moisture accounting and streamflow prediction in SWAT by incorporating a modified time-dependent Curve Number method. Hydrological Processes 30 (4): 603–624 DOI: 10.1002/hyp.10639

Rajib MA, Merwade V, Yu Z. 2016. Multi-objective calibration of a hydrologic model using spatially distributed remotely sensed/in-situ soil moisture. Journal of Hydrology 536: 192–207 DOI: 10.1016/j.jhydrol.2016.02.037

Ren P, Li J, Feng P, Guo Y, Ma Q. 2018. Evaluation of Multiple Satellite Precipitation Products and Their Use in Hydrological Modelling over the Luanhe River Basin, China. Water 10 (6): 677 DOI: 10.3390/w10060677

Revilla-Romero B, Beck HE, Burek P, Salamon P, de Roo A, Thielen J. 2015. Filling the gaps: Calibrating a rainfall-runoff model using satellite-derived surface water extent. Remote Sensing of Environment 171 (Supplement C): 118–131 DOI: 10.1016/j.rse.2015.10.022

Rippey BR. 2015. The U.S. drought of 2012. Weather and Climate Extremes 10: 57–64 DOI: 10.1016/j.wace.2015.10.004

Rockström J, Steffen W, Noone K, Persson Å, Chapin F, Lambin E, Lenton T, Scheffer M, Folke C, Schellnhuber H, et al.,2009. Planetary Boundaries: Exploring the Safe Operating Space for Humanity. Institute for Sustainable Solutions Publications Available at: http://pdxscholar.library.pdx.edu/iss_pub/64

Rouhani H, Willems P, Wyseure G, Feyen J. 2007. Parameter estimation in semi-distributed hydrological catchment modelling using a multi-criteria objective function. Hydrological Processes 21 (22): 2998–3008 DOI: 10.1002/hyp.6527

Royer TV, Tank JL, David MB. 2004. Transport and Fate of Nitrate in Headwater Agricultural Streams in Illinois. Journal of Environment Quality 33 (4): 1296 DOI: 10.2134/jeq2004.1296

Ruddy BC, Lorenz DL, Mueller DK. County-Level Estimates of Nutrient Inputs to the Land Surface of the Conterminous United States, 1982–200: 23

Russelle MP, Birr AS. 2004. Large-Scale Assessment of Symbiotic Dinitrogen Fixation by Crops: Soybean and Alfalfa in the Mississippi River Basin. AGRONOMY JOURNAL 96: 7

Samadi SZ. 2016. Assessing the sensitivity of SWAT physical parameters to potential evapotranspiration estimation methods over a coastal plain watershed in the southeastern United States. Hydrology Research: nh2016034 DOI: 10.2166/nh.2016.034

Sanchez PA. 2002. Soil fertility and hunger in Africa. (Policy forum: ecology). Science 295 (5562): 2019-

Santhi C, Kannan N, Arnold JG, Di Luzio M. 2008. Spatial Calibration and Temporal Validation of Flow for Regional Scale Hydrologic Modeling1. JAWRA Journal of the American Water Resources Association 44 (4): 829–846 DOI: 10.1111/j.1752-1688.2008.00207.x

Sawyer, John E., 'Nitrogen Use in Iowa Corn Production' (2015). Extension and Outreach Publications. 107. http://lib.dr.iastate.edu/extension_pubs/107. Available at: https://store.extension.iastate.edu/product/Nitrogen-Use-in-Iowa-Corn-Production [Accessed 15 March 2018]

Scavia D, Bertani I, Obenour DR, Turner RE, Forrest DR, Katin A. 2017. Ensemble modeling informs hypoxia management in the northern Gulf of Mexico. Proceedings of the National Academy of Sciences 114 (33): 8823–8828 DOI: 10.1073/pnas.1705293114

Schilling KE, Wolter CF. 2007. A GIS-based groundwater travel time model to evaluate stream nitrate concentration reductions from land-use change. Environmental Geology 53 (2): 433–443 DOI: 10.1007/s00254-007-0659-0

Schilling KE, Jha MK, Zhang Y-K, Gassman PW, Wolter CF. 2008. Impact of land-use and land cover change on the water balance of a large agricultural watershed: Historical effects and future directions. Water Resources Research 44 (7): W00A09 DOI: 10.1029/2007WR006644

Schlesinger WH. 2009. On the fate of anthropogenic nitrogen. Proceedings of the National Academy of Sciences 106 (1): 203–208 DOI: 10.1073/pnas.0810193105

Schneider K, Ketzer B, Breuer L, Vaché KB, Bernhofer C, Frede H-G. 2007. Evaluation of evapotranspiration methods for model validation in a semi-arid watershed in northern China. Adv. Geosci. 11: 37–42 DOI: 10.5194/adgeo-11-37-2007

Science Advisory Board 2011 Reactive Nitrogen in the United States: An Analysis of Inputs, Flows, Consequences, and Management Options Office of the U.S. EPA Administrator Washington,DC. Available at: https://yosemite.epa.gov/sab/sabproduct.nsf/WebBOARD/INCFullReport/$File/Final%20INC%20Report_8_19_11(without%20signatures).pdf [Accessed 3 March 2019]

Sebilo M, Mayer B, Nicolardot B, Pinay G, Mariotti A. 2013. Long-term fate of nitrate fertilizer in agricultural soils. Proceedings of the National Academy of Sciences 110 (45): 18185–18189 DOI: 10.1073/pnas.1305372110

Secchi S, Kurkalova L, Gassman PW, Hart C. 2011. Land-use change in a biofuels hotspot: The case of Iowa, USA. Biomass and Bioenergy 35 (6): 2391–2400 DOI: 10.1016/j.biombioe.2010.08.047

Seibert J, McDonnell JJ. 2002. On the dialog between experimentalist and modeler in catchment hydrology: Use of soft data for multicriteria model calibration. Water Resources Research 38 (11): 1241 DOI: 10.1029/2001WR000978

Seitzinger S, Harrison JA, Böhlke JK, Bouwman AF, Lowrance R, Peterson B, Tobias C, Drecht GV. 2006. Denitrification Across Landscapes and Waterscapes: A Synthesis. Ecological Applications 16 (6): 2064–2090 DOI: 10.1890/1051-0761(2006)016[2064:DALAWA]2.0.CO;2

Seo B-C, Cunha LK, Krajewski WF. 2013. Uncertainty in radar-rainfall composite and its impact on hydrologic prediction for the eastern Iowa flood of 2008. Water Resources Research 49 (5): 2747–2764 DOI: 10.1002/wrcr.20244

Shafii M, Basu N, Craig JR, Schiff SL, Van Cappellen P. 2017. A diagnostic approach to constraining flow partitioning in hydrologic models using a multiobjective optimization framework. Water Resources Research 53 (4): 3279–3301 DOI: 10.1002/2016WR019736

Shirinian-Orlando AA, Uchrin CG. 2007. Modeling the Hydrology and water quality using BASINS/HSPF for the upper Maurice River watershed, New Jersey. Journal of Environmental Science and Health, Part A 42 (3): 289–303 DOI: 10.1080/10934520601134254

Six J, Conant RT, Paul EA, Paustian K. 2002. Stabilization mechanisms of soil organic matter: Implications for C-saturation of soils. Plant and Soil 241 (2): 155–176 DOI: 10.1023/A:1016125726789

Skahill BE. 2004. Use of the Hydrological Simulation Program - FORTRAN (HSPF) Model for Watershed Studies: Defense Technical Information Center, Fort Belvoir, VA. DOI: 10.21236/ADA434883

Sloan BP. 2013. Hydrologic impacts of tile drainage in Iowa.MS, University of Iowa, Iowa City, Iowa, USA. DOI: 10.17077/etd.s65i2rmj

Smil, V. (2011) Nitrogen Cycle and World Food Production. World Agriculture, 2, 9-13.

Smith P. 2008. Land-use change and soil organic carbon dynamics. Nutrient Cycling in Agroecosystems 81 (2): 169–178 DOI: 10.1007/s10705-007-9138-y

Smith RA, Schwarz GE, Alexander RB. 1997. Regional interpretation of water-quality monitoring data. Water Resources Research 33 (12): 2781–2798 DOI: 10.1029/97WR02171

Soil Survey Staff (n.d.). Web Soil Survey. Washington, DC: Natural Resources Conservation Service, United States Department of Agriculture. Retrieved from <http://websoilsurvey.nrcs.usda.gov/>.

Sperna Weiland FC, Tisseuil C, Dürr HH, Vrac M, van Beek LPH. 2012. Selecting the optimal method to calculate daily global reference potential evaporation from CFSR reanalysis data for application in a hydrological model study. Hydrol. Earth Syst. Sci. 16 (3): 983–1000 DOI: 10.5194/hess-16-983-2012

Spies RR, Franz KJ, Hogue TS, Bowman AL. 2014. Distributed Hydrologic Modeling Using Satellite-Derived Potential Evapotranspiration. Journal of Hydrometeorology 16 (1): 129–146 DOI: 10.1175/JHM-D-14-0047.1

Sprague LA, Hirsch RM, Aulenbach BT. 2011. Nitrate in the Mississippi River and Its Tributaries, 1980 to 2008: Are We Making Progress? Environmental Science & Technology 45 (17): 7209–7216 DOI: 10.1021/es201221s

Srinivasan, R., X. Zhang, and J. G. Arnold. 2010. SWAT ungauged: Hydrological budget and crop yield predictions in the Upper Mississippi River basin. Trans. ASABE 53(5): 1533- 1546. Available at: http://ssl.tamu.edu/media/30637/sw8281.pdf [Accessed 18 December 2017]

State of the Bay, 2018. Chesapeake Bay Foundation, Report on state of the bay. Available at: https://www.cbf.org/document-library/cbf-reports/2018-state-of-the-bay-report.pdf [Accessed 16 February 2019]

Stisen S, Jensen KH, Sandholt I, Grimes DIF. 2008. A remote sensing driven distributed hydrological model of the Senegal River basin. Journal of Hydrology 354 (1): 131–148 DOI: 10.1016/j.jhydrol.2008.03.006

Sudheer KP, Chaubey I, Garg V, Migliaccio KW. 2007. Impact of time-scale of the calibration objective function on the performance of watershed models. Hydrological Processes 21 (25): 3409–3419 DOI: 10.1002/hyp.6555

Suir GM. 2002. Validation of AnnAGNPS at the field and farm-scale using an integrated AGNPS/GIS system: 115

Teshager AD, Gassman PW, Secchi S, Schoof JT, Misgna G. 2016. Modeling Agricultural Watersheds with the Soil and Water Assessment Tool (SWAT): Calibration and Validation with a Novel Procedure for Spatially Explicit HRUs. Environmental Management 57 (4): 894–911 DOI: 10.1007/s00267-015-0636-4

Thiemig V, Rojas R, Zambrano-Bigiarini M, De Roo A. 2013. Hydrological evaluation of satellite-based rainfall estimates over the Volta and Baro-Akobo Basin. Journal of Hydrology 499: 324–338 DOI: 10.1016/j.jhydrol.2013.07.012

Thieu V, Bouraoui F, Aloe A, Bidoglio G. 2012. Scenario analysis of pollutants loads to European regional seas for the year 2020. EUR 25159 EN: 80

Tolson BA, Shoemaker CA. 2007. Dynamically dimensioned search algorithm for computationally efficient watershed model calibration. Water Resources Research 43 (1) DOI: 10.1029/2005WR004723

Tomer MD, Moorman TB, Rossi CG. 2008. Assessment of the Iowa River's South Fork watershed: Part 1. Water quality. Journal of Soil and Water Conservation 63 (6): 360–370 DOI: 10.2489/jswc.63.6.360

Townsend AR, Howarth RW, Bazzaz FA, Booth MS, Cleveland CC, Collinge SK, Dobson AP, Epstein PR, Holland EA, Keeney DR, et al.,2003. Human health effects of a changing global nitrogen cycle. Frontiers in Ecology and the Environment 1 (5): 240–246 DOI: 10.1890/1540-9295(2003)001[0240:HHEOAC]2.0.CO;2

Trautmann T. 2016. Macroscopic diagnostic modeling of the hydrological cycle: Understanding the dynamics of water pools in snow affected regions.Master's Thesis, Friedrich-Schiller-Universität, Jena.

Trybula EM, Cibin R, Burks JL, Chaubey I, Brouder SM, Volenec JJ. 2014. Perennial rhizomatous grasses as bioenergy feedstock in SWAT: parameter development and model improvement. GCB Bioenergy: n/a-n/a DOI: 10.1111/gcbb.12210

United States Department of Agriculture-National Resorces Conservation Services USDA-NRCS, 2004. Part 630 Hydrology National Engineering Handbook, Chapter 9 Hydrologic Soil-Cover Complexes. Available at: https://directives.sc.egov.usda.gov/OpenNonWebContent.aspx?content=17758.wba [Accessed 17 December 2018]

United States Environmental Protection Agency (US-EPA). 2013. Weather Bureau Army Navy (WBAN) - Station Notes. US EPA Available at: https://www.epa.gov/ceam/weather-bureau-army-navy-wban-station-notes [Accessed 3 December 2018]

U.S. Geological Survey (USGS) (2012). County fertiliser data. Data downloaded from <http://water.usgs.gov/GIS/dsdl/sir2012-5207_county_fertilizer.zip>.

U.S. Geological Survey (USGS) (2013). National Elevation Dataset. Data downloaded from <http://ned.usgs.gov>.

U.S. Geological Survey (USGS) (2016). National Water Information System data available on the World Wide Web (USGS Water Data for the Nation), accessed [December 19, 2017], at URL [http://waterdata.usgs.gov/nwis/]. Available at: http://waterdata.usgs.gov/nwis/

US National Weather Service (NWS). Cooperative Observer Program (COOP) Available at: https://www.weather.gov/coop/overview [Accessed 3 December 2018]

USDA. 2012. U.S. Department of Agriculture (USDA). (2012). Crop Data Layer. Washington, DC: National Agricultural Statistics Service. Data downloaded from <http://nassgeodata.gmu.edu/CropScape/>

USDA-National Agricultural Statistics Service, Census of Agriculture. (USDA-Agricultural Census) (2012). Published state and county level data [Online]. Available at [https://www.agcensus.usda.gov/Publications/2012, accessed 2017-12-18]. USDA-NASS, Washington, DC. Available at: https://www.agcensus.usda.gov/Publications/2012/ [Accessed 19 December 2017]

USDA-National Agricultural Statistics Service, Census of Agriculture. (USDA-Agricultural Survey) (2012). QuickStats Ad-hoc Query Tool [Online]. Available at [https://quickstats.nass.usda.gov/?source_desc=CENSUS, accessed 2017-12-18]. USDA-NASS, Washington, DC. Available at: https://quickstats.nass.usda.gov/?source_desc=CENSUS [Accessed 19 December 2017]

USDA-National Agricultural Statistics Service, Cropland Data Layer. (USDA-CDL) (2012). Published crop-specific data layer [Online]. Available at [https://nassgeodata.gmu.edu/CropScape, accessed 2017-12-18]. USDA-NASS, Washington, DC.

USEPA, 2017. United States Environmental Protection Agency (USEPA), National Water Quality Inventory: Report to Congress.: 22

Van Meter KJ, Basu NB. 2015. Catchment Legacies and Time Lags: A Parsimonious Watershed Model to Predict the Effects of Legacy Storage on Nitrogen Export. PLoS ONE 10 (5): e0125971 DOI: 10.1371/journal.pone.0125971

Van Meter KJ, Basu NB. 2017. Time lags in watershed-scale nutrient transport: an exploration of dominant controls. Environmental Research Letters 12 (8): 084017 DOI: 10.1088/1748-9326/aa7bf4

Van Meter KJ, Basu NB, Van Cappellen P. 2017. Two centuries of nitrogen dynamics: Legacy sources and sinks in the Mississippi and Susquehanna River Basins. Global Biogeochemical Cycles 31 (1): 2016GB005498 DOI: 10.1002/2016GB005498

Van Meter KJ, Van Cappellen P, Basu NB. 2018. Legacy nitrogen may prevent achievement of water quality goals in the Gulf of Mexico. Science: eaar4462 DOI: 10.1126/science.aar4462

Van Meter KJ, Basu NB, Veenstra JJ, Burras CL. 2016. The nitrogen legacy: emerging evidence of nitrogen accumulation in anthropogenic landscapes. Environmental Research Letters 11 (3): 035014 DOI: 10.1088/1748-9326/11/3/035014

Varvel GE. 1994. Rotation and Nitrogen Fertilization Effects on Changes in Soil Carbon and Nitrogen. Agronomy & Horticulture -- Faculty Publications Available at: http://digitalcommons.unl.edu/agronomyfacpub/323

Veenstra J. 2010. Fifty years of agricultural soil change in Iowa. Graduate Theses and Dissertations Available at: http://lib.dr.iastate.edu/etd/11428

Vero SE, Basu NB, Van Meter K, Richards KG, Mellander P-E, Healy MG, Fenton O. 2018. Review: the environmental status and implications of the nitrate time lag in Europe and North America. Hydrogeology Journal 26 (1): 7–22 DOI: 10.1007/s10040-017-1650-9

Vitousek PM, Aber JD, Howarth RW, Likens GE, Matson PA, Schindler DW, Schlesinger WH, Tilman DG. 1997. Human alteration of the global nitrogen cycle: sources and consequences. Ecological Applications 7 (3): 737–750 DOI: 10.1890/1051-0761(1997)007[0737:HAOTGN]2.0.CO;2

Wang J-Y, Yan X-Y, Gong W. 2015. Effect of Long-Term Fertilization on Soil Productivity on the North China Plain. Pedosphere 25 (3): 450–458 DOI: 10.1016/S1002-0160(15)30012-6

Wang R, Bowling LC, Cherkauer KA. 2016. Estimation of the effects of climate variability on crop yield in the Midwest USA. Agricultural and Forest Meteorology 216: 141–156 DOI: 10.1016/j.agrformet.2015.10.001

Wang S, Zhang Z, Sun G, Strauss P, Guo J, Tang Y, Yao A. 2012. Multi-site calibration, validation, and sensitivity analysis of the MIKE SHE Model for a large watershed in northern China. Hydrol. Earth Syst. Sci. 16 (12): 4621–4632 DOI: 10.5194/hess-16-4621-2012

Wang X, Melesse A, Yang W. 2006. Influences of Potential Evapotranspiration Estimation Methods on SWAT's Hydrologic Simulation in a Northwestern Minnesota Watershed. Transactions of the ASABE (American Society of Agricultural and Biological Engineers) 49: 1755–1771 DOI: 10.13031/2013.22297

Weyer PJ, Cerhan JR, Kross BC, Hallberg GR, Kantamneni J, Breuer G, Jones MP, Zheng W, Lynch CF. 2001. Municipal drinking water nitrate level and cancer risk in older women: the Iowa Women's Health Study. Epidemiology (Cambridge, Mass.) 12 (3): 327–338

Wi S, Yang YCE, Steinschneider S, Khalil A, Brown CM. 2015. Calibration approaches for distributed hydrologic models in poorly gaged basins: implication for streamflow projections under climate change. Hydrol. Earth Syst. Sci. 19 (2): 857–876 DOI: 10.5194/hess-19-857-2015

Worrall F, Burt TP. 1999. The impact of land-use change on water quality at the catchment scale: the use of export coefficient and structural models. Journal of Hydrology 221 (1): 75–90 DOI: 10.1016/S0022-1694(99)00084-0

Worrall F, Howden NJK, Burt TP. 2015. Evidence for nitrogen accumulation: the total nitrogen budget of the terrestrial biosphere of a lowland agricultural catchment. Biogeochemistry 123 (3): 411–428 DOI: 10.1007/s10533-015-0074-7

X. Wang, R. D. Harmel, J. R. Williams, W. L. Harman. 2006. EVALUATION OF EPIC FOR ASSESSING CROP YIELD, RUNOFF, SEDIMENT AND NUTRIENT LOSSES FROM WATERSHEDS WITH POULTRY LITTER FERTILIZATION. Transactions of the ASABE 49 (1): 47–59 DOI: 10.13031/2013.20243

Xue Xianwu, Zhang Ke, Hong Yang, Gourley Jonathan J., Kellogg Wayne, McPherson Renee A., Wan Zhanming, Austin Barney N. 2016. New Multisite Cascading Calibration Approach for Hydrological Models: Case Study in the Red River Basin Using the VIC Model. Journal of Hydrologic Engineering 21 (2): 05015019 DOI: 10.1061/(ASCE)HE.1943-5584.0001282

Yan X, Ti C, Vitousek P, Chen D, Leip A, Cai Z, Zhu Z. 2014. Fertilizer nitrogen recovery efficiencies in crop production systems of China with and without consideration of the residual effect of nitrogen. Environmental Research Letters 9 (9): 095002 DOI: 10.1088/1748-9326/9/9/095002

Yang J, Reichert P, Abbaspour KC, Xia J, Yang H. 2008. Comparing uncertainty analysis techniques for a SWAT application to the Chaohe Basin in China. Journal of Hydrology 358 (1–2): 1–23 DOI: 10.1016/j.jhydrol.2008.05.012

Yang Q, Zuo H, Li W. 2016. Land Surface Model and Particle Swarm Optimization Algorithm Based on the Model-Optimization Method for Improving Soil Moisture Simulation in a Semi-Arid Region. PLoS ONE 11 (3) DOI: 10.1371/journal.pone.0151576

Yen H, Bailey RT, Arabi M, Ahmadi M, White MJ, Arnold JG. 2014. The role of interior watershed processes in improving parameter estimation and performance of watershed models. Journal of Environmental Quality 43 (5): 1601–1613 DOI: 10.2134/jeq2013.03.0110

Yilmaz KK, Gupta HV, Wagener T. 2008. A process-based diagnostic approach to model evaluation: Application to the NWS distributed hydrologic model. Water Resources Research 44 (9): W09417 DOI: 10.1029/2007WR006716

Yilmaz KK, Hogue TS, Hsu K, Sorooshian S, Gupta HV, Wagener T. 2005. Intercomparison of Rain Gauge, Radar, and Satellite-Based Precipitation Estimates with Emphasis on Hydrologic Forecasting. Journal of Hydrometeorology 6 (4): 497–517 DOI: 10.1175/JHM431.1

Zaehle S. 2013. Terrestrial nitrogen–carbon cycle interactions at the global scale. Philosophical Transactions of the Royal Society B: Biological Sciences 368 (1621): 20130125 DOI: 10.1098/rstb.2013.0125

Zessner M, Schönhart M, Parajka J, Trautvetter H, Mitter H, Kirchner M, Hepp G, Blaschke AP, Strenn B, Schmid E. 2017. A novel integrated modelling framework to assess the impacts of climate and socio-economic drivers on land-use and water quality. Science of The Total Environment 579: 1137–1151 DOI: 10.1016/j.scitotenv.2016.11.092

Zhang Q, Ball WP, Moyer DL. 2016. Decadal-scale export of nitrogen, phosphorus, and sediment from the Susquehanna River basin, USA: Analysis and synthesis of temporal and spatial patterns. Science of The Total Environment 563–564 (Supplement C): 1016–1029 DOI: 10.1016/j.scitotenv.2016.03.104

Zhang X. 2016. Spatio-Temporal Patterns in Net Anthropogenic Nitrogen and Phosphorus Inputs Across the Grand River Watershed Available at: https://uwspace.uwaterloo.ca/handle/10012/10900 [Accessed 24 February 2019]

Zhang X, Izaurralde RC, Arnold JG, Williams JR, Srinivasan R. 2013. Modifying the Soil and Water Assessment Tool to simulate cropland carbon flux: model development and initial evaluation. The Science of the Total Environment 463–464: 810–822 DOI: 10.1016/j.scitotenv.2013.06.056

Zhang Y, Chiew FHS, Zhang L, Li H. 2009. Use of Remotely Sensed Actual Evapotranspiration to Improve Rainfall–Runoff Modeling in Southeast Australia. Journal of Hydrometeorology 10 (4): 969–980 DOI: 10.1175/2009JHM1061.1

Zuo D, Xu Z, Peng D, Song J, Cheng L, Wei S, Abbaspour KC, Yang H. 2015. Simulating spatiotemporal variability of blue and green water resources availability with uncertainty analysis. Hydrological Processes 29 (8): 1942–1955 DOI: 10.1002/hyp.10307

Appendix A: Supplementary Information for Chapter 3

Table A1. SWAT calibration parameters with the description, adjustments made, initial range and final calibrated values for BS through S3

Parameters	Description	Adjustment[a]	Calibration Range	Calibrated values			
				BS	S1	S2	S3
Hydrology							
CN2	Runoff curve number	Relative	-0.10-0.25	0.213	0.199	-0.022	-0.053
CHN2	Main Channel Manning's "n" value	Relative	-0.10-0.10	-0.032	-0.020	0.008	-0.023
SURLAG	Surface Runoff Lag Coefficient	Relative	-0.50-0.50	-0.224	-0.294	-0.423	-0.093
DEP_IMP	Depth to impervious layer, mm	Replace	2400-2600	2438	2400	2534	2547
ESCO	Soil evaporation compensation coefficient	Replace	0.85-1.00	0.997	0.997	0.926	0.983
EPCO	Plant uptake compensation coefficient	Replace	0.90-1.00	0.954	0.957	0.978	0.969
SOL_Z	Depth from soil surface to bottom of layer (mm)	Relative	-0.15-0.10	-0.128	-0.034	0.056	-0.049
SOL_AWC	Available water capacity of soil layers (mmH_20/mm soil)	Relative	-0.10-0.20	-0.005	0.022	-0.005	0.027
SOL_K	Saturated hydraulic conductivity (mm/hr)	Relative	-0.15-0.10	-0.051	-0.054	-0.001	-0.058
GW_REVAP	Groundwater re-evaporation coefficient	Relative	-0.10-0.15	0.117	0.055	0.048	0.059
GW_DELAY	Groundwater delay time (days)	Relative	-0.10-0.10	0.038	0.031	-0.006	0.040
ALPHA_BF	Baseflow recession constant (days)	Relative	-0.15-0.10	-0.046	-0.045	-0.031	0.029
Crop yield							
BIO_E_CORN	Plant radiation use efficiency for corn, MJ/m^2	Relative	-0.10-0.10	-	-0.008	-0.001	-0.014
BIO_E_SOYB	Plant radiation use efficiency for corn, MJ/m^2	Relative	-0.10-0.10	-	0.044	0.028	-0.013
HVSTI_CORN	Harvest Index for corn	Relative	-0.10-0.10	-	-0.014	-0.018	0.020
HVSTI_SOYB	Harvest Index for soybean	Relative	-0.10-0.10	-	-0.046	-0.094	0.054
BLAI_CORN	The maximum potential leaf area index for corn	Relative	-0.10-0.10	-	-0.002	-0.033	-0.006
BLAI_SOYB	The maximum potential leaf area index for soybean	Replace	3.00-5.00	-	3.885	3.678	3.424
HEATUNITS_CORN	Heat units of corn (cumulative ^oC)	Replace	1000-1150	-	1032	1104	1078
HEATUNITS_SOYB	Heat units of soybean (cumulative ^oC)	Replace	1300-1600	-	1309	1595	1595
Tile drain Parameters	**Description**		**Adjustment**		**Values**		
DDRAIN	Depth at which tile drains are installed (mm)		Fixed		1000		
TDRAIN	Time required to drain the soil to field capacity (hr)		Fixed		48		
GDRAIN	Drain tile lag time (hr)		Fixed		96		

[a] Type of change applied over the SWAT's default values during calibration, where (i) Relative means: SWAT's default value is multiplied by the adjustment factor (1 + "a given value within the calibration range which is identified by the calibration algorithm during each run") (ii) Replace means: SWAT's default parameter value is replaced with a given value within the calibration range which is identified by the calibration algorithm during each run and (iii) Fixed means: Constant values, where the tile drain parameters are based on Green *et al.* (2006) and Nair *et al.* (2011)

Appendix B: Supplementary Information for Chapter 4

Section B1: Estimation of crop yield, mineral N fertilizer, and manure application rates

Annual corn and soybean yield data for counties in the study area (Franklin, Hamilton, Hardin, and Wright counties) were downloaded from USDA-Agricultural Survey (2012) and converted to the watershed scale using proportional areas. Where annual data was not available, the USDA-Agricultural Census (2012) (1 in 5 years) data was interpolated to estimate the annual yield. Since SWAT simulates yield on a dry weight basis, observed corn and soybean yield were corrected for moisture based on the procedure outlined in (Gassman, 2008). For oats, alfalfa and other hay observed yields were multiplied by dry matter percentages 89.4%, 90.4%, and 86.7% respectively, based on Hong *et al.* (2013).

County-scale fertilizer application data were obtained from Alexander and Smith (1990) and USGS (2012). County-scale magnitudes were converted to watershed-scale magnitudes based on the area proportions of each county within the watershed. Mineral N application rates estimated by this method varied between 2 kg/ha/yr and 211 kg/ha/yr, with the lower numbers representative of application rates in the 1950s, and the higher values corresponding to current typical N application rates recommended for cropland in Iowa (Sawyer, 2015)

It was assumed that all manure generated in the watershed was used as fertilizer. This assumption is reasonable considering the costs of transporting manure over long distances. Animal counts at county scale were obtained from the USDA-Agricultural Census (2012). Based on the "N in animal excretion" parameters obtained from Hong et al.,(2011), manure N was computed by multiplying the animal count with respective "N in animal excretion" values. County-scale magnitudes were converted into watershed-scale magnitudes based on the area proportions of each county within the watershed. The typical manure N application rates varied from 37 kg/ha/yr to 105 kg/ha/yr.

Section B2: Synthesis of Publications to Estimate acceptable ranges for the Kling-Gupta Efficiency

There is a lack of information on the range of KGE values that are acceptable in watershed modeling. To address this, we synthesized 11 studies (Formetta *et al.,* 2014; Hoch *et al.,* 2017; Hublart *et al.,* 2015; Kuentz *et al.,* 2013; Pechlivanidis *et al.,* 2010; Pechlivanidis and Arheimer, 2015; Rajib *et al.,* 2016; Revilla-Romero *et al.,* 2015; Thiemig *et al.,* 2013; Trautmann, 2016; Yang *et al.,* 2016) that used KGE as a performance metric to calibrate streamflow, rainfall estimates, snow water equivalent, soil moisture and evapotranspiration at daily / monthly / annual time step. Based on the distribution of KGE values obtained in these studies, the acceptance criteria ranges were formulated, as shown in **Table S3**. Specifically, KGE values between the 1st quartile and the median (0.64 to 0.79) of the dataset were categorized as "good", values between the median and the 3rd quartile (0.79 to 0.86) of the dataset were categorized as "Very good", and values between the 3rd quartile and maximum (0.86 to 0.98) of the dataset were categorized as "Excellent"

Section B3: Modifications to the SWAT source code

The SWAT2012 – rev.659 version was used for all the analyses in this thesis. The SWAT-M model version (Zhang et al., 2013) could be availed by setting the CSWAT option in basins.bsn file to "2" (note that, option "0" indicates default C-N cycling routines, referred to as "SWAT" in this study, and option "2" denotes CENTURY based C-N routines, referred to as SWAT-M in this study). However, this version was not able to appropriately capture soil nitrogen accumulation. Furthermore, there were some inconsistencies in the equations described by Zhang *et al.* (2013) and the published equations in SWAT. To address these issues, the following modifications were made to SWAT-M that were then coupled to the TTD model to create SWAT-LAG.

Subroutine	Changes	Explanation

soil_chem.f in SWAT -M	Changed
	IF (FHP<1.E-10) FHP=.7-.4*EXP(-.0277*100) to
	
	IF (FHP<1.E-10) FHP=.97
		Changed SWAT-M's passive pool size to be 97%, slow pool size to be 1%, and active pool size to be 2% of initial soil organic nitrogen mass (**Table B4**).

carbon_zhang2.f90 in SWAT -M	Changed ABP=.003+.00032*sol_clay(k,j) to ABP=.003+.02*sol_clay(k,j)	This parameter (slope of the equation) helps to change the allocation of decomposed carbon/nitrogen from the active pool to passive pool. A discrepancy in slope value was observed between Zhang *et al.* (2013) and SWAT source code. In Zhang *et al.* (2013), the slope value was reported as 0.032, whereas, in the SWAT source code, the slope value was reported as 0.00032. However, this value was manually calibrated and fixed at 0.02 (during each trial, we checked whether the simulated soil organic nitrogen accumulation magnitudes are closer to observed soil organic nitrogen accumulation magnitudes)
	Changed ASP=MAX(.001,PRMT_45-.00009*sol_clay(k,j)) to ASP=MAX(.001,PRMT_45+.00009*sol_clay(k,j))	Zhang *et al.* (2013) used positive sign before the slope value (0.00009) whereas, SWAT source code used negative sign before the slope value. The authors changed the negative sign before the slope value (0.00009) to positive based on Supplementary Information of Zhang *et al.* (2013), page 6, equation 24
SWAT-LAG	The parameter NO3GW (HRU-scale NO_3-N in kg/ha/month, available in output.hru file) from SWAT-M model was coupled with the travel time distribution (TTD) model written in MATLAB (external to SWAT) to create SWAT-LAG (**Figure B5**).	

Section B4: Biogeochemical loss pathways for nitrate

Loss of nitrate from the system can occur via uptake (plant or algal) and denitrification in the hillslope and stream network. In SWAT, denitrification in the shallow aquifer is captured by the half-life parameter (HLIFE_NGW) that describes the time taken (days) to reduce nitrate concentration by a factor of two (Neitsch *et al.,* 2011). We assumed this parameter to capture the decay of nitrate in the groundwater system and calibrated this parameter (Table 4.1) to match the simulated nitrate load values with observed values.

SWAT has the option to simulate in-stream N cycling and removal processes. In general, in-stream N removal occurs through biotic N uptake and denitrification in the streambed (Mulholland *et al.,* 2008; Basu *et al.,* 2011). Default SWAT parameters were used for simulating biotic N uptake processes since site-specific information was not available. SWAT does not simulate streambed denitrification; however, it is well established that the majority of denitrification (87%) occurs in soils and groundwater (Seitzinger *et al.,* 2006; Beaulieu *et al.,* 2011), and thus it is reasonable to neglect this component of the N budget (Royer *et al.,* 2004; Seitzinger *et al.,* 2006; Alexander *et al.,* 2009; Gentry *et al.,* 2009; Beaulieu *et al.,* 2011).

Table B1. Watershed area under various crop rotation types from 1950 to 2012

S. No	Land-use / Rotation Description	Land-use Code	Percent watershed area (%) from 1950 to 1960	Percent watershed area (%) from 1961 to 2003	Percent watershed area (%) from 2004 to 2012
1	Continuous Alfa	AAAA			0.14
2	Continuous corn	CCCC	-	-	20.2
3	2-year alfa – 2-year	AACC	5.48	2.21	0
4	2-year corn – 2-year	CCAA	5.48	2.21	0
5	2-year corn - soybean	CCSC	0.86	3.32	2.54
6	Soybean – 2-year	SCCS	0.54	1.93	2.06
7	Corn - soybean	CSCS	9.67	37.21	28.46
8	Deciduous forest	FRSD	2.47	2.47	2.47
9	Pasture	PAST	15.20	7.59	4.09
10	Soybean - corn	SCSC	8.63	31.03	33.12
11	Hay-Oats-Corn	HOCH	4.93	0.87	0
12	Oats-Corn-Hay	OCHO	4.93	0.87	0
13	Corn-Hay-Oats	CHOC	4.93	0.87	0
14	Oats-Corn	OCOC	14.99	1.25	0
15	Corn-Oats	COCO	14.99	1.25	0
16	Urban	URBN	6.59	6.59	6.59
17	Waterbody	WATR	0.10	0.10	0.10
18	Wetland	WETF	0.23	0.23	0.23
	Total area		**100.00**	**100.00**	**100.00**

Note: Column 4, 5 and 6 represent percent watershed area under each land-use/rotation types for three different time-blocks

Table B2. Crop yield calibration ranges and final calibrated values

Variables	Range	Calibrated Values	Variables	Range	Calibrated Values
BIOE_CORN1	28.9 – 34	31.87	**BLAI_CORN1**	5 – 5.75	5.56
BIOE_CORN2	31.45 - 37	35.47	**BLAI_CORN2**	5.1 – 6	5.22
BIOE_CORN3	37 – 42.5	39.9	**BLAI_CORN3**	5.6 – 6.44	6.1
BIOE_SOYB1	19 – 21.8	20.76	**BLAI_SOYB1**	3.8 – 4.37	3.96
BIOE_SOYB2	19.5 – 23	22.92	**BLAI_SOYB2**	3.4 - 4	3.93
BIOE_SOYB3	23.5 – 27	25.11	**BLAI_SOYB3**	3.7 – 4.25	4.14
BIOE_ALFA	19 – 20	19.45	**BLAI_ALFA**	3.6 – 4	3.76
BIOE_OATS	10 – 20	14.29	**BLAI_OATS**	3.6 – 4	3.82
BIOE_HAY	20 – 25	20.07	**BLAI_HAY**	3.6 – 4	3.76
HVSTI_CORN1	0.32 – 0.37	0.33	**HEATUNITS_CORN1**	1000-1400	1001
HVSTI_CORN2	0.38 – 0.45	0.41	**HEATUNITS_CORN2**	1000-1400	1299
HVSTI_CORN3	0.52 – 0.59	0.58	**HEATUNITS_CORN3**	1000-1400	1146
HVSTI_SOYB1	0.19 – 0.22	0.21	**HEATUNITS_SOYB1**	1400-1600	1535
HVSTI_SOYB2	0.22 – 0.26	0.22	**HEATUNITS_SOYB2**	1400-1600	1474
HVSTI_SOYB3	0.27 – 0.31	0.28	**HEATUNITS_SOYB3**	1400-1600	1549
HVSTI_ALFA	0.85 – 0.90	0.86	**HEATUNITS_ALFA**	1000-1300	1267
HVSTI_OATS	0.36 – 0.42	0.36	**HEATUNITS_OATS**	1400-1600	1402
HVSTI_HAY	0.85 – 0.9	0.86	**HEATUNITS_HAY**	1000-1300	1162

Description of calibration variables: Note that we had used three different corn and soybean traits so that CORN1/SOYB1, CORN2/SOYB2, and CORN3/SOYB3 represents the crop traits used during 1950-1960,1961-2003 and 2003-2012, respectively; BIOE_CORN/SOYB/ALFA/OATS/HAY represents the Plant radiation use efficiency of respective crops, MJ m^{-2}, HVSTI_CORN/SOYB/ALFA/OATS/HAY: Harvest index of respective crops; BLAI_CORN/SOYB/ALFA/OATS/HAY: The maximum potential leaf area index of respective crops; HEATUNITS_CORN/SOYB/ALFA/OATS/HAY: Heat units of respective crops, cumulative ^{o}C

Table B3. KGE performance criteria

KGE Ranges	Range description	Performance
0.00 - 0.31	Zero to minimum	Poor
0.31 - 0.64	Minimum to 1st quartile	Moderate
0.64 - 0.79	1st quartile to the median	Good
0.79 - 0.86	Median to 3rd quartile	Very good
0.86 - 0.98	3rd quartile to maximum	Excellent

Table B4. Changes made to pool sizes of SWAT-M / SWAT-LAG model version

Initial Pool sizes	SWAT	SWAT-M / SWAT-LAG
Active	2% of initial soil organic nitrogen mass	5% of initial soil organic nitrogen mass (changed to 2%)
Slow	-	28% of initial soil organic nitrogen mass (changed to 1%)
Passive	98% of initial soil organic nitrogen mass	67% of initial soil organic nitrogen mass (changed to 97%)
		For a fair comparison with SWAT's soil organic nitrogen accumulation values, SWAT-M's initial pool sizes were made similar to SWATs

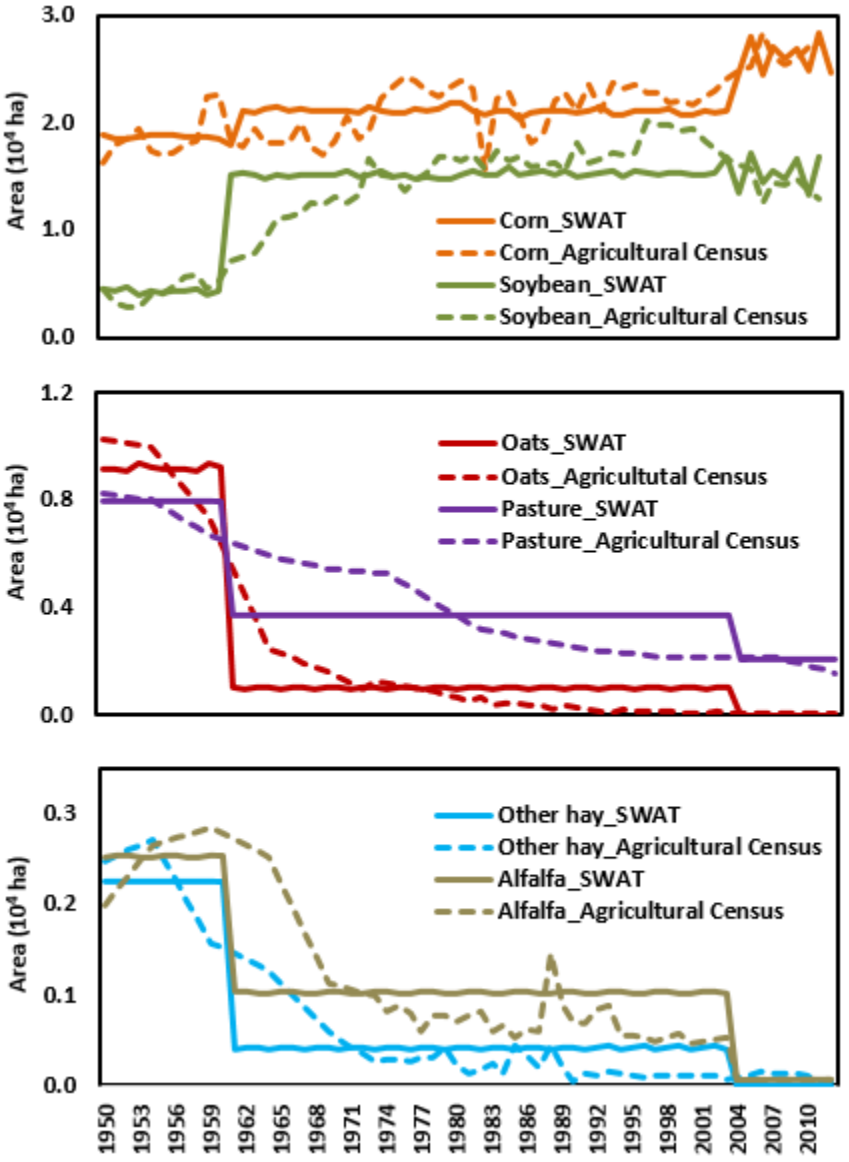

Figure B1. Crop harvested area trends (Agricultural Census vs. SWAT simulated) over the last 68 years in the South Fork Iowa Watershed. Note that simulated land-use is constant within each time block (1949-1960, 1961-2003 and 2004-2012)

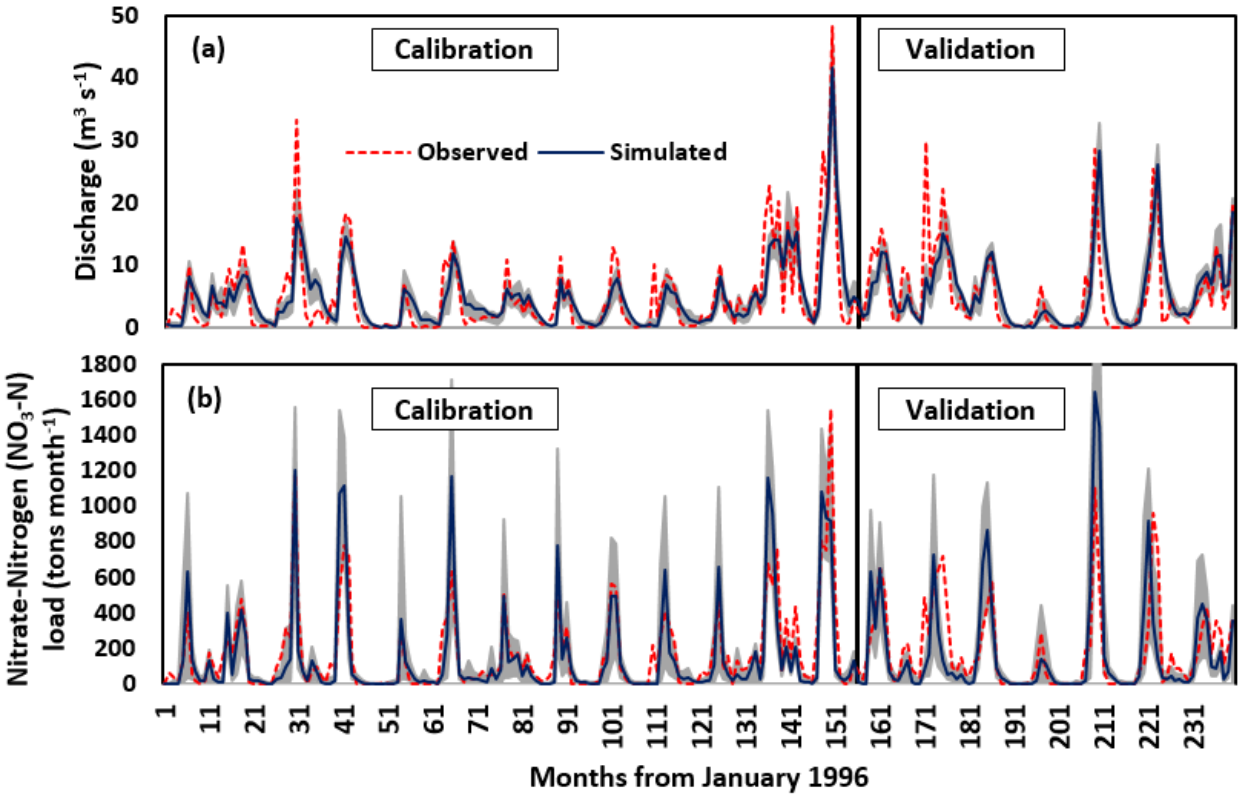

Figure B2. Observed vs. simulated monthly (a) discharge and (b) nitrate load from 1996 to 2015, using SWAT-LAG model version. Note: A grey area represents the 95% Prediction Uncertainty (95 PPU) band

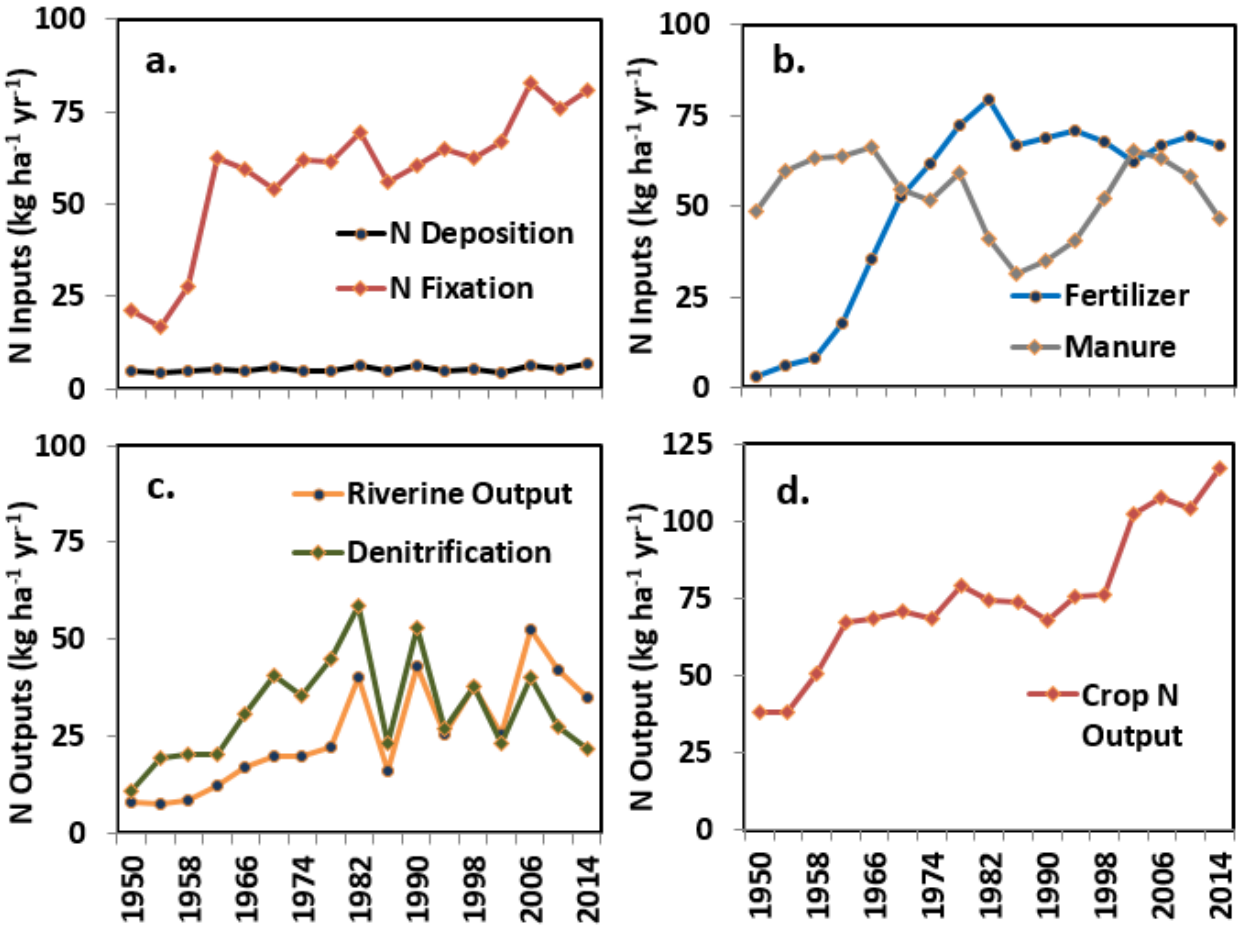

Figure B3. Model simulated trends in N fluxes for the SFIRW: (a) N deposition and N fixation, (b) fertilizer and manure application, (c) riverine output and denitrification and (d) crop N output and N surplus. Note that each data point represents a four-year average value

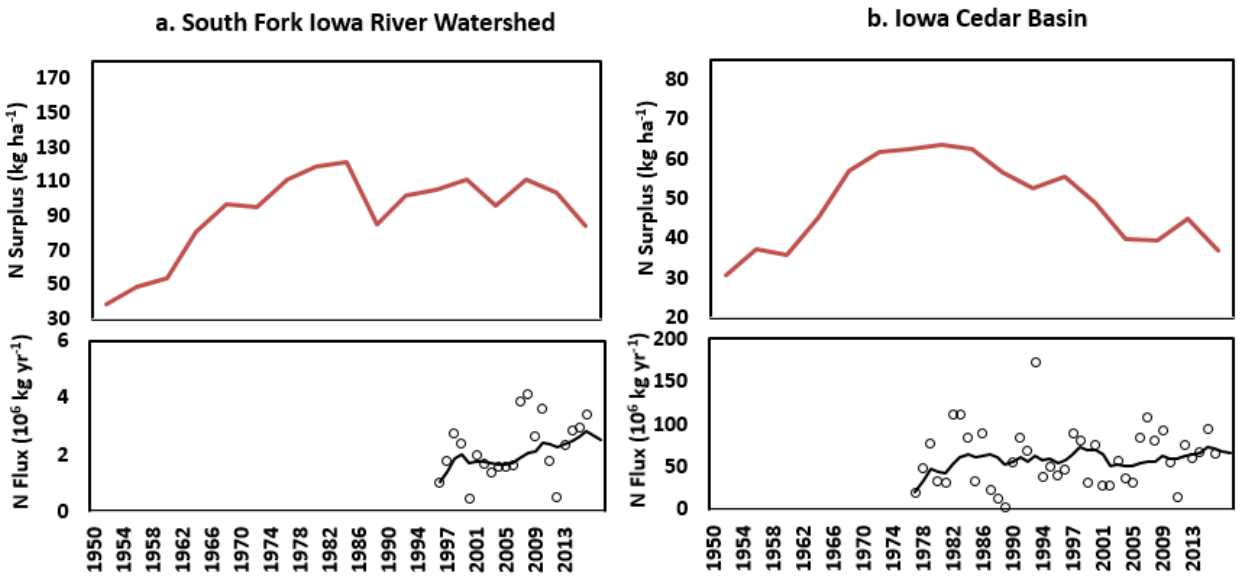

Figure B4. Comparison of N Surplus and Observed nitrate flux for (a) South Fork Iowa River Watershed (SFIRW) and Iowa Cedar Watershed (with an outlet at Wapello). The circles in the bottom plot denote observed nitrate flux values (estimated using WRTDS), and the solid line denotes the 10-year moving average of observed nitrate flux

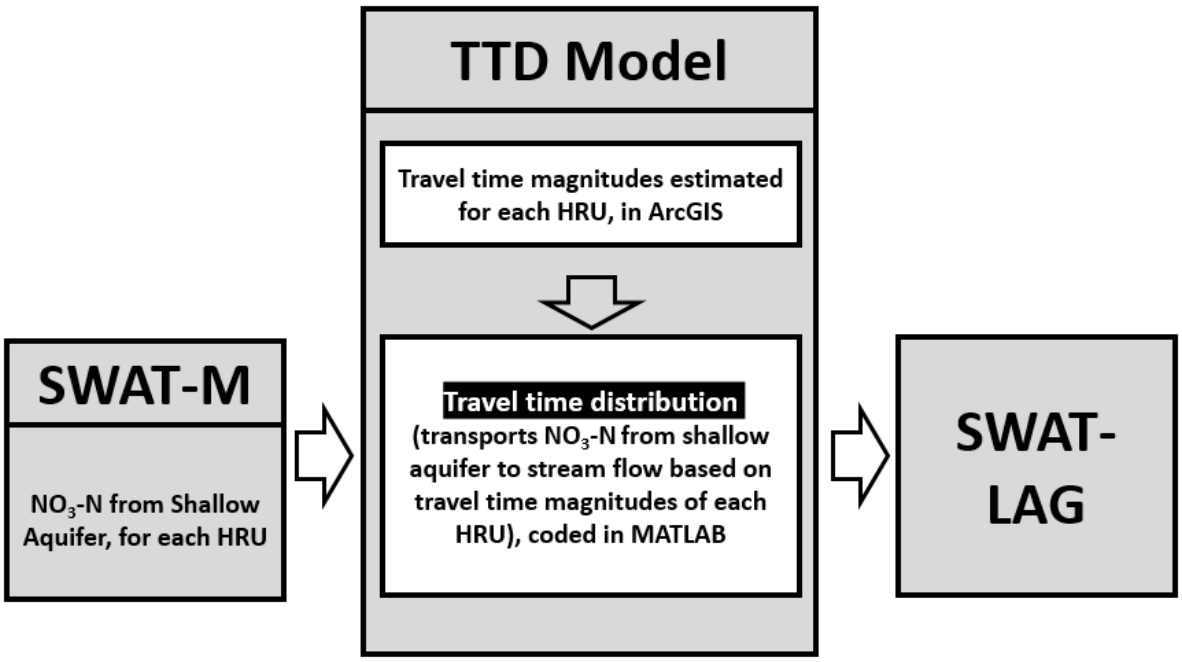

Figure B5. Schematic of SWAT-LAG model development. Nitrate-nitrogen of each HRU in the watershed, from shallow aquifer of SWAT-M, was transported to the stream outlet based on travel time magnitudes of the HRUs obtained from ArcGIS

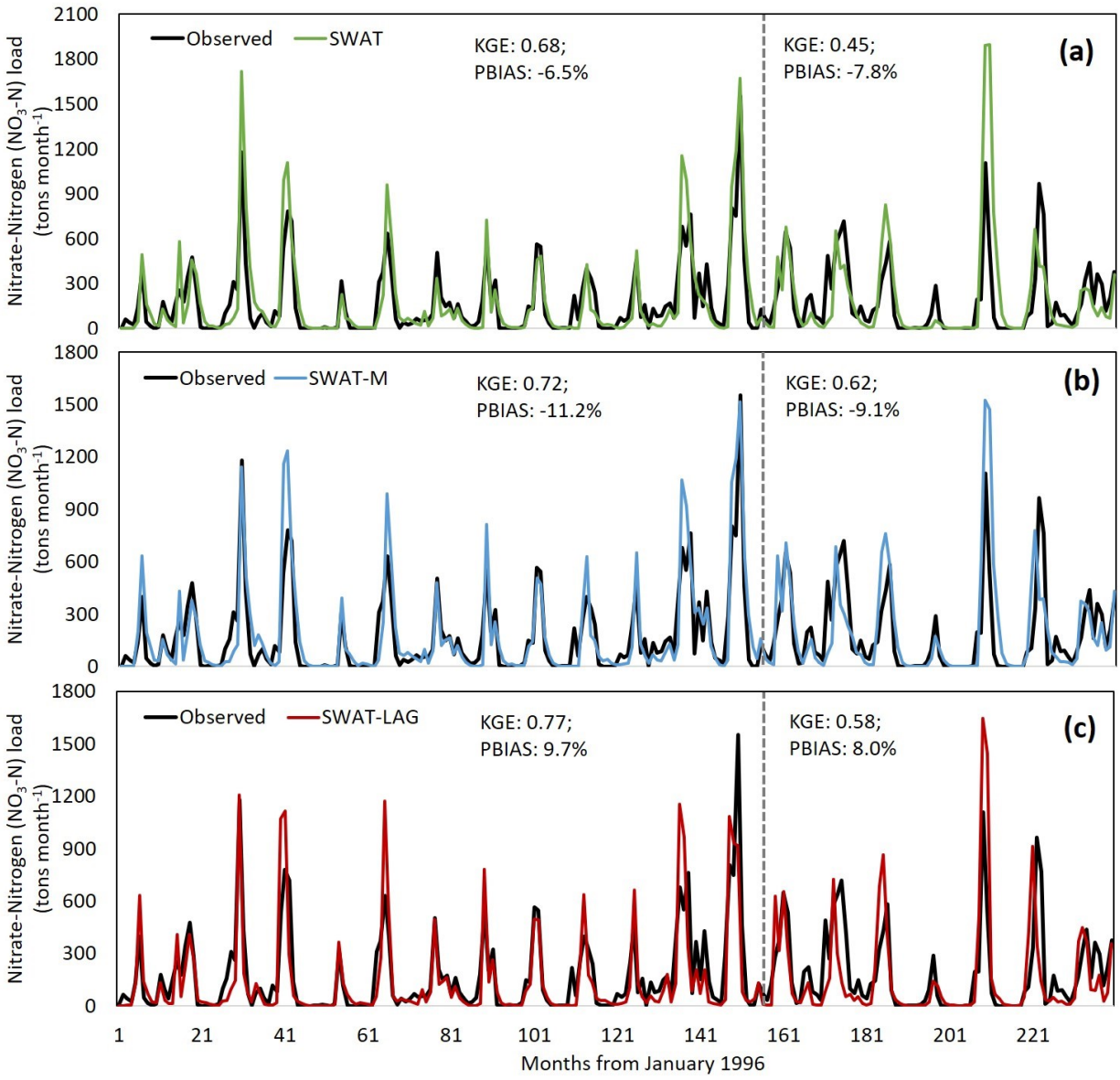

Figure B6. Observed vs. simulated monthly nitrate load from 1996 to 2015 for (a) SWAT, (b) SWAT-M, and (c) SWAT-LAG model versions, where SWAT and SWAT-M's nitrate load were obtained by using SWAT-LAG's calibration parameters. The dashed line separates calibration and validation periods

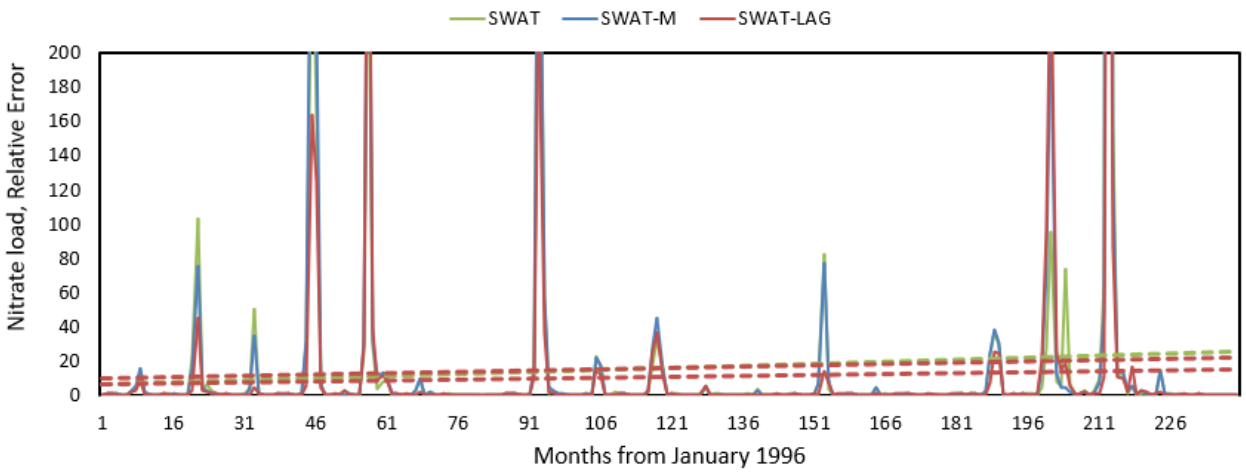

Figure B7. Relative error (abs(observed-simulated)/observed) of monthly nitrate load from 1996 to 2015 for (a) SWAT, (b) SWAT-M, and (c) SWAT-LAG model versions, where SWAT and SWAT-M's nitrate load were obtained by using SWAT-LAG's calibration parameters. Though the relative error of all the three model versions was increasing insignificantly, SWAT-LAG's mean relative error (11) was 31% lesser than the mean relative error of both SWAT and SWAT-M (16) versions. Note: p-values obtained from Mann-Kendall trend test are as follows: SWAT = 0.9; SWAT-M = 0.8; SWAT-LAG = 0.2.

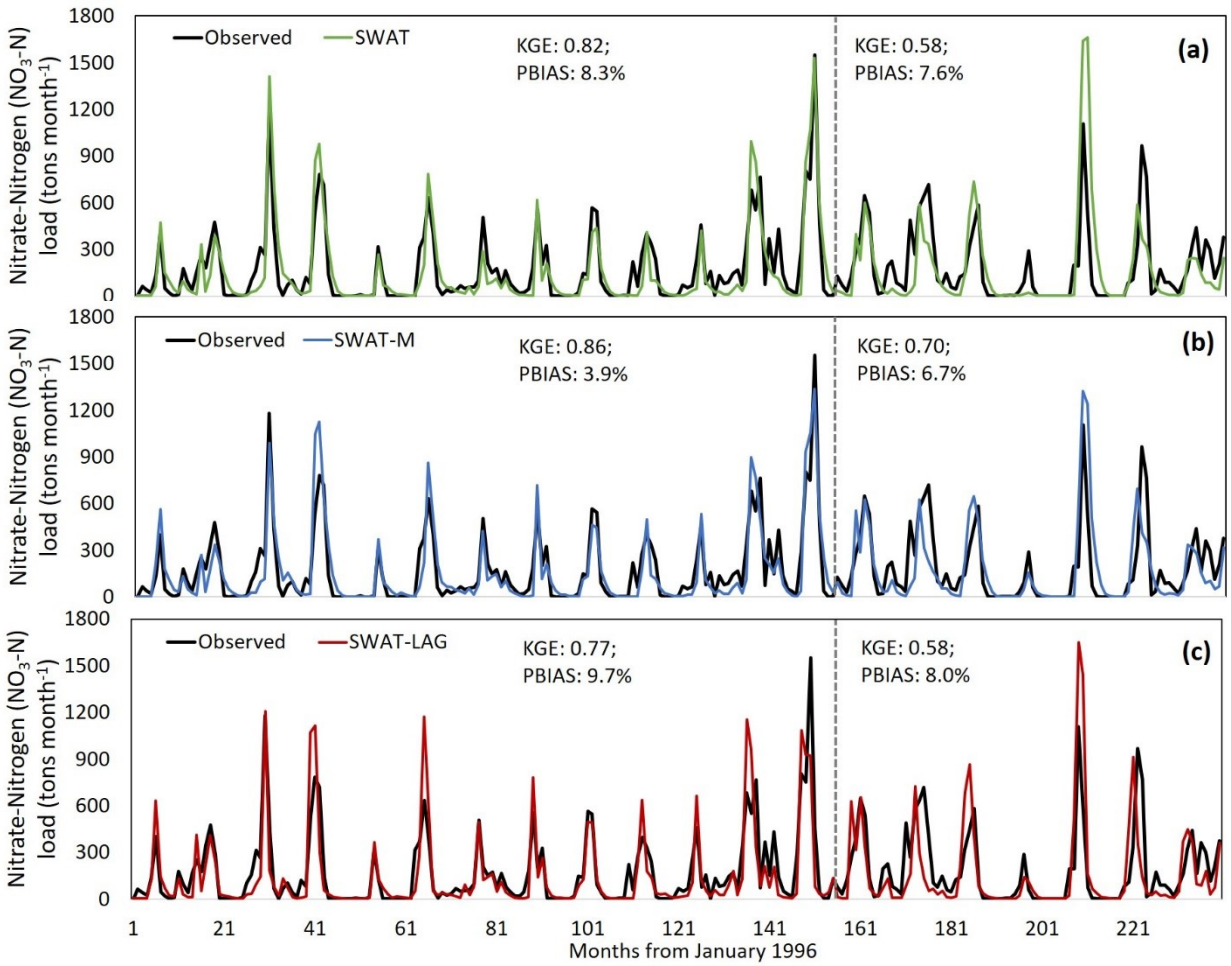

Figure B8. Observed vs. simulated monthly nitrate load from 1996 to 2015 for (a) SWAT, (b) SWAT-M, and (c) SWAT-LAG model versions. The simulated nitrate load of each model version was obtained from the individual model calibration. The dashed line separates calibration and validation periods

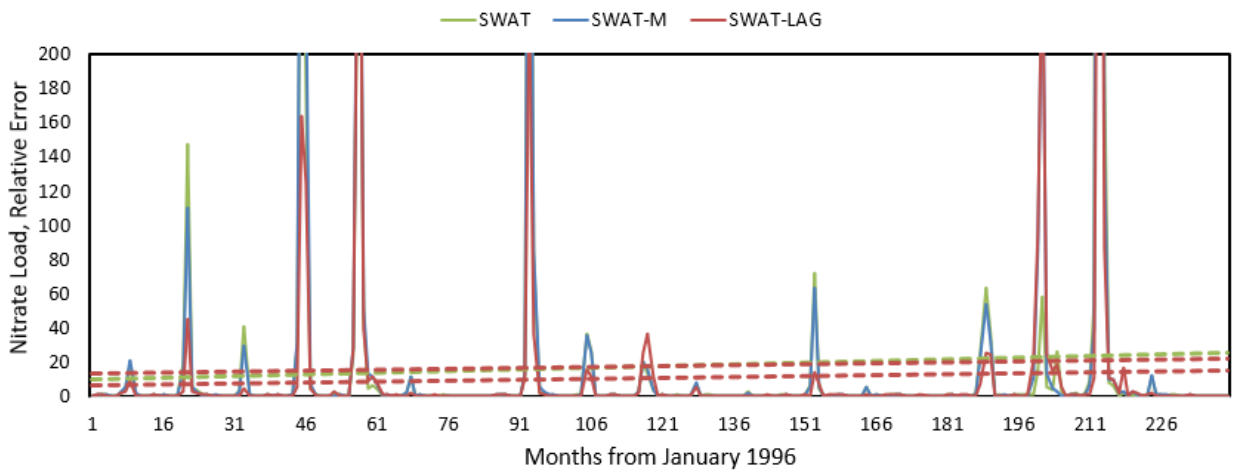

Figure B9. Relative error (abs(observed-simulated)/observed) of monthly nitrate load from 1996 to 2015 for (a) SWAT, (b) SWAT-M, and (c) SWAT-LAG model versions. The simulated nitrate load of each model version was obtained from the individual model calibration. Though the relative error of all the three model versions was increasing insignificantly, SWAT-LAG's mean relative error (11) was 38% lesser than the mean relative error of both SWAT and SWAT-M (18) versions. Note: p-values obtained from Mann-Kendall trend test are as follows: SWAT = 0.6; SWAT-M = 0.7; SWAT-LAG = 0.2.

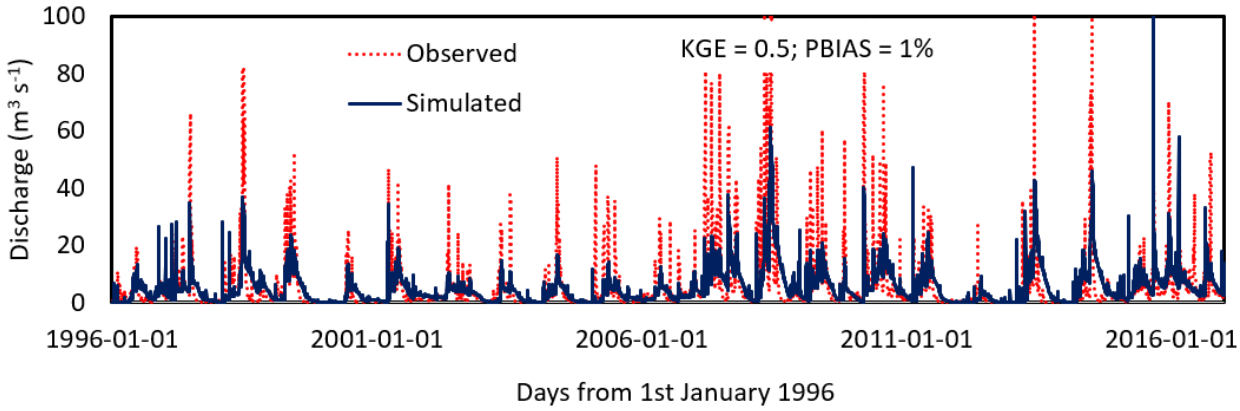

Figure B10. Observed vs. Simulated daily discharge from 1996 to 2015, using SWAT-LAG model version. Note: The monthly calibrated SWAT-LAG model version was checked for daily discharge simulation. The daily discharge was simulated adequately with a KGE value of 0.5 and a PBIAS value of 1%.

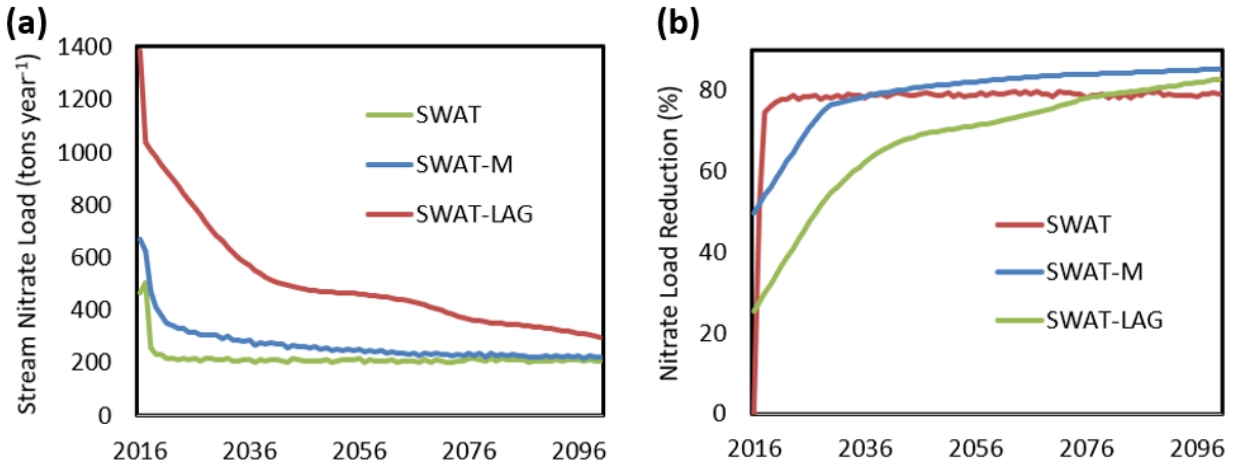

Figure B11. (a) Stream N load and (b) N load reduction as a function of time, simulated by SWAT, SWAT-M and SWAT-LAG for NM4 (100% fertilizer reduction in Corn HRUs). The stream nitrate load reduction trajectory was obtained by subtracting N load for the NM4 scenario from that of the BAU scenario. Longer lag times are observed for the SWAT-LAG and SWAT-M scenarios, compared to the SWAT scenario. Note that, the simulated nitrate load of each model version was obtained from the individual model calibration.

Appendix C: Supplementary Information for Chapter 5

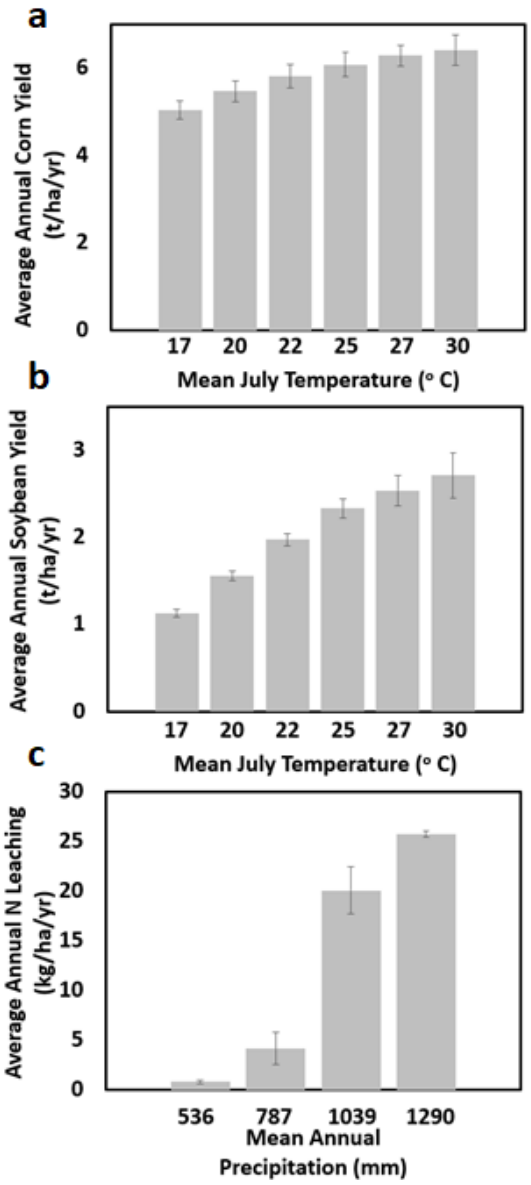

Figure C1. Improvements in average annual corn (a) and soybean yield (b) with increase in Mean July Temperature (ºC) and the error bars in (a) and (b) represent the standard error obtained from the four precipitation scenarios; (c) Dependence of average annual N leaching on Mean Annual Precipitation (mm). Average annual N Leaching magnitudes increase with an increase in Mean Annual Precipitation, and the error bars represent the standard error obtained from the six temperature scenarios.

Table C1. Crop yield and biological nitrogen fixation calibration parameters and final values

Years	Crop Varieties	PRDX	HIMAX	Crop Varieties	PRDX	SNFXMX
1875-1924	Corn1	10	0.4	Oats Alfalfa	8 15	- 0.11
1925-1934	Corn2	10	0.6	Soy1	10	0.11
1935-1936	Corn2	10	0.6	Soy2	30	0.034
1937-1948	Corn3	90	0.8	Soy2	30	0.034
1949-1956	Corn3	90	0.8	Soy3	90	0.012
1957-1960	Corn4	150	0.8	Soy3	90	0.012
1961-1966	Corn5	230	0.8	Soy3	90	0.012
1967-1980	Corn5	230	0.8	Soy4	110	0.012
1981-1986	Corn6	150	0.7	Soy4	110	0.012
1987-1990	Corn6	150	0.7	Soy5	130	0.012
1991-1996	Corn7	150	0.7	Soy5	130	0.012
1997-2000	Corn7	150	0.7	Soy6	150	0.012
2001-2010	Corn8	100	0.8	Soy6	150	0.012
2011-2012	Corn9	250	0.8	Soy6	150	0.012
2013-2014	Corn10	300	0.8	Soy6	150	0.012

PRDX: Potential aboveground monthly production for crops, g-C/m^2; HIMAX: Maximum harvest index for crops;
SNFXMX: Maximum symbiotic N fixation, grams N fixed per gram C fixed
Crop rotations: 1875-1924 – Corn-Oats-Alfalfa Hay; 1925-2014 – Corn-Soybean
HIMAX: Oats = 0.28; Alfalfa Hay = 0.8 and All soybean varieties = 0.52